Multilayer thin film thickness measurement method

to measure thickness of liquid thin film within a layer stack

Julian Bleeker

Report no	: 2023.039
Coach	: Ir. J. (Jelle) Snieder
Professor	: Dr.ir. R.A.J. (Ron) van Ostayen
Specialisation	: Mechatronic System Design
Type of report	: Master of Science Thesis
Date	: 16-06-2023

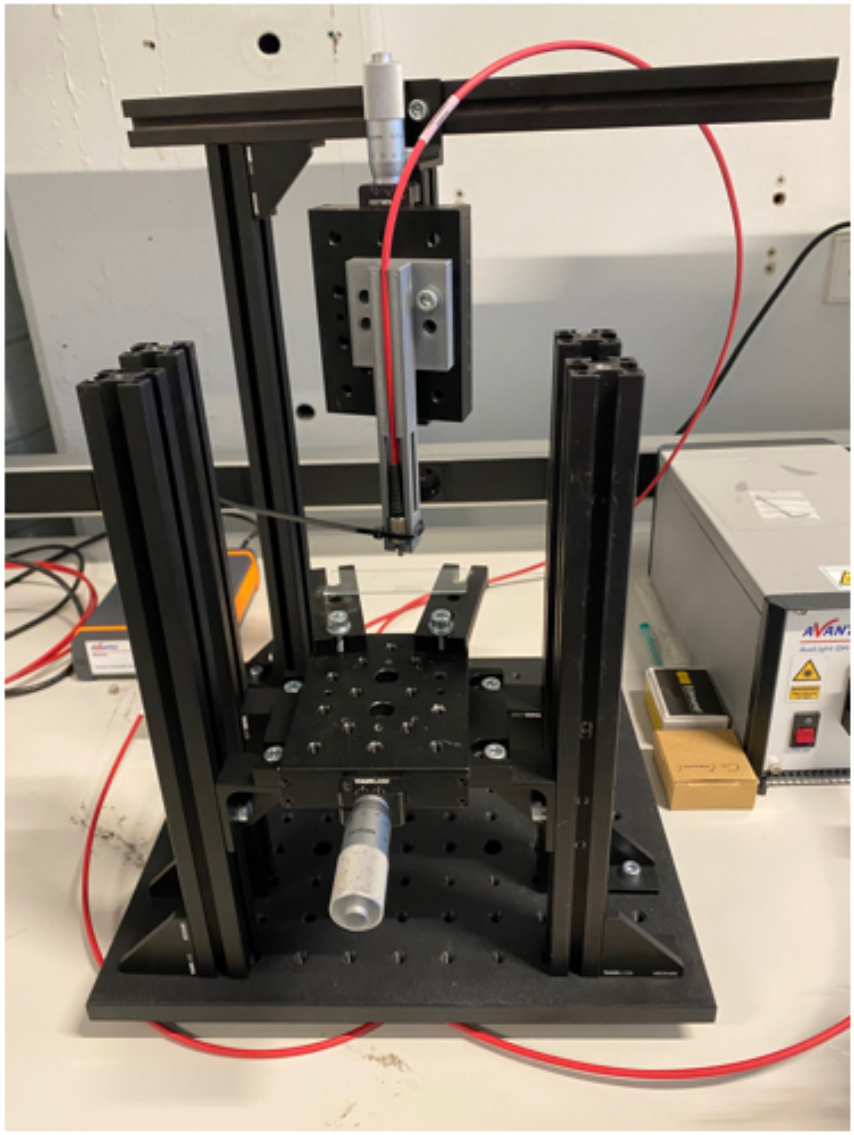

TU Delft Delft University of Technology

Challenge the future

Department of Precision and Microsystems Engineering

Multilayer thin film thickness measurement method

to measure thickness of liquid thin film within a layer stack

by

Julian Bleeker

to obtain the degree of Master of Science
at the Delft University of Technology,
to be defended publicly on June 27th, 2023 at 13:30.

Student number:	4433084	
Thesis committee:	Dr.ir. R.A.J. (Ron) van Ostayen,	TU Delft, supervisor
	Ir. J. (Jelle) Snieder	TU Delft
	Dr. N. (Nandini) Bhattacharya ,	TU Delft

TU Delft Delft University of Technology

Abstract

Roll-to-Plate (R2P) nanoimprint lithography (NIL) is used to imprint textures at nano scale into large surface areas. In the process an excess volume of liquid acrylic is deposited on a substrate. What follows is the lamination of a stamp, this means rolling a stamp over the substrate which spreads out the liquid acrylic and imprints the texture at the same time. The stamp contains the inverse texture and is pressed into the liquid acrylic, where excess volume of liquid forms a residual layer which is flat and below the texture. Here the texture is the useful part and the residual layer is desired to be as thin as possible. After the stamp is pressed onto the liquid acrylic and the texture is formed, the liquid acrylic is cured with UV light. A last step is delamination of the stamp from the substrate. The process is used for various applications such as an anti-reflective texture on solar panels. Other examples where R2P NIL is used is for example to create flexible electronics, micro lenses, LEDs and Architectural glass. The process effectively imprints desired textures on flat substrates. However, often the substrates are not perfectly flat which causes a non-uniform residual layer in the imprint. The non-uniform residual layer negatively impacts the performance of the imprint. In order to improve the process a uniform residual layer has to be maintained during the imprinting process. A first step in the improvement of this process is to inline measure the film thickness. Inline measuring of the film thickness allows one to tune the process and make adjustments to ensure a more uniform residual layer. It is desired to measure the film thickness before the liquid acrylic is cured, at this phase one can still have an influence on the layer by making adjustments to the process. Measuring of the film thickness is nontrivial since the acrylic film is situated between various other layers throughout the process.

The research objective of this thesis is to develop a measurement method that can measure thin film thicknesses through a multilayer that consists of both surrounding thick layers and in between thin films. The thick layers in this case are a stamp and a glass substrate while the thin films are the inverse texture film and the liquid acrylic based thin film where the texture is to be created into. A first step in the development of the measurement method, the multilayer sample is simplified and the textures are neglected. The resulting multilayer consists of several flat layers. An optical non-contact measurement method is researched and developed to non-destructively measure the thickness of a liquid thin film, which is situated between other layers. The liquid thin film represents the residual layer from the R2P-NIL process.

The optical measurement method used in this research is called spectral reflectance. The method is able to measure the thickness of a layer or several layers in a multilayer. The method works by analyzing the reflectance spectrum from a light beam which is directed perpendicularly and with a wide range of wavelengths on the surface of the layer. The reflectance spectrum that is measured with a spectrometer includes oscillations that result from the interference of light that reflects at the different interfaces between the different media within the layer. The oscillation contains frequency content which is used to determine the thickness of the layer. At first, the frequency of the signal can be determined with the use of the fast fourier transform. In the next step, this frequency can be related to the optical thickness of the layer. The final step is to translate the optical thickness into a geometrical thickness by using the average refractive index of the material over the measured wavelength range. To verify the performance of the spectral reflectance technique, reference layers were used. It is important that the thickness of these reference layers was known or could be determined accurately. These reference layers could then be used by measuring with the spectral reflectance method to compare the measured thickness with the reference thickness. The reference layers that have been used are a thin film of water and a cured layer of acrylic.

This research shows that the spectral reflectance technique can be used to measure the thickness of a stack of thin films with the condition that the thin films are all coherent. Also the layers in the multilayer exist of non-absorbing materials only. In order to measure the thickness, the refractive indices of the layers in the multilayer must be known and for some of the layers the orders of magnitude of their thickness are needed. It is also reasoned in this research why the method will become more and more

tedious as more than three layers are added due to peak recognition limitations. It is still possible to determine the film thickness of a stack coherent thin films, which are surrounded by incoherently thick layers. The outer layers can be assumed to be incoherently thick based on a combination of factors such as the layer thickness of the thick layer, the measured wavelength range and the resolution of the spectrometer.

Preface

Here I am working on the final part of the Master Thesis for the Master Mechanical Engineering after spending more time than I initially planned. Nonetheless am I extremely proud to have made it, without giving up, to the point where I will give the final presentation of my research before obtaining my Master's degree.

Right here I would like to express my gratitude to my initial supervisor Ir. J. Spronck and later on Dr. Ir. R.A.J. van Ostayen for brainstorming with me on potential topics and the weekly sessions, my supervisor Ir. J. Snieder for helping me throughout all my stumbling and all the weekly discussions, M. Ballottin from Morphotonics and Dr. S. Dutta for their assistance with the equipment and knowledge in their specialization, friends and family for supporting me and last but not least the incredible help from the PME Technical Support Staff.

Julian Bleeker
Delft, June 16, 2023

Contents

1 Introduction

In this chapter, the technique nanoimprint lithography is introduced. Also, the extensive literature study that has been done on thin film thickness measurement techniques is discussed. Besides that, the project objective is stated. Finally, to give an impression of the thesis structure, an overview of contents is given.

1.1. Nanoimprint lithography

As Chou et all mention in their work [10], nanoimprint lithography (NIL) is a technique for producing micro or nano-scale features and patterns over large surface areas, with high throughput and at a low cost. It is a technology that works based on a mechanical deformation of a resin. NIL works with a mold that transfers an inverse geometry in a resin onto a desired surface. An advantage of this technique is that it allows for the mold to be reused and therefore enables for a long-life cycle. This comes down to a large area, high throughput, low-cost micro/nanoimprint application suitable for a large range of industries. Back in 1995 Chou et all were the first to publish about the concept of nanoimprinting [9]. The mentioned paper from 1995 is the first ever published attempt of imprinting sub-25 nm structures with high aspect ratios into polymers.

As Lan presents in his work [18] one can divide NIL into two main categories. The full wafer NIL and the roller type NIL [17]. Full wafer is often referred to as plate to plate (P2P). It works by pressing a flat plate which can be seen as a mold or stamp into a resin layer which lays on a rigid substrate see figure 1.2. This creates full surface contact of two plates which results in high imprint and demolding forces.

To further improve the development of NIL, the issues concerning P2P had to be described. Four important issues had been identified:

1. Achieving uniform pressure distribution across the full wafer
2. Ensuring entirely conformal contact on the imprint full field
3. Avoiding trapped air bubble defects
4. Reducing imprinting forces

Roller type NIL was initially invented to increase imprint surfaces and throughput of the process. However, it also gave solutions for the mentioned issues. The main difference between full wafer NIL and roller type NIL is that the roller type works with a line contact rather than full surface contact. This highly reduces the imprint and demolding forces. This line contact also reduces the trapped air bubbles effect and variation in thickness. Besides this, the roller type NIL can imprint continuously whereas the full wafer technique can imprint one substrate at the time.

The roller type NIL can be further divided into two subcategories, roll to roll (R2R) and roll to plate (R2P) as can be seen in figure 1.1. R2P works with a stamp wrapped around one or multiple rollers and a flat rigid substrate. Instead of a stamp wrapped around rollers one often uses a textured roller. This rigid substrate is supported on top of different rollers in such a way that it can be guided through the rollers with the stamp. This creates a line contact between the stamp and the rigid substrate which has a resin deposited onto it.

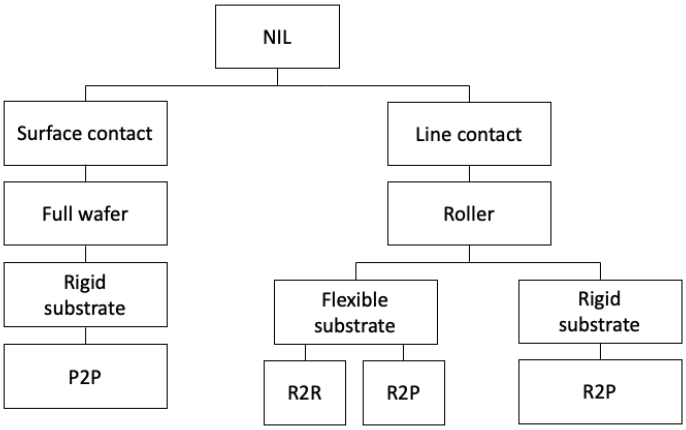

Figure 1.1: Nanoimprint lithography (NIL) categorization

Since R2P works with this line contact it has great advantages over the conventional P2P method. However, the R2P still has some problems in realizing an imprint process that works continuously. Figure 1.2 shows an schematic of both methods where the dimensions of the structures are exaggerated for illustrative purposes.

The R2R method uses a stamp around a roller to transfer a nano or micro-structure onto a substrate. With this method a flexible substrate is used to imprint structures. The R2R process is generally a continuous process. On the other hand, the R2P method uses substrates with a finite length and is therefore not continuous. An advantage of the R2P method is that it enables you to imprint structures on both flexible as well as rigid substrates.

With all three of the previously described nanoimprint methods initially a fluid resin is used. The molds imprint the structures while the resin stays a fluid. An important step is the curing of the resin. This is done by either of the two fundamental types, either with UV NIL or with thermal NIL [17] Where thermal NIL [24, 31] works with imprinting onto a thermally softened thermoplastic polymer resin, UV NIL [6, 19] makes use of a liquid photopolymer resin that cures by exposure to ultra violet light.

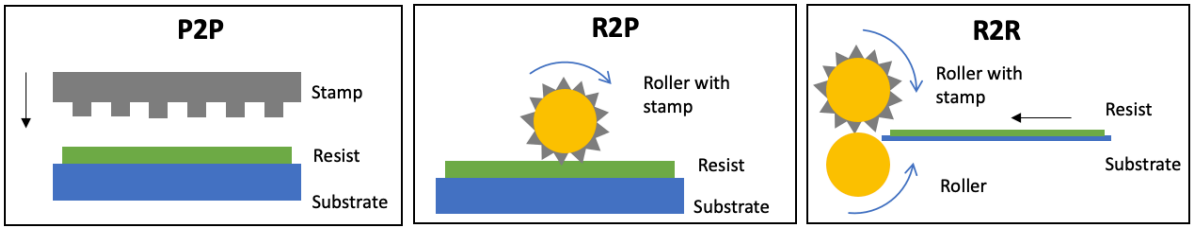

Figure 1.2: Illustration of the different NIL methods.

Nano textures have been an important research area for some time in the high-tech industry now. Different nano textures are applied to improve the performance for a wide range of applications such as the brightness of LEDs, improved efficiency solar panels, high density storage to high clearness (HD) display.

Since large-area NIL is the most cost-efficient way to do this, it is already used to create micro/nanostructures and features for multiple applications in nanoelectronics optoelectronics, optical components, nanostructured glass and biological applications. Micro- and nanostructures are used to enhance performance of these applications. Figure 1.3 shows the representative industrial applications and products that fit into the different NIL categories as given by H. Lan [18]. For the roller type NIL category the application are AR films, solar cells, patterning of flexible films, architectural glass, TV with AR structures, flexible electronics, HD displays and OLED. While full wafer NIL is mainly utilized for LEDs but also for HDD and micro lenses.

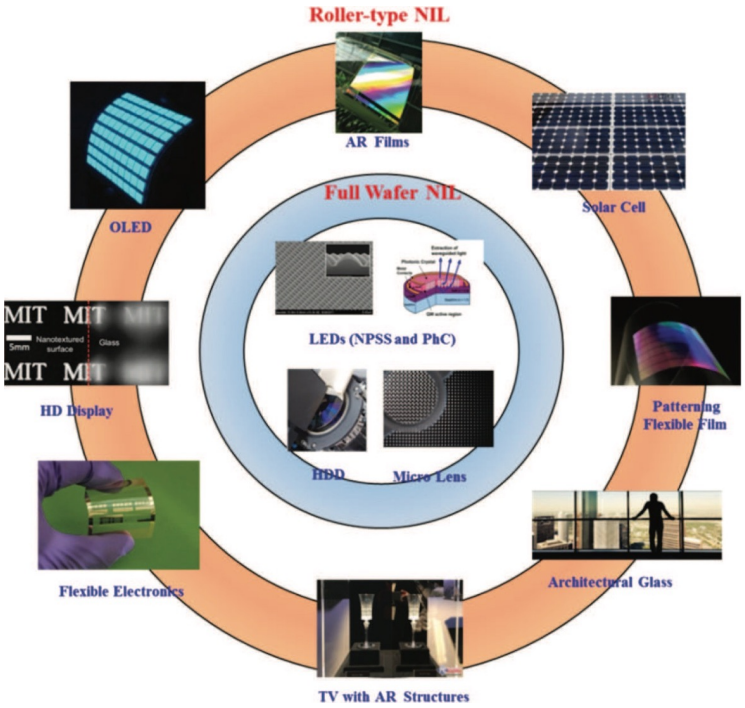

Figure 1.3: Large area NIL applications per category [18]

Morphotonics is our research partner in this project. A company that is specialized in developing and delivering machines that are able to imprint micro- and nano-textures onto substrates for customers. At Morphotonics the R2P NIL technique is used in a process to imprint textures onto substrates with a wide range of applications. One of the applications where this process is often used for is the process of imprinting anti-reflection textures on solar panels. The texture that is desired on the solar panels enables increased efficiency for the solar panel by trapping light. The texture causes more light to transmit while limiting the reflection away from the panel. This R2P NIL process is used in Veldhoven in the Portis NIL600 (see figure 1.4), a machine developed and produced by Morphotonics.

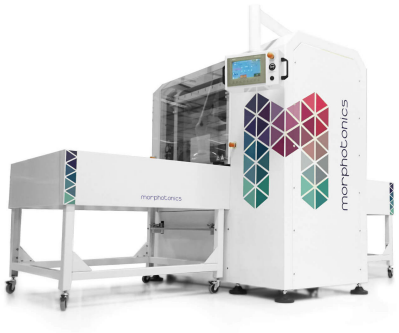

Figure 1.4: Portis NIL600 from Morphotonics. [23]

The process of Morphotonics can be divided into five separate phases. See figure 1.5 for a schematic of these phases. The five different phases are listed and explained next:

1. Lamination phase

In this phase the mold (flexible stamp) gets laminated over the substrate. This mold is a thin film that includes the inverse texture and is made from a comparable acrylic material but is cured. By laminating this mold, the dispensed droplets are spread out over the surface. Since the roller ensures a continuous line contact, air bubbles are eliminated. An important aspect of this phase is that the textures in the flexible stamp are filled with liquid resin.

2. Liquid film phase

In this phase we are dealing with a liquid film which is in between the substrate and the flexible stamp.

3. UV curing phase

In this part of the process, the thin film is cured by UV light. This phase can be seen as a transitioning phase from liquid to solid imprinted textures.

4. Cured film phase

In this phase the thin film is completely cured but is still under the stamp.

5. Delamination phase

The last phase is the delamination phase which is where the flexible stamp is delaminated from the imprint and where we have the cured thin film on a substrate. This gives the final result of the imprint process. This result can be a flat thin film or a thin film with texture. The objective of the imprint process is to create a textured film with uniform thickness on top of the substrate.

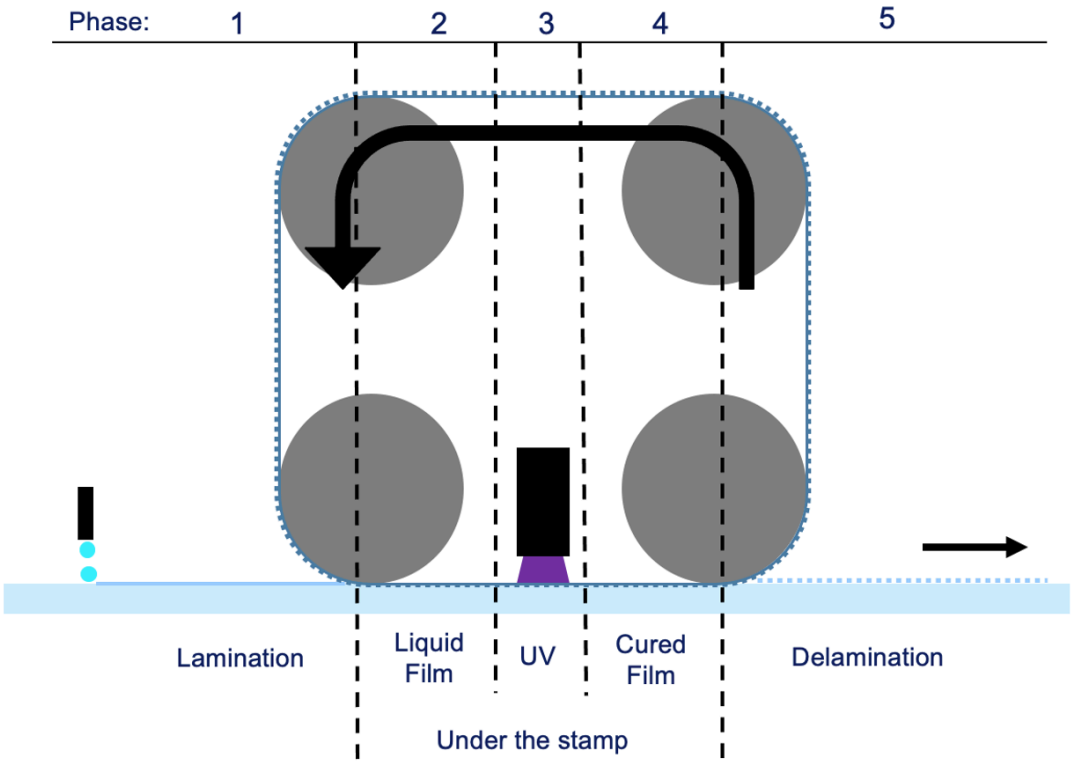

Figure 1.5: A representation of the phases in the process.

The described process works well whenever there is a flat substrate. The process of imprinting a uniform texture becomes significantly more challenging whenever the substrate contains non-uniformities such as waviness. A consequence of such uniformities in the substrate can be that the imprint pressure is not uniformly distributed over the surface of the substrate. This results in non-uniform imprinted texture thicknesses. This problem often occurs when imprints need to be made on solar panels. Multiple attempts have been made by Morphotonics to solve this problem. Such as initially depositing an excess volume of resist onto the substrate and changing the formation of droplet deposition. Besides this there is also a certain pressure on the flexible stamp. Different pressures have been used to try and change the result of the process.

To come closer to a solution for this problem, one needs to have a better understanding of what happens to the resin during the imprinting process. One steps is to measure the thickness of the thin film in each of the individual phases. A first step would be to measure the film thickness of the thin film in phase two where the thin film is still a liquid. It is important to measure the liquid at this point in the process (phase 2 in figure 1.5) since we are not yet dealing with a cured layer which means that it is still possible to adjust the layer thickness. It will not be possible or at least significantly more challenging to make adjustments to the layer in phase three or four once it is already cured. The inline measurement would allow one to tune the process by changing a variety of parameters such as, the speed at which the substrate is guided or the pressure that is used in the R2P NIL process.

1.2. Layer thickness measurement methods

A literature study has been performed to find out which measurement techniques exist. From the techniques that were determined to be eligible, an optical measurement method which is known as spectral reflectance was selected. The technique makes use of a light beam with a wide range of wavelengths and looks at reflection when it travels perpendicular to a multilayer. This method was chosen since it is a technique that measures non-destructively, without contact and can measure thin film thicknesses by looking at the interference between reflections from the different interfaces within a multilayer stack. The measurement technique must not be destructive as that would negatively impact the performance of the layer for the application it was made for. While non-contact was a requirement since the thickness of a layer is to be measured while the layer is in the middle of a multilayer.

The literature study contains a study on the state- of-the-art measurement techniques for thin film thickness measurements. The different measurement techniques have been divided into separate groups based on what physics the techniques cover. These different physics groups are:

1. Mechanical methods
2. Electrical methods
3. Optical methods
4. Electromagnetical methods
5. Chemical methods
6. Acoustical methods

Most of these methods were not useful because certain conditions were required such as measurements in vacuum, destructive measurements, contact measurements or single layer measurements only. For more information on the individual techniques see Appendix A. From all the individual methods, eventually three potential techniques were compared. The study reasons towards spectral reflectance as being the most suitable technique for the given problem. As spectral reflectance does not require any moving parts since it only looks at the reflectance spectrum over a specific wavelength range for a fixed angle of incidence. A spectral reflectance measurement setup requires relatively simple parts such as a light source, spectrometer and an optical cable which makes building a setup feasible within the duration of the master thesis.

A lot of research has been done on the measurement technique for both single thin film as well as multilayer thin film measurements [25]. This research makes use of the available knowledge to check whether this method can potentially be used for inline measurements to improve the imprint process at Morphotonics. This will be done by creating and measuring the thickness of a layer in a multilayer that is comparable to the multilayer from the process of Morphotonics.

1.3. Project objective

This thesis will focus on measuring the thickness of a liquid thin film between 1 and 10 µm, since the thickness of the residual layer in the R2P NIL process is of that order of magnitude. The objective is to measure the thickness of this liquid thin film in phase two while it is surrounded by other layers. The multilayer consists of two surrounding relatively thick layers which are the stamp and a glass substrate. Besides the thick layers, there is another thin film with thickness of comparable order of magnitude as the liquid thin film which is the cured resin (see figure 1.6). The thick layers are often glass substrates with a thickness of 500 µm while the stamp is generally more in the range of 250 µm. Morphotonics is currently only able to measure one thin film thickness at once. This means that the thin film can only be measured after the thin film is cured and removed from the machine. Meaning that any method suitable to measure through a multilayer to measure the thickness of the desired resin thin film is already an improvement on what is currently possible, regardless of the accuracy of the method. To summarize, the measurement method should be:

1. Non-destructive
2. Able to measure thickness of a liquid thin film of around 10 µm
3. Able to measure through a multilayer including thin and thick films
4. Implementable into the Morphotonics R2P NIL process at the liquid layer phase

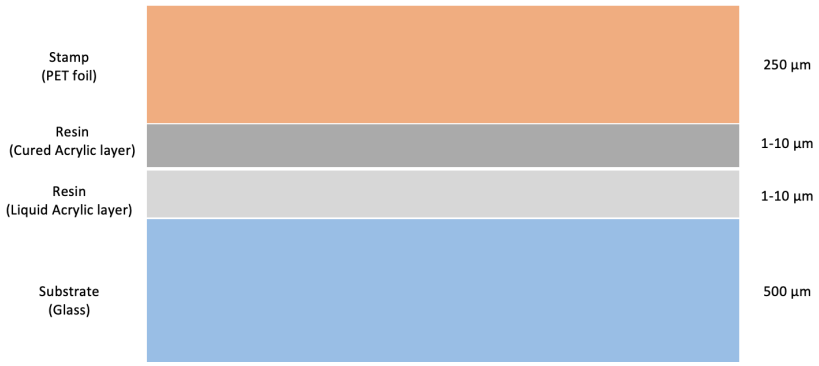

Figure 1.6: Multilayer including the thin film thickness to be measured.

1.4. Thesis overview

In Chapter 2 a theoretical model will be laid out and explained in detail. The theoretical model looks at the reflection of a light beam that travels perpendicular to the surface of the multilayer. While the reflectance spectrum can be used to determine the thickness of the layers in the multilayer. Followed by Chapter 3 which includes an approach to come close to the situation from the R2P NIL process by using the theoretical models. In Chapter 4 the experimental setup is presented, including an overview of the different parts. Lastly, the results from the measurements on the experimental setup are shown in Chapter 5. Furthermore, Appendices with additional information including the literature study that has been done prior to this research can be found at the end of this document.

2

Spectral Reflectance Principle

This chapter will look into the principle behind the optical measurement method called spectral reflectance used for the research described in this thesis. A theoretical model is explained including the applicable conditions such as incident material and the materials that can be measured. Besides those, important conditions are the angle of incidence, the refractive index of the materials and the thicknesses of the involved layers.

2.1. Introduction

As described in the previous chapter it is known that the objective is to measure the thickness of a liquid thin film that is located between other layers thereby forming a multilayer including another thin film of comparable thickness as well as two thicker layers.

If one is looking into the principle of spectral reflectance to measure the thickness of a thin film it is important to understand what steps are involved with the measurement technique. In this chapter we will attempt to describe the steps needed for the simulation of a single thin film, followed by a more complex scenario which is the multilayer scenario and finally the steps needed to go from measuring the reflection of light into determination of the thickness of the layers that are measured. Equations used in this chapter originate from the work of Quinten et al [25] unless mentioned otherwise.

2.2. Governing equations

Consider a single thin film (medium 1) with thickness d, which is positioned between an incident material (medium 0) and a substrate (medium 2) as depicted in figure 2.1. Each medium has its own characteristics, such as thickness and refractive index. Assume we are dealing with infinite thicknesses for media 0 and 2 while medium 1 has a finite thickness. Now consider light that is traveling through medium 0 falls onto the interface between medium 0 and medium 1 with angle of incidence of α with respect to the normal on the thin film.

Part of this incident light reflects on the interface back into medium 0 (B_1) while another part of the light transmits through this interface and into medium 1. The part that now travels in medium 1 hits the second interface between medium 1 and 2 with an angle of incidence β. Again part of the light reflects back now into medium 1 while another part transmits into medium 2.

The part that travels in medium 1 hits the initial interface but from the other side. Part of the light transmits through this interface into medium 0 (B_2) while another part of the light reflects back into medium 1. In theory this process continues an infinite amount of times which means that we eventually end up with infinite amounts of reflected rays (B_1 up to B_i) in medium 0. However, once light reflects or transmits, the intensity of the reflected ray decreases. After continuously reflecting and transmitting, the intensity of the light becomes insignificant. The intensity of reflection B_1 (see figure 2.1) scales down by just one reflection coefficient (Fresnel equation which will be explained in detail below), while the intensity of reflection B_2 already scales down by two transmission coefficients and one reflection coefficient, the intensity of reflection B_3 scales down even faster and adds another two reflection coefficients. Depending on the materials used, reflections up to B_4 are having significant impact. After B_4, the terms becomes decreasingly important until they are negligible.

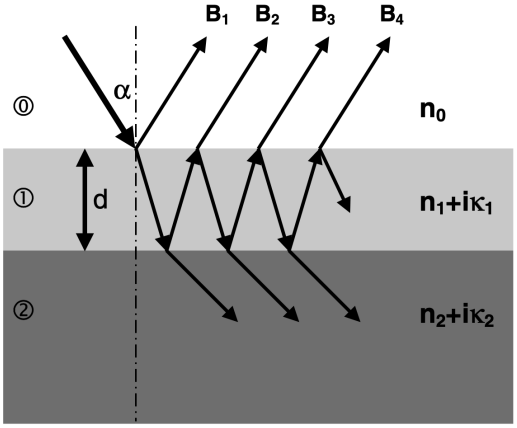

Figure 2.1: Spectral reflectance principle for a single thin film [25].

The incident light results in individual reflections B_1 up to B_i. In order to find the resultant reflection from the thin film a combined expression of these individual reflections has to be determined. These individual reflections interfere with each other and together form an interference pattern. As a result one will see bright and dark fringes with a certain frequency in the signal due to constructive and destructive interference. A graph showing the interference pattern of these light rays is referred to as a reflectance spectrum which shows the reflected light intensity over a wide range of wavelengths.

The reflection B_1 on the interface between the incident medium and the layer can be calculated with the reflection coefficient from the Fresnel equations (equations 2.1). Where the reflection coefficient is related to the refractive indices n_0 and n_1 of two media. What follows is the expression for B_1 (equation 2.2) where A_0 contains the incident light magnitude and phase content, but is irrelevant for the reflectance spectrum.

$$t_{ij} = \frac{2 \cdot n_i}{n_i + n_j}$$
$$r_{ij} = \frac{n_j - n_i}{n_i + n_j} \tag{2.1}$$

$$B_1 = r_{01} A_0 \tag{2.2}$$

Followed by B_2, the reflection at the bottom interface between the layer and the rear media. This reflection can be determined by using the Fresnel equations for a transmission coefficient through interface 1 from medium 0, a reflection coefficient at interface 2 from medium 1 and another transmission coefficient through interface 1 back into medium 0. The light that transmits through the first interface into the layer travels back and forth in the layer. meaning that B_2 travels a longer distance than B_1. This path length difference causes a phase difference between B_1 and B_2. This phase factor is defined as equation 2.3. The total reflection B_2 now consists of two transmission coefficients, one reflection coefficient, a phase factor, and A_1 see equation 2.4. Where A_1 still represents the incident light magnitude but will be set as equal to 1 for the remainder of this research. Variables and constants in the equations

are the layer thickness d, the angle β is the angle at which the light travels through the layer towards the bottom interface after transmitting through the top interface, the wavelength of the light λ and the refractive index n_1 of the layer.

$$\delta\phi_1 = \exp\left(i\frac{4\pi}{\lambda}\frac{n_1(\lambda)\cdot d}{\cos(\beta)}\right) \tag{2.3}$$

$$B_2 = t_{10}r_{12}t_{01}A_0 \cdot \delta\phi_1 \tag{2.4}$$

Followed by the expression for B_3 which adds two more reflection coefficients and additional path length difference (taken into account by the m in the exponent) which gives us a more general expression for B_{m+1} where m is a positive integer ($m \geq 1$) according to equation 2.5.

$$B_{m+1} = t_{10}r_{12}t_{01}(r_{10}r_{12})^{(m-1)}A_0 \cdot \delta\phi_{1,m} \tag{2.5}$$

$$\delta\phi_{1,m} = \exp\left(i\frac{4\pi}{\lambda}\frac{n_1(\lambda)\cdot m\cdot d}{\cos(\beta)}\right) \tag{2.6}$$

At this point it is clear to see that the individual reflection B_1 is dependent only on the Fresnel equation while B_2 and higher orders are also dependent on a phase term. The thickness dependence is only included in the phase term. From here on the incidence angle will be taken as perpendicular to the thin film which allows for a simplification of the phase term (Equation 2.7). Besides this, an assumption is made that the thin film is a non absorbing transparent material. This means that the complex part of the refractive indices can be set to zero ($\hat{n} = n + i\kappa$ where $\kappa = 0$).

$$\delta\phi_{1,m} = \exp\left(i\cdot n_1(\lambda)\cdot m\cdot d\frac{4\pi}{\lambda}\right) \tag{2.7}$$

Now that we have determined expressions for the individual reflections from figure 2.1 the next step is to form an expression for the combined reflectance. This can be achieved by applying superposition of B_1 with B_{m+1}.

$$B = A_0\,(B_1 + B_{m+1}) \tag{2.8}$$

By filling in the expressions from equations 2.2 and 2.5 we get the following resultant expression for the total reflectance as per equation 2.9.

$$B = A_0\left(r_{01} + \sum_{m=1}^{\infty}\left(t_{10}r_{12}t_{01}(r_{10}r_{12})^{(m-1)}\cdot\ \exp\left(i\cdot n_1(\lambda)\cdot m\cdot d\frac{4\pi}{\lambda}\right)\right)\right) \tag{2.9}$$

Equation 2.9 can be rewritten to the form $a\cdot\sum_{m=0}^{\infty}(r)^m$ as shown below:

$$B = A_0\left(r_{01} + t_{10}r_{12}t_{01}\exp\left(i\cdot n_1(\lambda)\cdot d\frac{4\pi}{\lambda}\right)\cdot\sum_{m=0}^{\infty}\left(r_{10}r_{12}\exp\left(i\cdot n_1(\lambda)\cdot d\frac{4\pi}{\lambda}\right)\right)^m\right) \tag{2.10}$$

With the use of the infinite geometric series rule, equation 2.10 which can be seen as $a\cdot(r)^m$ can be rewritten to $\frac{a}{1-r}$ since $|r| < 1$. Besides the infinite geometric series rule, two other assumptions are made (see Appendix F for the derivations), $r_{10} = -r_{01}$ and $t_{10}t_{01} = 1 - r_{01}^2$ which all together results in the following equation for the reflectance simulation of an unsupported, non absorbing single thin film:

$$B = A_0\frac{r_{01} + r_{12}\exp\left(i\cdot n_1(\lambda)\cdot d\frac{4\pi}{\lambda}\right)}{1 + r_{01}r_{12}\exp\left(i\cdot n_1(\lambda)\cdot d\frac{4\pi}{\lambda}\right)} \tag{2.11}$$

$$R = |B|^2 \tag{2.12}$$

Here equation 2.12 shows the total reflectance from the layer.

At this point it is possible to simulate the reflectance spectrum of a single thin film as long as the surrounding materials can be assumed infinitely thick. One could also say that the equation is valid as long as it concerns an unsupported thin film. In this example a thin film of glass, in this case SiO_2 of thickness 30 µm is simulated. The simulation results are given in the form of the refractive index of the material for the simulated wavelength range (see figure 2.2a) and the reflectance spectrum (see figure 2.2b) which are shown together in figure 2.2. It is clear that bright and dark fringes are visible with a certain frequency according to the interference theory due to the phase term. The frequency that can be found in this reflectance spectrum will become important in section 2.4.1 where the frequency content of the reflectance spectrum will be used to determine the layer thickness. The simulation model that has been used to create the figures can be found in Appendix G.1.

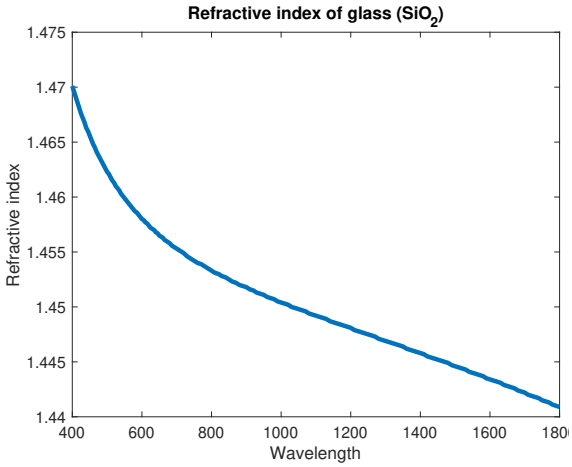

(a) Refractive index of the material [12].

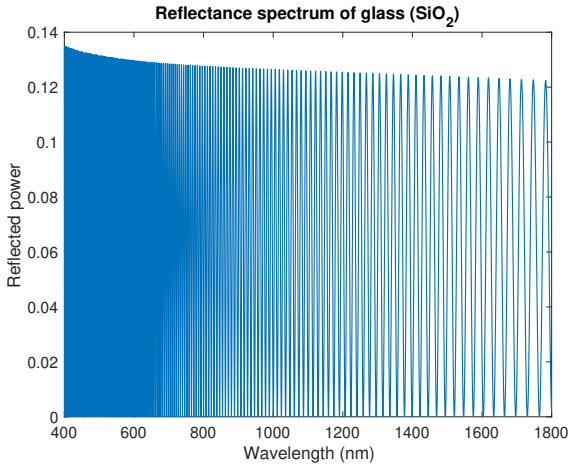

(b) Reflectance spectrum of the thin film with thickness 30 µm.

Figure 2.2: The simulation of a thin film of SiO_2 resulted in the following reflectance spectrum.

The thickness of the thin film can be determined from the reflectance spectrum with the use of the Fast Fourier Transform. This can be done due to the fact that the frequency content can be related to the thickness of the layer, refractive index of the material and the wavelength of the light. More on this in section 2.4.1. For now it is important to realise that the thickness determination is indirectly done from measuring a thin film. The first step is to measure the reflectance spectrum followed by postprocessing of the data and using Fast Fourier Transform technique which enable you to determine the thickness using the frequency content from the reflectance spectrum.

2.3. Multilayer simulation

In the previous section a method to simulate the reflectance spectrum of a single thin film has been discussed. This section covers a follow up which highlights a method that can be used to determine the reflectance spectrum of a stack of layers, often called a multilayer. The method used to determine the reflectance spectrum of a multilayer is referred to as the transfer matrix method. The transfer matrix method is an elegant method with characteristic matrices for each individual layer in the stack of coherent layers to account for all the individual reflections and transmissions that occur within the multilayer. One speaks of coherent layers when the combination of the resolution used to create the reflectance spectrum, the simulated wavelength range and the thicknesses of the layers result in a reflectance spectrum where the frequencies of the individual layers are fully resolved. This will be explained in more detail in Chapter 3. In order to find the total reflectance one needs to combine the individual characteristic matrices of the layers by multiplication of the matrices which results in the characteristic matrix of the multilayer.

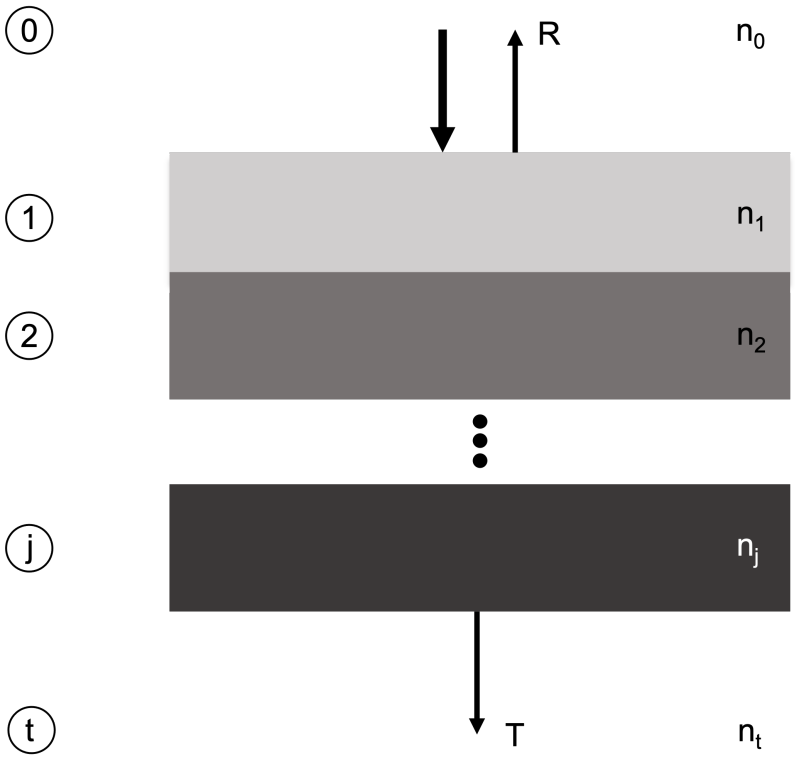

Figure 2.3: Overview of a stack of layers.

Polarization effects play a role when light interacts with a surface while traveling towards the surface at an angle relative to the normal of the surface. Light exists of electric and magnetic fields which are always perpendicular to each other. The polarization state of the light tells something about the propagation direction of those electric and magnetic fields before and after reflection on a surface. This gives two sets of Fresnel equations, one set for p-polarized light and one for s-polarized light. The p- and s-polarization is the typical sign convention that is used in optics. In this research the assumption is made that light travels normal to the surface (see figure 2.3). This allows for a simplification of the more general case since the angle dependency can be neglected. In other words, the polarization effects can be neglected. What follows is that both Fresnel equations for p- and s-polarization are identical. Another assumption must be made which is that the multilayer only contains coherent layers meaning that the thickness of the film is thin enough. If the layer becomes thicker one speaks of an incoherent layer which will be covered in more detail in chapter 3.

In Section 2.2 the total reflection on a single thin film is described as interference between reflection components at the different interfaces. This was including the internal reflection components (B_2 up to B_{m+1} in figure 2.1). With multiple layers, these individual internal reflection components are best taken into account with the use of a matrix method. For the case of a multilayer, it is assumed to consists of j coherent layers. Where each layer has characteristics such as layer thickness, material and refractive index, see figure 2.3. In order to calculate the total reflection that comes from the multilayer, equation 2.13 in combination with equations 2.14 and 2.15 can be used. Equation 2.13 shows the characteristic matrix for the jth layer in the multilayer. For this method, each layer will have a characteristic matrix which are then combined to get the transfer matrix of the multilayer. The transfer matrix (equation 2.14) is simply the product of the individual characteristic matrices. The transfer matrix elements are needed in the next step which shows the equation that is used for the reflectance of a multilayer [7, 25, 28, 29]. The characteristic matrix includes the refractive index n and thickness d of the jth layer but is also dependent on the wavelength λ of the lightsource:

$$M_j = \begin{pmatrix} \cos\left(\frac{2\pi}{\lambda} n_j(\lambda) d_j\right) & -\frac{i}{n_j(\lambda)} \sin\left(\frac{2\pi}{\lambda} n_j(\lambda) d_j\right) \\ -i n_j(\lambda) \sin\left(\frac{2\pi}{\lambda} n_j(\lambda) d_j\right) & \cos\left(\frac{2\pi}{\lambda} n_j(\lambda) d_j\right) \end{pmatrix} \tag{2.13}$$

$$T = \prod_{j=1}^{N} M_j \tag{2.14}$$

$$r = \frac{(T_{11} + n_t \cdot T_{12}) - \frac{1}{n_0}(T_{21} + n_t \cdot T_{22})}{(T_{11} + n_t \cdot T_{12}) + \frac{1}{n_0}(T_{21} + n_t \cdot T_{22})} \tag{2.15}$$

Equation 2.15 shows how the reflection of the multilayer is calculated. Where T_{ij} represent the individual transfer matrix elements, n_0 and n_t represent the refractive index of the incident and rear medium respectively (see figure 2.3). While the resulting reflectance from the multilayer is determined by the following equation:

$$R = |r|^2 \tag{2.16}$$

By using the described equations a simulation has been done for two coherent thin films from materials Acrylic and PET with thicknesses of 20 and 10 µm, respectively. For this simulation the incident and rear media are assumed to be air. The resulting reflectance spectrum can be seen in figure 2.4 which has been created with the help of the simulation model that can be found in Appendix G.2. In the reflectance spectrum two different frequencies are visible, each representing a layer. Important here is that the refractive indices are not identical over the measured wavelength range. In the section that follows a method will be presented to determine the thickness from reflectance spectra.

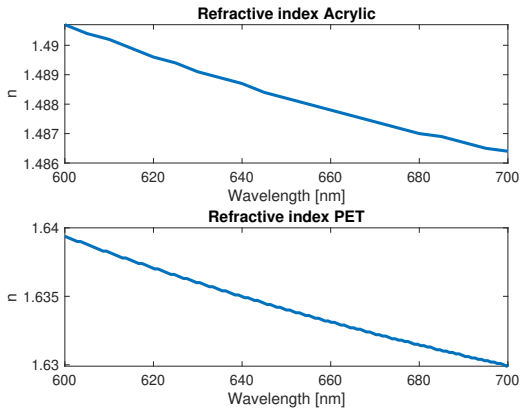

(a) Refractive indices of the two different materials [12].

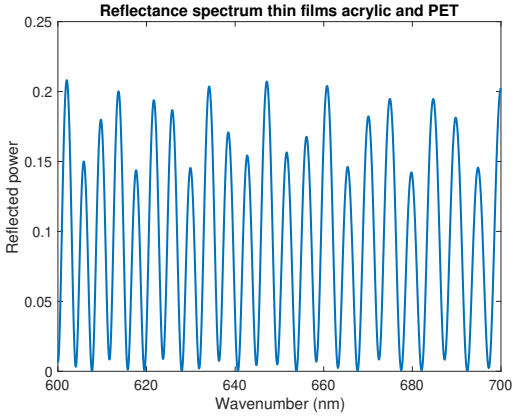

(b) Reflectance spectrum of the two thin films.

Figure 2.4: The simulation of two thin films of Acrylic and PET resulted in the following reflectance spectrum.

2.4. Thickness determination

At this stage it is possible to simulate reflectance spectra for both single thin films and multilayers that consist of coherent thin films. This section will look into how these reflectance spectra can be related to the layer thickness. One method is to calculate the frequency of the oscillation and relate that to a thickness this is done with the fast Fourier transform. Another method is the regression analysis, which simulates reflectance spectra for thin films in an attempt to fit it to a measured reflectance spectrum. The FFT method is often used for thicknesses as thin as approximately 1 µm. For film thicknesses below this, no complete periods are shown in the reflectance spectra, which will be explained in this section. For thin films thinner than that, regression analysis can be used instead. However, this research only focuses on the FFT method as that is sufficient for the thin film thicknesses that will be measured.

2.4.1. Single layer thickness determination

As mentioned before a reflectance spectrum usually contains an oscillating pattern. The pattern results from interference between reflections from the different interfaces of different materials. The oscillation can be used to determine the thickness of a thin film with the use of the fast Fourier transform (FFT). The FFT mathematically calculates the frequency of the oscillation. This frequency is then related to a film thickness. Let us take the example used in section 2.2, figure 2.2. See figure 2.5 here again.

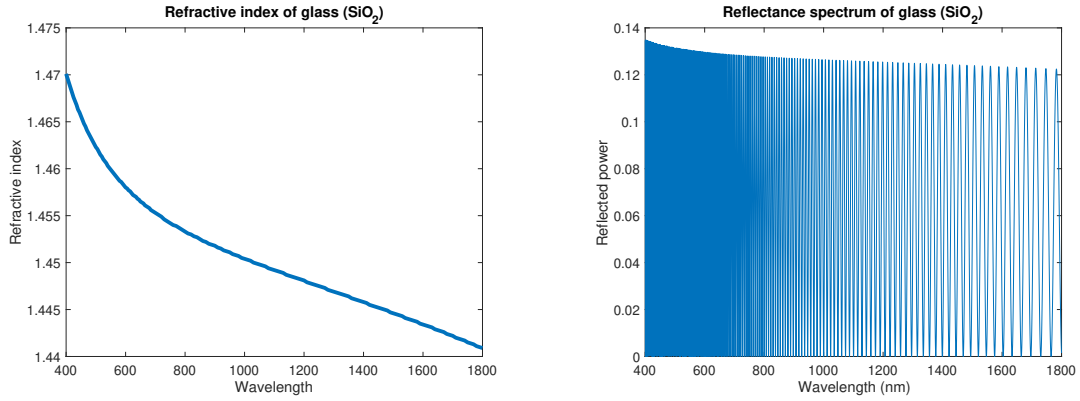

(a) Refractive index of the material [12].

(b) Reflectance spectrum of the thin film.

Figure 2.5: The simulation of a thin film of SiO_2 resulted in the following reflectance spectrum.

In order to determine a thickness from a reflectance spectrum, the FFT can be used. When a thin film with a certain thickness is simulated, an oscillation with a certain frequency will be visible in the reflectance spectrum. The FFT can used to mathematically determine this frequency. When the thickness of the thin film is lowered, the frequency decreases. The FFT requires at least a full period in the reflectance spectrum in order to determine a frequency. Once the thickness of a thin film is lowered to such an extend that less than a full period is visible, the FFT will no longer be able to determine a frequency. This means that the thickness will no longer be measurable with the FFT. This characterizes a minimal thickness limit of the spectral reflectance thickness measurement in combination with the FFT. On the other hand, when the thickness of the layer is increased, the frequency of the signal will increase. At some point the resolution used will not be high enough to measure the oscillation effectively. This characterizes a maximal thickness limit. A more detailed explanation of the mentioned limits of this method will be given in chapter 3, for now it is important to realize that these limits exist.

Before the FFT can be used on the reflectance spectrum simulated data, a couple of steps need to be taken first. By looking at the reflectance spectrum as shown in figure 2.5 it can be seen that the distance between the peaks and valleys increases for increasing wavelength, it is an aperiodic signal. This is due to the fact that $\frac{1}{\lambda}$ is included in the method used to create this reflectance spectrum (see equation 2.11) while the reflection is plotted versus λ. In order to make the signal periodic it needs to be plotted versus the wavenumber $v = \frac{1}{\lambda}$ instead, see figure 2.6. This is necessary before the FFT can recognize and determine a frequency from the signal [26].

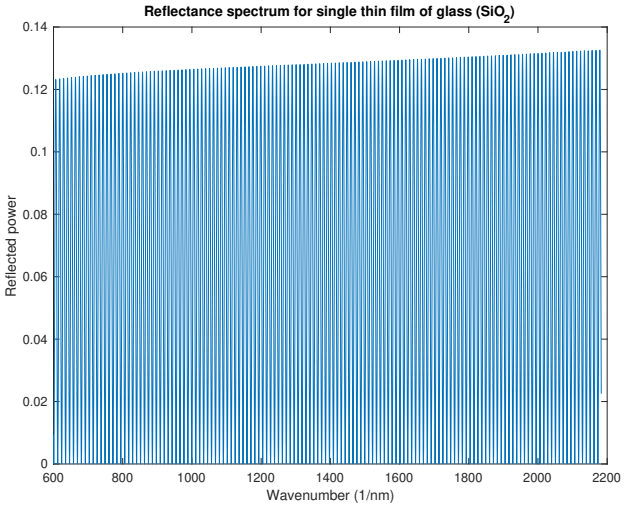

Figure 2.6: The reflectance spectrum plotted versus the wavenumber.

From here we can relate the reflectance data to the layer thickness with equation 2.17. Here the optical thickness t is determined with the FFT which is related to the geometrical thickness directly by multiplying the geometrical thickness with the refractive index of the layer (t is equal to $d_{\mathrm{FFT}} \cdot n$).

$$d_{\mathrm{FFT}} = \frac{m}{2 \cdot n \cdot (v_{\max} - v_{\min})} \tag{2.17}$$

In equation 2.17 m is the resulting frequency content from the periodic signal that follows directly from using the FFT. However, it has yet to be related to the layer thickness [25]. In the same equation, n is the refractive index of the layer, $v_{\max}$ and $v_{\min}$ is the measured wavenumber range of the dataset (either set manually when simulating or by the used spectrometer when doing measurements). The refractive index and wavenumber range are used to relate the frequency content of the periodic signal to a thickness. The way it is used in the simulation can be seen in Appendix G where a matlab code has been included.

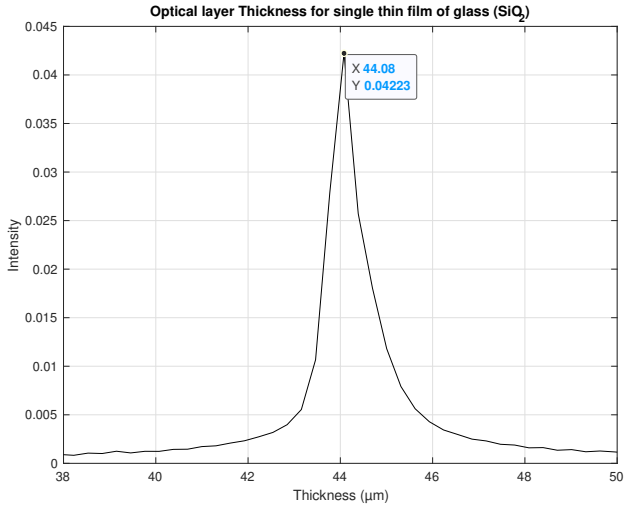

Figure 2.7: Example of a Fast Fourier Transform (FFT) calculation resulting in an optical thickness.

As an example let us have a look at the FFT result that follows from the situation with a single layer with thickness 30 μm of SiO_2 as simulated in figure 2.5. This results in the optical layer thickness graph as shown in figure 2.7. It can be seen that the optical layer thickness t is equal to 44.08 μm. In order to

find the geometrical thickness one has to divide by the refractive index from the material of the layer, in this case SiO_2. The refractive index is between roughly 1.465 at lower wavelength ranges and 1.441 at higher wavelength ranges (see figure 2.5a). By using the average refractive index over this range it results in a thickness determination as follows: $d_{\mathrm{FFT}} = \frac{44.08}{1.453}$ = 30.34 µm which has an error of 1.13% when compared to the thickness of 30 µm that was used for the simulation.

2.4.2. Multilayer thickness determination

The next step is to use the FFT method for a multilayer. The simulation result from section 2.3 is used to describe how the FFT can be utilized in the case of a multilayer simulation to determine the thicknesses from the reflectance spectrum (figure 2.4). The same figure is shown below here again.

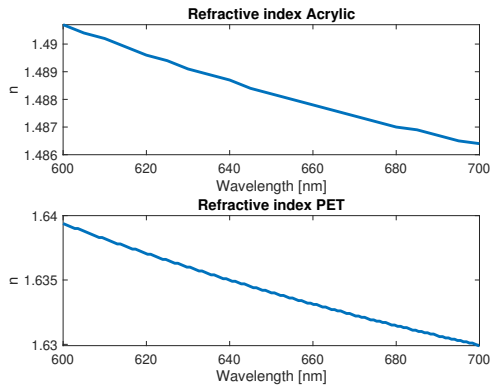

(a) Refractive indices of the two different materials [12].

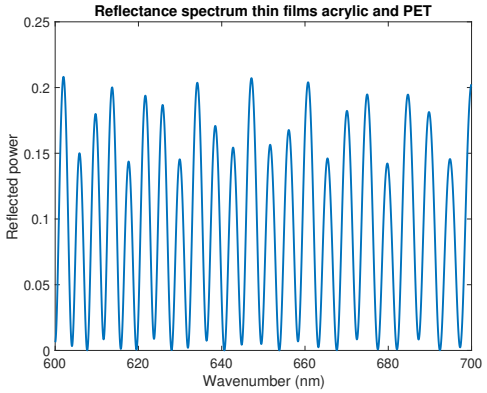

(b) Reflectance spectrum of the two thin films.

Figure 2.8: The simulation of two thin films of Acrylic and PET resulted in the following reflectance spectrum.

Again it is important to realize that the FFT from the reflectance spectrum calculates the optical thickness. Which means that the refractive indices of the materials need to be used in order to calculate the geometrical thicknesses. When one is dealing with a multilayer simulation it means that the reflectance spectrum contains multiple frequencies. The FFT method is then used to retrieve these different frequencies. The multilayer used here as an example contains interference patterns (frequencies) of both a 20 µm and 10 µm Acrylic and PET thin film. The average refractive indices of Acrylic and PET over simulated wavelength range are n_{acrylic} = 1.489 and n_{PET} = 1.634 respectively (see figure 2.8a).

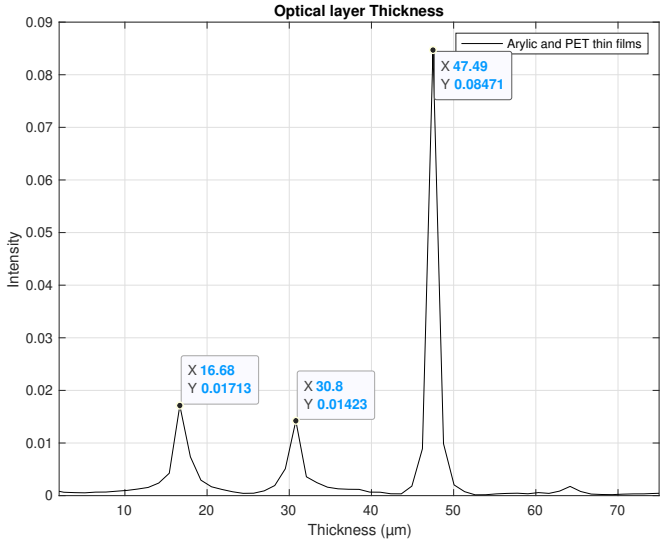

Figure 2.9: The FFT result for the two thin film simulation.

In figure 2.9 multiple peaks are visible. There are two individual layers so at least two peaks are expected resulting from those two layer thicknesses. From the Acrylic layer which is 20 µm thick, it is expected that the optical thickness peak is around $t_{\text{acrylic}} = n_{\text{acrylic}} \cdot d_{\text{acrylic}}$ = 1.489 · 20 µm = 29.78 µm. From the PET layer which is 10 µm, it is expected that the optical thickness peak is around $t_{\text{PET}} = n_{\text{PET}} \cdot d_{\text{PET}}$ = 1.634 · 10 µm = 16.34 µm. While having an error margin, those two peaks show up. However, a third peak is visible in the FFT result. This peak is a combination of the two individual layers which combines the optical thickness of both layers and is irrelevant in the thickness determination of the simulated layers.

It is important to realize that when using the FFT of a reflectance spectrum to determine thin film thicknesses, one must have certain information about the layers that are measured. First of all, the refractive indices over the measured wavelength range. Secondly, it is required to know to some extent what the thicknesses of the layers are when measuring a multilayer. In the above example the optical thickness peak of the thicker layer was placed after the optical thickness peak of the thinner layer. However, there are scenarios possible where this is not the case. Take for example a scenario where refractive indices have a huge difference. Where the thinnest film of the two layers has a refractive index which is much higher than the refractive index of the least thin film of the two layers. In this scenario it is theoretically possible that the optical thickness peak of the thinnest film of the two layers is placed after the optical thickness peak of the least thin film. Peak recognizing can become quite difficult when measuring multilayers where too many unknowns exist such as completely unknown thicknesses.

Another issue may arise when optical thicknesses of different layers are roughly the same and therefore overlap in the FFT result. This will make it rather difficult to recognize the individual thicknesses. Take for example the scenario where you have two thin films of d_1 = 15 µm and d_2 = 20 µm with average refractive indices over the measured wavelength range n_1 = 1.67 and n_2 = 1.25. Both optical thicknesses will be roughly 25 meaning that the optical thickness peaks will overlap. The overlapping can make the resulting FFT quite confusing when determining the thin film thicknesses.

Another scenario is where thin films from certain materials with refractive indices that have a small difference to no difference at all. As the difference in refractive indices between the two materials becomes smaller there is a certain point where determining the thicknesses can become impractical or not even possible anymore. This subject will be discussed in more detail in chapter 3.

As shown in the example of the two thin films, three peaks were visible in the FFT result. A peak for both layers and a peak for the combined thickness. The next thing to realize is that for three layers, even more peaks will be displayed in the FFT result. Since there are three layers in that scenario there will be three peaks visible for the individual layers. But also a peak for the combination of layer 1 and layer 2, as well as a peak for the combination of layer 1 and layer 3, a peak for the combination of layer 2 and layer 3 and finally a peak for the all layers combined resulting in 7 individual peaks. Clearly the more layers included in the measurement, the more advanced the peak recognition step becomes, especially when the thicknesses are completely unknown for all layers.

2.4.3. Accuracy of thickness determination

Even though the Fast Fourier Transform method allows us to determine thicknesses from the interference patterns of layers, the method is not perfect and brings errors for a number of reasons.

For starters, when a reflectance spectrum of a single thin film is taken, a certain frequency is visible. Depending on where the reflectance spectrum starts and ends in the oscillation, a symmetrical peak will or will not show up in the FFT result. In some cases, there may not even be a peak at all. In order to get the most accurate result, the FFT must begin and end measuring at the same point in the oscillation so that only complete periods are measured. This creates a symmetrical peak. An example of how to do this is shown in figure 2.10 with the green dotted lines in the reflectance spectrum of an arbitrary thin film simulation. It can be achieved with a window function or by manually adjusting the limits of the wavelength range. A symmetrical peak is desired as it ensures the smallest possible error due to this problem which is referred to as spectral leakage [22]. When the FFT begins the measurement at

the bottom of an oscillation and ends at the top of an oscillation, an error occurs. This error is due to the peak of the FFT being tilted towards either the left or right side meaning that there will no longer be a symmetrical peak. This spectral leakage error can be minimized by windowing the reflectance data. This has been done manually to achieve the smallest possible leakage error contributing to the results for the remainder of this research. Two examples of a peak being tilted and one without a clear peak are shown in figure 2.11. Where both examples have been simulated with almost the same wavelength range but starting at an insignificant higher or lower wavelength. This shows that the smallest shift in wavelength range (shifting either one of the green lines in figure 2.10 slightly to the left or the right), can already contribute to this error either by tilting the peak or not showing a clear peak at all.

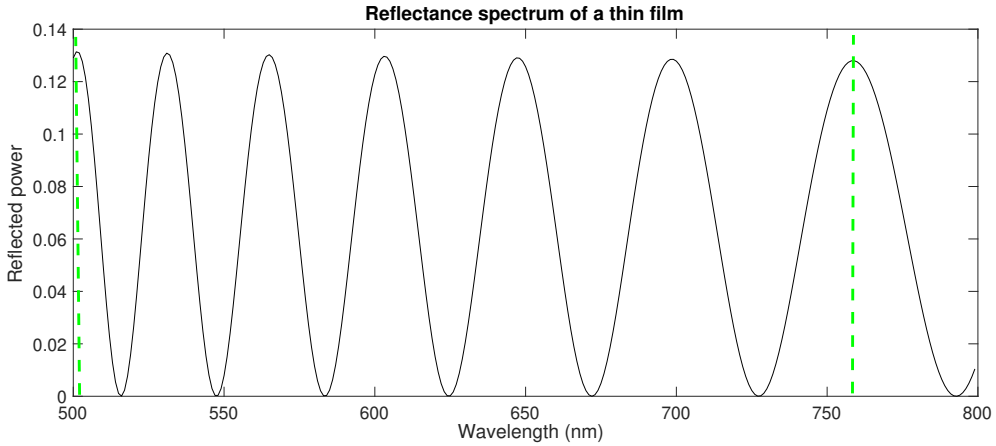

Figure 2.10: Windowing the signal to minimize spectral leakage errors.

Another contribution to the total error can originate from the fact that one works with a limited resolution on the measurement equipment. When simulating, there are no limits to the resolution. However, when doing practical measurements, one usually works with a spectrometer (this will be explained in more detail in chapter 4). A spectrometer has a fixed resolution which in some cases can be adjusted by replacing hardware. One might not always have the possibility to use the preferred resolution which can result in a measurement error. The thicker the layer becomes, the higher the frequency in the oscillation. As the layer becomes thicker, a higher resolution is needed which ensures that enough points are measured to display the correct oscillation pattern in the reflectance spectrum. If the resolution is insufficiently low, meaning that not enough points are measured, an error may occur since the wrong oscillation pattern will show up in the reflectance spectrum.

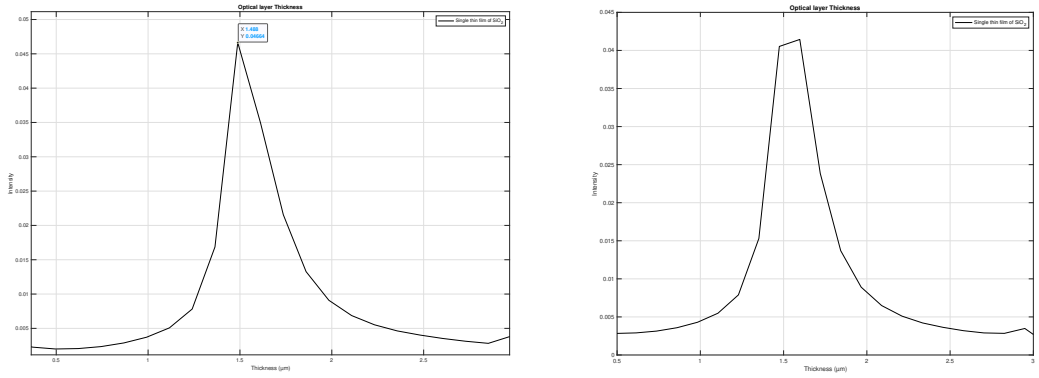

(a) Tilted peak

(b) No clear peak

Figure 2.11: Due to leakage, the FFT may not result in a symmetrical peak or in some cases not even a peak at all.

Another source of error can be due to the fact that the wavelength range is limited. Again in simulating there is not really any limit since any arbitrary large wavelength range can be used. While in reality one often has to deal with a light source that has a fixed wavelength range or a spectrometer that can only measure a part of that wavelength range. The FFT is often used in engineering applications where a time signal is plotted versus displacement. In these examples, frequencies are measured with relatively great amount of periods compared to the optical application in this research. The higher the number of periods in a signal, the sharper the peak will be. If the number of periods in a signal is limited, the error will be larger.

A final contribution to the error of the FFT can be due to the fact that an average value of the refractive index is used to translate the optical thickness result from the FFT into a geometrical thickness. When the refractive index has a huge slope in the measure wavelength range, the average refractive index may not be an accurate way to determine the geometrical thickness.

3

Spectral Reflectance Approach

3.1. Multilayer approach

The previous chapter described the theoretical model that can be used to simulate a thin film as well as a multilayer of thin films. This chapter will now come up with concrete steps that one needs to go through in order to simulate the preferred multilayer as described in the thesis objective. This multilayer consists of two thin films and one of these thin films is a liquid. The two thin films are between two thicker layers. The steps include the simulation of coherent thin films, the simulation of thick incoherent films, the influence of difference in refractive index between layers and finally a specific multilayer scenario is simulated. All steps have been done with the use of the simulation model that can be found in Appendix G.

3.1.1. Thin film simulation

By dividing the multilayer up into single layers first and finding out what is needed to measure these layers on their own one gets a better understanding of how to measure the multilayer. In this section the focus will be on simulations to try and find where the limits of this method lie in the case of simulating single thin films.

The thickness of both thin films in the multilayer are between 1 and 10 µm. To start with, a simulation is done for a thin film of glass from material SiO_2 that is surrounded by air. The thickness is assumed to be 10 µm and then gradually lowered to 5 µm, then 1 µm and finally 0.5 µm to find out how the layer thickness influences the oscillation. Figure 3.1 shows the reflectance spectra for the four individual thicknesses. Where the wavelength range has been set between 400 and 1000 nm. The lower limit has been set to 400 nm since this is where the UV light range begins. The liquid thin film within the multilayer is from acrylic and will become cured when being exposed to UV light. This thesis focusses on measuring the thickness while this layer is still a liquid and therefore limits the use of wavelength ranges below that number. The upper limit is more of an arbitrary number and can be higher depending on the type of light source that is used and the capabilities of the spectrometer. Besides choosing a wavelength range for the simulation, one also needs to think about the resolution that is used. The resolution tells you how many data points will be measured within the wavelength range and is a specification that comes from the spectrometer. For this simulation, a resolution of 1.4 nm has been used. This resolution has been used since that is the resolution from a spectrometer that is available which will be highlighted in chapter 4.

In the reflectance spectrum for 10 µm a relatively high frequency can be recognized. As the wavelength increases, the distance between the peaks increases as discussed in the previous chapter. By looking at the lower wavelength range, a unusual pattern is seen. This is due to the fact that there are too many peaks and valleys in the signal to properly display with the used resolution. If it is desired to perfectly display it in the lower wavelength range, one needs to increase the number of data points measured by increasing the resolution. Another solution is to move towards higher wavelength ranges. However, in this case there is more than enough available signal within the given wavelength range to determine the thickness with the FFT method.

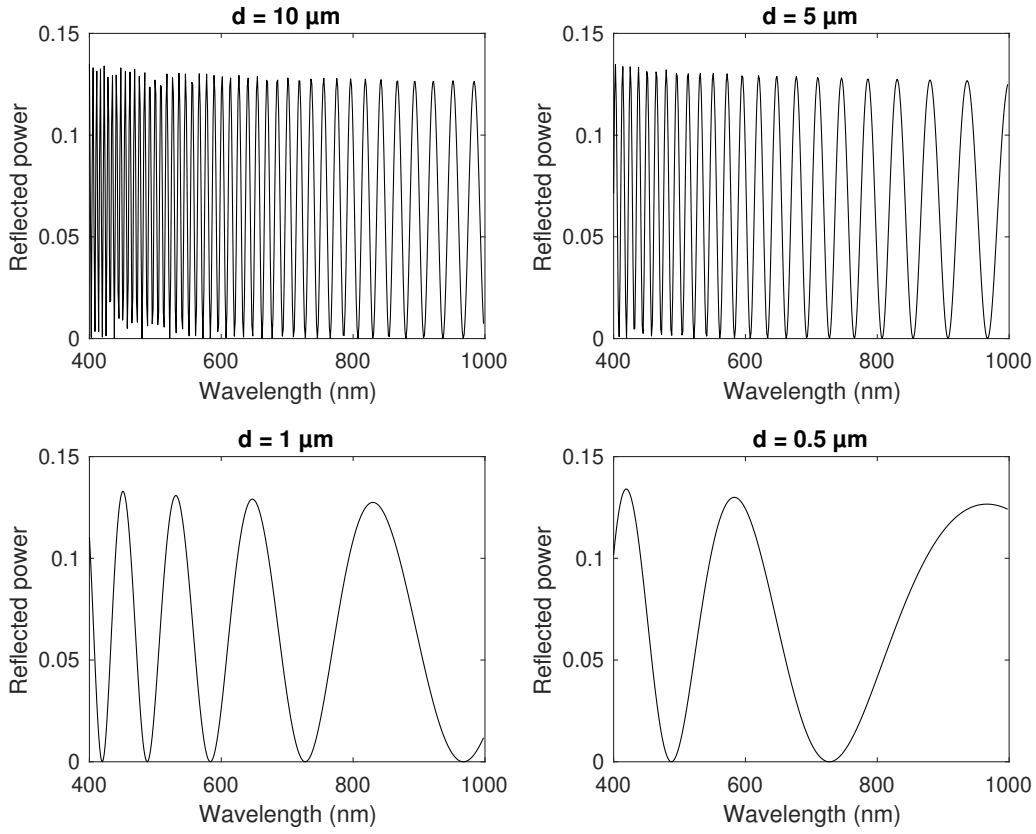

Figure 3.1: The reflectance spectra for four different thicknesses.

When the thickness is decreased from 10 to 5 µm, it can be seen that the frequency of the signal is lower. One could also say that less periods are visible within the same wavelength range. However, still more than enough signal is displayed which still enables one to use the FFT to determine the thickness. A further decrease in thickness brings us to 1 µm and yet again the frequency is lowered. Followed by decreasing the thickness even further to 0.5 µm. Even though the frequency of the signal is again lowered, in both cases there are still at least two peaks visible meaning that there is at least one period available to measure the thickness with FFT. However, as you can imagine, by further decreasing the thickness, at some point there will no longer be a full period of the oscillation visible within the reflectance spectrum. Once there is no longer a full period within the signal, it means that a limit of the spectral reflectance measurement method is reached. The measurement method is in this case limited by a minimal thickness that can be measured. This limit is due to the fact the FFT will no longer be able to determine a frequency from the signal at that point.

To show the lower limit, an even thinner film is simulated, in this case to 0.4 µm. In this example the frequency is lowered to such an extend that barely one full period is visible within this wavelength range. Further decreasing of the thickness will mean that less than one full period will be displayed within this wavelength. Therefore is means that this is where the lower limit of thickness for this specific scenario with the given conditions reached. Without a full period of signal, the FFT will no longer be able to extract a frequency and hence the thickness will not be measurable. The minimum thickness for a given wavelength range and refractive index of a material can be determined with equation 3.1 [25] and is equal to roughly 0.22 µm in the case of the thin film SiO_2 with the given wavelength range between 400 and 1000 nm.

$$d_{min} = \frac{1}{2 \cdot ((n(\lambda_{min})/\lambda_{min}) - (n(\lambda_{max})/\lambda_{max})} \tag{3.1}$$

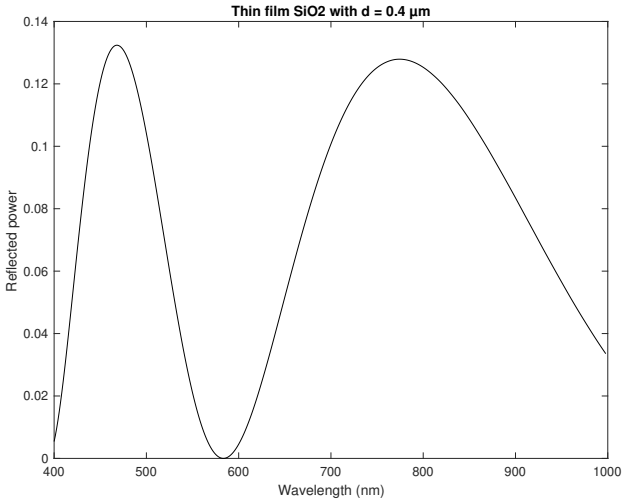

Figure 3.2: Reflectance spectrum for the minimal thickness showing the limits of the FFT.

3.1.2. Incoherent layer simulation

This section will attempt to give a better understanding of how thicker layers can be simulated. It is now known that when the thickness decreases, the frequency of the signal in the reflectance spectrum is lowered. The inverse is also true, when increasing the thickness, the frequency of the signal increases. In the case where the thickness was 10 µm (figure 3.1) relatively many periods were visible in the reflectance spectrum. In order to correctly show (fully resolve) the signal one needs a minimum resolution. If the resolution is not high enough, so when not enough data points are measured (or calculated in case of simulating) the reflectance spectrum will not be able to show the correct signal in the reflectance spectrum. When this happens, a signal in the reflectance spectrum is not fully resolved. This means that the limit for relatively thick layers depends on what wavelength range and what resolution is used. Shifting to the left or right in the wavelength range also influences the number of peaks and valleys as described previously [21].

For the case where the thickness of a layer becomes relatively large, while the resolution is not sufficiently high enough, no frequency will be measured at all. This is because there will be an extreme amount of peaks and valleys in the signal. With the relatively low resolution, not enough data points are measured to show the correct oscillating pattern in the reflectance spectrum. When one takes such a thick layer in combination with a relatively low resolution the signal is said to be non resolvable. If it is desired to retrieve the frequency from the reflectance spectrum with the FFT, one needs to increase the resolution. By doing this, the correct oscillation can be plotted in the reflectance spectrum. In some cases it might not be desired to show a fully resolved signal.

When a layer is sufficiently thick compared to the used wavelength range and resolution a layer can be seen as an incoherent layer. This means that a simplification can be made in the method used to simulate the reflectance spectrum. The case of incoherent layers will be further explained in section 3.2. With thin films, the expression for the total reflectance is achieved by superposition of the reflections including their phase factor. This phase factor in particular is responsible for the interference pattern see equation 2.11). As discussed, when a incoherently thick layer is assumed, the phase factor may be neglected. A result of this simplification in the method is shown in a reflectance spectrum (figure 3.3) for a relatively thick substrate of SiO_2 with thickness 500 µm while using a wavelength range of 200 up to 1200 nm and a resolution of again 1.4 nm.

The below figure shows the simulation of a incoherently thick layer. This assumption is made due to the combination of resolution, layer thickness and wavelength range used for the simulation. It means that there is no longer a frequency in the signal. Since there is no longer a frequency in the signal it means that the reflectance of a thick, incoherent layer will no longer influence the frequency content in the reflectance spectrum once such a layer is included in a multilayer with a thin film. When equation 2.11 is used and the phase factor is ignored in case of incoherently thick layers, it means that the reflection is a function of the Fresnel equations. This means that the total reflected power is a function of the refractive index of the material. For the material glass which is used in the simulation in figure 3.3, one can see that the reflected power decreases as wavelength increases. This is directly correlated with the refractive index of glass (see figure 2.5a).

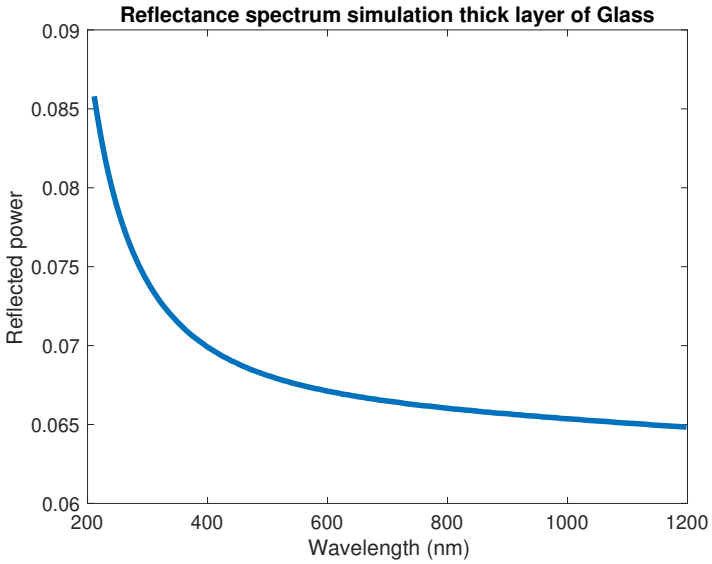

Figure 3.3: Reflectance spectrum for an incoherently thick layer.

An attempt has been made to approximate when a layer can be considered incoherent which allows for the simplified method and essentially allows one to ignore that layer in a multilayer simulation [29]. The equation that describes the minimal thickness for this approximation:

$$d_{\text{incoherent}} > \frac{\lambda^2}{2\pi n \Delta\lambda} \tag{3.2}$$

Equation 3.2 shows what the minimal thickness ($d_{\text{incoherent}}$) has to be before one can make the assumption of incoherent layer and neglect the phase factor while simulating the reflectance spectrum. In this equation, the wavelength λ in the signal, the refractive index n of the material and the resolution $\Delta\lambda$ are used. When using equation 3.2 it makes sense that the minimum thickness is correlated to the resolution. As described, while the resolution is lowered (less data points in the wavelength range are measured), the resolution value goes up and consequentially the minimal thickness is lowered. Meaning that by decreasing the resolution, a layer can be treated as incoherent with decreasing layer thickness.

3.1.3. Influence of difference in refractive index between layers

By now, both the limits for thin film as well as for incoherently thick layer simulations have been defined and illustrated. However, there is another subject that has to covered before the single layers can be combined into a multilayer.

Assume a single thin film surrounded by the material SiO_2 in both incident and rear media (which is assumed to be infinitely thick). Depending on how thick the thin film is there will be an oscillation with a certain frequency when reflectance is measured. However, besides a frequency, the signal will also contain a certain amplitude. The amplitude is related to the difference in refractive index between the surrounding media and the refractive index of the thin film. The bigger the absolute difference between the refractive indices is, the larger the amplitude becomes and vice versa.

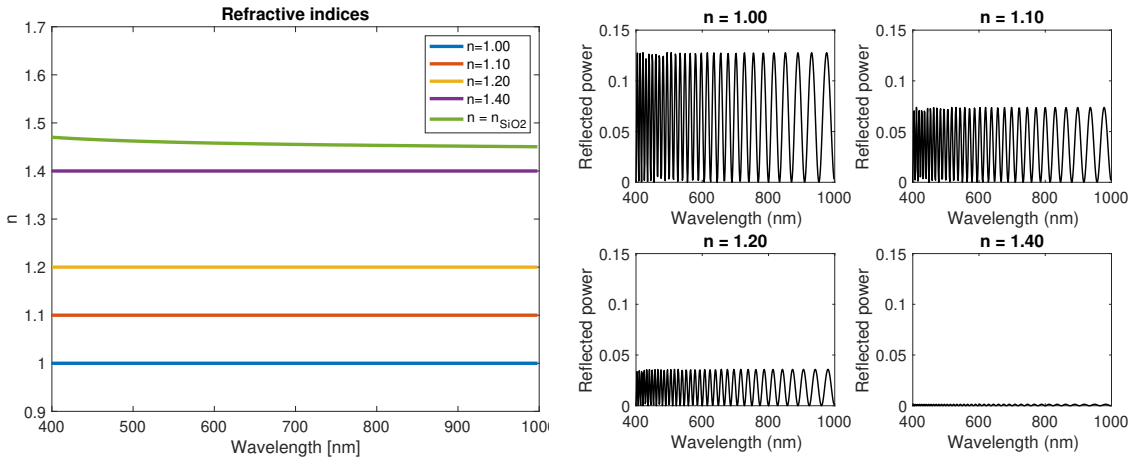

(a) Refractive indices [12, 27].

(b) Reflectance spectra.

Figure 3.4: The simulation of a thin film with constant refractive indices step by step getting closer to SiO_2 (green line).

The relation between difference of refractive indices and amplitude of the signal is visible in figure 3.4. Figure 3.4a shows the refractive indices for the surrounding material SiO_2 and for four different materials for the thin film. For the thin film, arbitrary constant refractive indices have been used. These refractive indices step by step come closer to the refractive index of the surrounding material (n=1.00, n=1.10, n=1.20, n=1.40). For the described situation with a thin film surrounded by glass, four different scenarios have been simulated in figure 3.4b. In this figure, the relation between the amplitude of the signal and the difference in refractive index is shown. For all four of the sub figures, the same surrounding material (SiO_2) is used. For the thin film in between, the four different constant refractive indices have been used. On the top left, a material with arbitrary constant refractive index of 1.00 is assumed for the thin film. On the top right, the thin film is changed to a material with refractive index of 1.10, meaning that the gap between the refractive indices of the surrounding and thin film material is decreasing. For the bottom left figure, the thin film has refractive index of 1.20 and the bottom right 1.40. The effect on the amplitude is clearly seen with the biggest amplitude when the layers have the largest refractive index gap which can be seen on the top left (n_{SiO_2}-$n_{1.00}$) and then step by step decreasing amplitude as the refractive index gap decreases with the smallest amplitude for n_{SiO_2}-$n_{1.40}$ on the bottom right. This effect can be explained with the equation for the reflection on thin films (equation 2.11), which is related to the reflection coefficients (Fresnel equations 2.1). Where the reflection coefficients are calculated based on difference in refractive index.

In theory, while the amplitude decreases significantly when the refractive index difference becomes smaller, one can still determine a thickness since the frequency content remains unchanged. However, this is only true for simulations without noise in the signal. In reality, one often has to deal with a noise in the signal. As the difference in refractive index decreases, the amplitude at some point may be of the same order of magnitude as the noise in the signal. As the amplitude/noise ratio nears one, it will no longer be possible to determine the thickness which is another limit of this method.

3.2. Modelling of specific multilayer scenario

Coming back to the figure shown in Chapter 1 concerning the multilayer structure (figure 1.6) we know that we are dealing with four individual layers. From these layers, it is known that the bottom and top layers are relatively thick, while the other two layers are thin films of comparable thickness. The thin films have different refractive indices while one of the layers is cured acrylic and the other one is water. The thickness of the thicker layers are both 500 µm while the thinner layers will 10 and 15 µm for water and cured acrylic respectively. The structure of the multilayer including the materials, refractive indices and thicknesses is shown in figure 3.5. The multilayer that was shown in the initial research objective contained a layer of liquid acrylic which has been replaced by water since the liquid acrylic is not a straight forward material to perform multiple tests with since contact of the liquid with human skin is not preferred. However the situation is comparable since it is still dealing with a liquid thin film that is non-absorbing and transparent. Besides the thin film, the thick stamp is also assumed to be glass instead of PET foil. This assumption was also made for the ease of testing. Similar to the thin film, is the stamp material also non-absorbing and transparent and therefore does not change the situation in an important way.

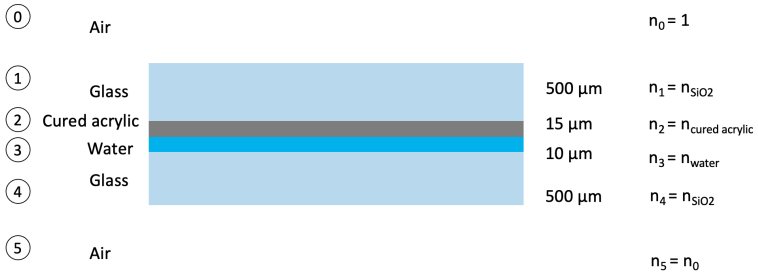

Figure 3.5: Structure of the multilayer.

In order to measure the multilayer as a whole, it is useful to approach the situation step by step. This can be done by individually simulating the layers so that one can determine the necessary settings for the equipment that is needed to conduct the measurements. One obvious setting that has to be determined is the wavelength range of the light source that will be used as discussed in Chapter 2. Besides this, the spectrometer that measures the reflection of the light will be included in the measurement setup. It will be important to figure out what the resolution requirement of this spectrometer should be. This will be approached by looking at reflectance spectra for the individual layers initially and later on combining the individual reflectance spectra to find a way to measure the layers all together with a possible set of settings.

Let us start by simulating the reflection of light with normal incidence onto a thin film of water with a thickness of 10 µm surrounded by air (unsupported) and see what the result of the reflectance spectrum is. A sketch of this situation is shown in figure 3.6. While this is not a situation that can be created in reality, the simulation does give important insights for this research. By picking a wavelength range for the simulated light source and a resolution of the spectrometer we can recreate the expected signal. The first step is to get a sense of the bigger picture spectrum. For a wavelength range between 450 upto 1000 nm and a resolution of 1.4 nm the following reflectance spectrum results from the simulation, see figure 3.7.

Figure 3.6: Structure of the multilayer.

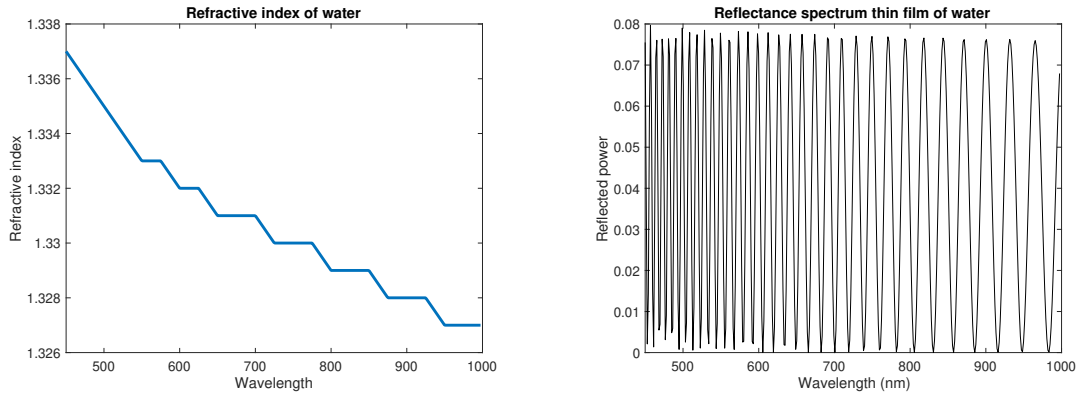

(a) Refractive index of the material [27].

(b) Reflectance spectrum of the thin film.

Figure 3.7: Refractive index of water and reflectance spectrum of a 10 µm thin film of water.

Clearly there is a frequency visible in the signal. Besides this, it is also clear that in the higher wavelength range (rightside of the spectrum) the signal is well developed where as the lower wavelength range (leftside) shows irregularities in the oscillations. On the left of the spectrum the wavelength is lower which means that more waves fit in between the given thickness and therefore more fringes should be visible. In order to measure the signal, enough individual data points need to be measured. This means that we need a higher resolution on the lower wavelength range in this example with the given thickness. Once the resolution is lowered it will result in the signal not being fully resolved and starts creating errors in determining the frequency content of the true signal. On the other hand, if the signal is fully resolved, further increasing the resolution will no longer have an influence. Another solution to measure a fully resolved signal in this wavelength range would be to lower the thickness of the layer as that would result in less periods in the signal and therefore a lower resolution would suffice to measure a fully developed signal. But since the thickness is a given that is not an option. The way to achieve a fully resolved signal is to shift further into higher wavelength ranges. Doing this will also cause the signal to have less periods which will be measurable with the resolution that is too low for the lower wavelength ranges. However, the wavelength range is limited by the lightsource.

The next step is to create the reflectance spectrum with similar condition for a thick layer of glass (which we take the material $\mathrm{SiO_2}$ for) with a thickness of 500 µm. This means that we are dealing with a layer that is significantly thicker than the previous layer, see figure 3.8.

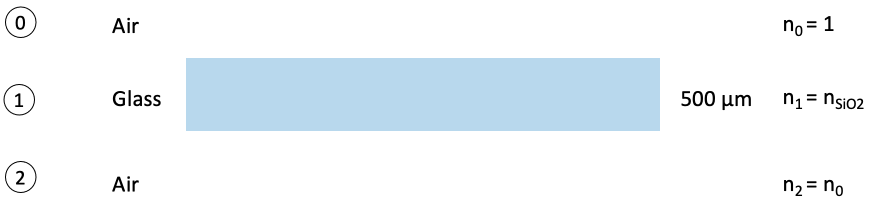

Figure 3.8: Sketch of the thick layer of glass.

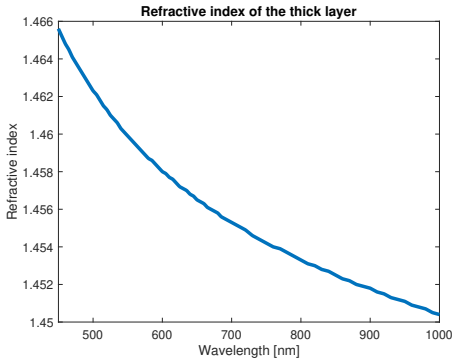

(a) Refractive index of the material [12].

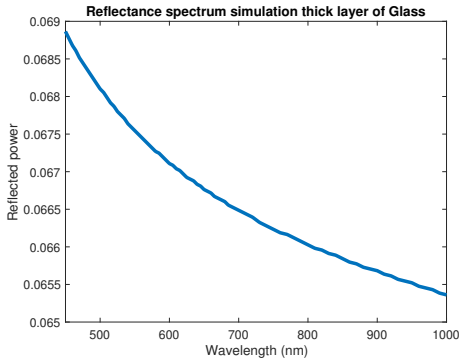

(b) Reflectance spectrum of the thick layer.

Figure 3.9: Refractive index and reflectance spectrum of a thick layer of glass.

As previously discussed the assumption can be made that it concerns an incoherently thick layer. Meaning that the signal consists of an excessive amount of periods in combination with the used resolution. This will not allow to achieve a fully resolved signal. Since the same resolution is used as before (1.4 nm) we are not able to measure all those individual periods accurately. This allows for the simplification (as discussed in Chapter 2) of the simulation method and leaves out the interference pattern. The result can be seen in figure 3.9. Since there will be no interference pattern, there is no frequency content in the reflectance spectrum of this thick layer.

To prove the point that has been made, it makes sense to show the reflectance spectrum for the thick layer but with a significantly higher resolution, see figure 3.10. Since it concerns a rather thick layer there will be an extreme amount of periods within the same wavelength range compared to the reflectance spectrum for the much thinner layer. However, since we significantly increased the resolution, the signal is now fully resolved within the same wavelength range which is shown in figure 3.10a. In the figure, a black shape can be seen since there are too many periods which makes it difficult to read the signal. Therefore, instead of looking at the entire wavelength range, only part of the wavelength range is shown from 980 to 1000 nm, see figure 3.10b. Right now we can see a similar amount of periods compared to the reflectance spectrum of the thin film on the entire wavelength range of 450 up to 1000 nm. By now it is clear that with a significant increase in resolution, one can change a incoherently thick layer that is not fully resolved to a coherent layer making the frequency content show up in the reflectance spectrum. However, it makes the task of measuring a multilayer easier if there are less layers that influence the frequency content.

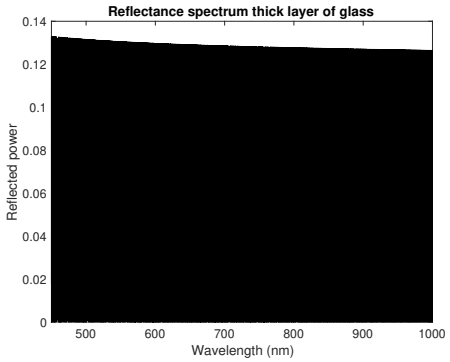

(a) Reflectance spectrum entire wavelength range.

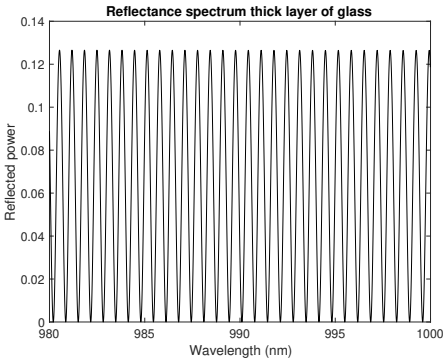

(b) Reflectance spectrum small part of wavelength range.

Figure 3.10: Reflectance spectrum of thick layer with both the entire and part of the wavelength range

It can be concluded that thicker layers can simply not be measured if the resolution of the spectrometer is not high enough for a given wavelength range. This is because the frequency of the signal will be too high. Meaning that if the thin film that is being measured, is on top of a thick enough substrate, one will not be able to measure any frequency content of the thick layer if a low enough resolution is used. While at the same time one can measure the thin film with that same resolution. This means that the incoherently thick layer can be ignored while measuring the thickness of thin films. Though, one has to be certain that the combination of wavelength range, layer thickness and used resolution, allows for the assumption that the thick layer is incoherent.

Continuing with the second thin film which is a cured acrylic thin film of thickness 15 µm while surrounded by air, see figure 3.11. The reflectance spectrum of this layer while using the same wavelength range of 450 up to 1000 nm and the same resolution of 1.4 nm gives the result as can be seen in figure 3.12. The reflectance spectrum shows a properly developed signal that can be used with the FFT method to determine a thickness. So the combination of resolution and wavelength range are valid for this thin film.

Figure 3.11: Sketch of the thin film of cured acrylic.

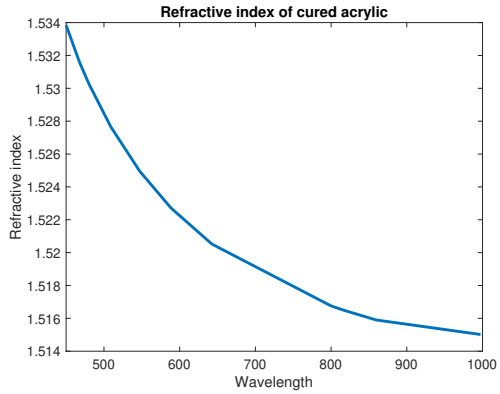

(a) Refractive index of the material (data measured on material from and by Morphotonics).

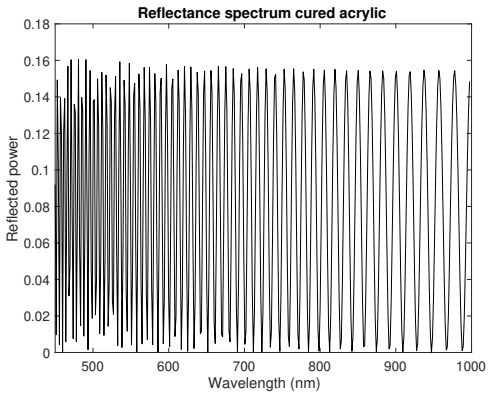

(b) Reflectance spectrum of the thin film.

Figure 3.12: Refractive index of water and reflectance spectrum of a 15 µm thin film of cured acrylic.

The next step is to combine the two thin films in one simulation. The situation sketched in figure 3.13 is simulated. To begin with, the simulation is done with surrounding media of air of which the reflectance spectra and refractive indices can be seen in figure 3.14. As has already been proven, the frequencies of both layers are fully resolved within the signal and will be measurable with the FFT technique.

Figure 3.13: Multilayer while surrounded by air.

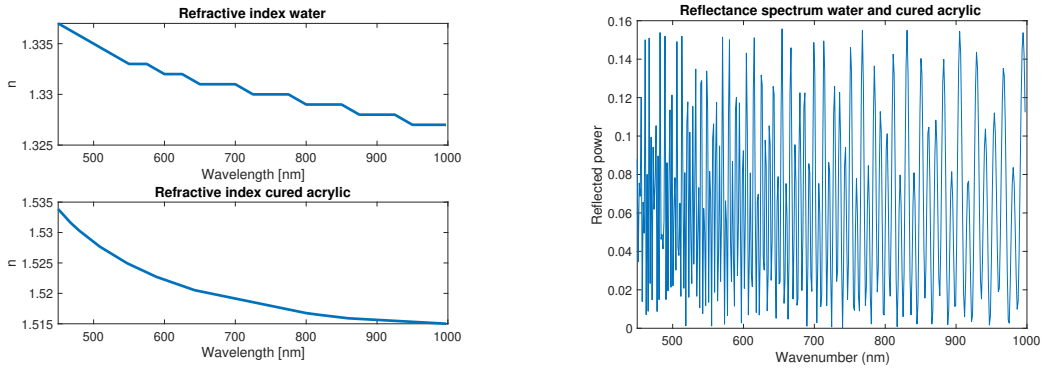

(a) Refractive index of the two materials [27].

(b) Reflectance spectrum of the two thin films.

Figure 3.14: Refractive index of water and reflectance spectrum of a 10 µm thin film of water and 15 µm cured acrylic.

In fact, the thin films are not surrounded by air, but by thick, incoherent layers of glass (see sketch in figure 3.15). Since the layers are thick enough and are therefore incohrent, we can assume that they are infinitely thick. This allows one to change the incident and rear media to be glass instead of air. The simulation of the previous figure will now be done but with surrounding media being glass, see figure 3.16b again for the same wavelength range and resolution.

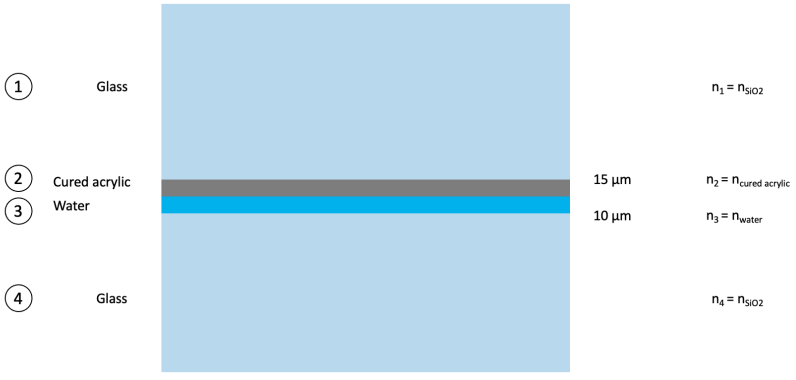

Figure 3.15: Multilayer while surrounded by glass.

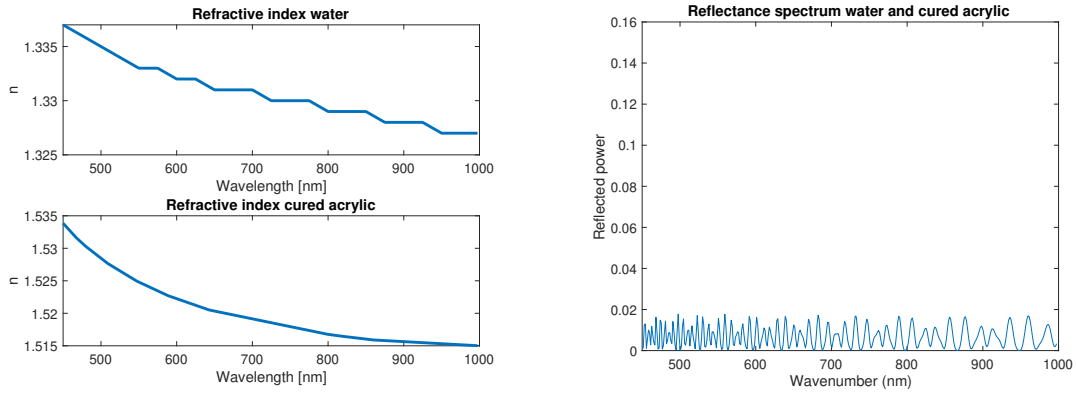

(a) Refractive index of the material [27].

(b) Reflectance spectrum of the thin film surrounded by glass.

Figure 3.16: Refractive index of water and cured acrylic followed by the reflectance spectrum of a 10 µm thin film of water and 15 µm cured acrylic now surrounded by glass instead of air.

The signal still contains the same frequency content of the two thin films. However, the amplitude of the oscillation is significantly lower. This is due to the fact that the refractive index differences between the thin films and the surrounding media are smaller when the surrounding media is glass compared to the situation where the surrounding media is air, as explained in chapter 2.

With the use of the FFT technique, the optical thicknesses can be determined from the reflectance spectra of both the situations. These situations are while the thin films are surrounded by air as well as when the thin films are surrounded by glass. By using the average refractive index of the materials over the measured wavelength range, the geometrical thickness can be derived, see the result in figure 3.17.

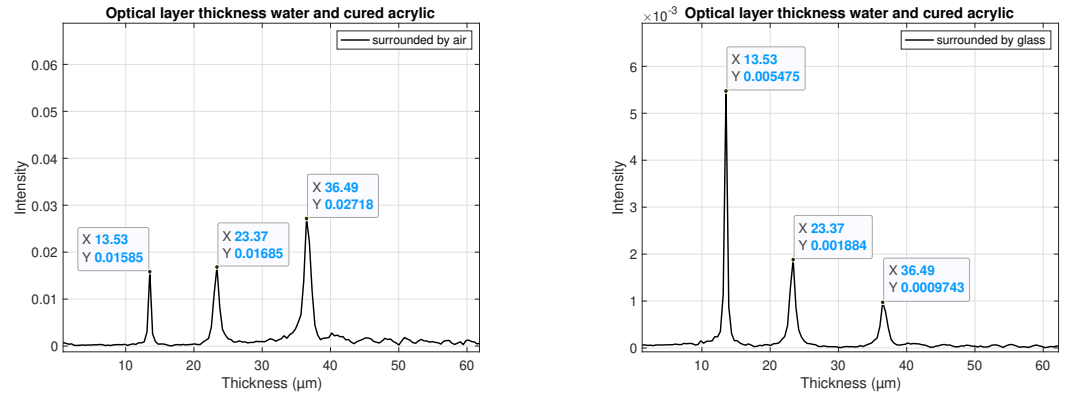

(a) Surrounding material air.

(b) Surrounding material glass.

Figure 3.17: The optical thickness determination of the reflectance spectra for both the situations while surrounded by air as well as by glass.

For both the situation with surrounding material of glass and air, the same optical thicknesses are to be expected. However, since the refractive index differences change, the amplitude of the peaks change. This will result in the height of the peaks in the FFT to become smaller. The optical thicknesses of the water and cured acrylic are $t_{\text{water}} = d_{\text{water}} \cdot n_{\text{water}}$ and $t_{\text{acrylic}} = d_{\text{acrylic}} \cdot n_{\text{acrylic}}$. This results in t_{water} = 13.53 µm and t_{acrylic} = 23.37 µm.

For figure 3.17a We know that the surrounding media is air while the thin films in the middle are water and cured acrylic. This means that the thin film of water ($n_{\text{water}} = 1.33$) is surrounded by air ($n_{\text{air}} = 1$) and cured acrylic ($n_{\text{acrylic}} = 1.53$). The thin film of cured acrylic is surrounded by water and air. The amplitude of the thin film of water is related to the differences of 1.33 with 1 and 1.53. While the am-

plitude of the thin film of cured acrylic is related to the differences of 1.53 with 1.33 and 1 this should result in a slightly larger peak for the peak that is related to the optical thickness of the cured acrylic thin film. This can be seen in the figure. The amplitude of the combined optical thickness is based partly on the difference of the refractive index of water (1.33) with air (1) but also on the difference between cured acrylic (1.53) and air (1). These differences are larger than for the individual thin films. Which is why the amplitude of the peak related to the combination of optical thicknesses is the largest.

The situation that follows is where the thin films are surrounded by thick layers of glass. As explained, the thick layers are assumed to be the infinitely thick similar to the previous situation with air. For that situation these layers were also incoherently thick. This time we are dealing with refractive indices of $n_{\text{water}} = 1.33$, $n_{\text{acrylic}} = 1.53$ and $n_{\text{glass}} = 1.46$. The thin film of water is now surrounded by glass and cured acrylic. Meaning that the amplitude is related to the differences of 1.33 with 1.46 and 1.53. The thin film of cured acrylic is surrounded by water and glass. The amplitude of this thin film is related to the differences in refractive index of 1.53 with 1.33 and 1.46. Clearly, the peak of the water layer has bigger differences with the surrounding material refractive indices compared to the thin film of cured acrylic. This means that the peak of the water thin film is expected to be larger than the peak of the cured acrylic thin film. This can also be seen in figure 3.17b which differs from the previous situation where the peaks had similar size. The amplitude of the combined optical thickness is based partly on the difference of the refractive index of water (1.33) with glass (1.46) but also on the difference between cured acrylic (1.53) and glass (1.46). These differences are much smaller than for the individual thin films. Which is why the amplitude of the peak related to the combination of optical thicknesses is the smallest.

4

Experimental Setup

In this chapter, the equipment that has been used to create a reflectance measurement setup will be presented. An outlay of the technical specifications of the equipment as well as a systematic overview of the entire measurement setup will be given. Besides that, a short description of the corresponding software and usage of the software will be given. Lastly, a couple of remarks on how to use and tune the equipment will be presented.

4.1. The setup

4.1.1. Equipment

In order to conduct the spectral reflectance measurements, a setup has been built. With the use of the simulation results, necessary specifications have been determined. Based on these results, applicable equipment has been chosen. In this case it concerns a light source type with a certain wavelength range, resolution of an optical spectrometer and the wavelength range that the spectrometer can measure.

The first important piece of equipment used in the measurement setup is the light source which is from the manufacturer Avantes [5], see figure 4.1a. The light source consists of two individual sources. A deuterium source and a halogen source. In the measurements that will be performed for this research, only the halogen source has been used as it contains the wavelength range that is required. The wavelength range of the used halogen source is between 500 and 2500 nm. It is important to turn on the light source roughly 20 minutes in advance so that it can warm up. Warming up the source is necessary as it allows the halogen cycle to begin and ensures the source signal to be as stable as possible. See Appendix B for more information [3].

(a) (b)

Figure 4.1: The Avantes equipment implemented in the final setup that has been used to conduct the measurements, see appendices B and C.

The next important piece of equipment in the measurement setup concerns the optical spectrometer (See figure 4.1b). When looking at spectrometers it is important to focus on two different specifications, the wavelength range it can observe and with what resolution it can measure this wavelength range. The resolution tells you in what minimum increments the wavelength can be measured. While the light source contains a rather wide range of wavelengths, the spectometer is able to observe a smaller range of wavelengths which is between 200 and 1100 nm. The resolution can be adjusted by changing either the used grating or by replacing the slit for different slit sizes.

The slit size can easily be adjusted since it is located at the outside of the frame. The used slit for the measurements that have been conducted is 25 µm. Besides the slit, one can also adjust the number of lines per mm grating. Adjusting this piece of hardware is not as convenient as the slit size. The manufacturer has given instruction to not do this on your own but rather send back the spectrometer if one desires to use a different grating. The grating used for this research is 300 lines per mm grating. This means that the resolution of the spectrometer is 1.4 nm. More details on the spectrometer but also about the resolution (see resolution table), see Appendix C [1].

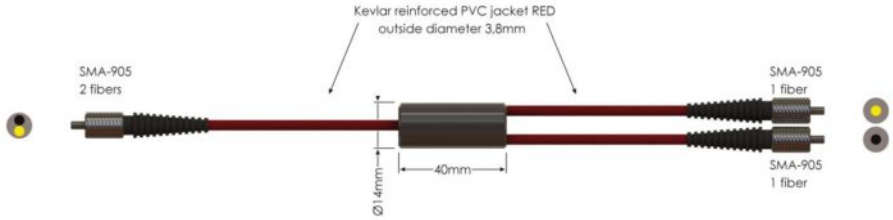

Figure 4.2: Used optical fiber with SMA-905 connectors that is connected to both the spectrometer and light source at once [4].

An optical fiber is used where the light travels through towards the substrate which consists out of a y-splitter (see figure 4.2) so that it can be connected to both the spectrometer as well as the light source at the same time while the single end is the light tip attachted to a 3D printed mount which ensures the position is steady. The connection is made with SMA-905 type.

The mount of the light source tip is attached onto a z stage allowing the user of the setup to change the height of the tip. While the positioning of the substrate can also be adjusted with a single y stage.

4.1.2. Overview setup

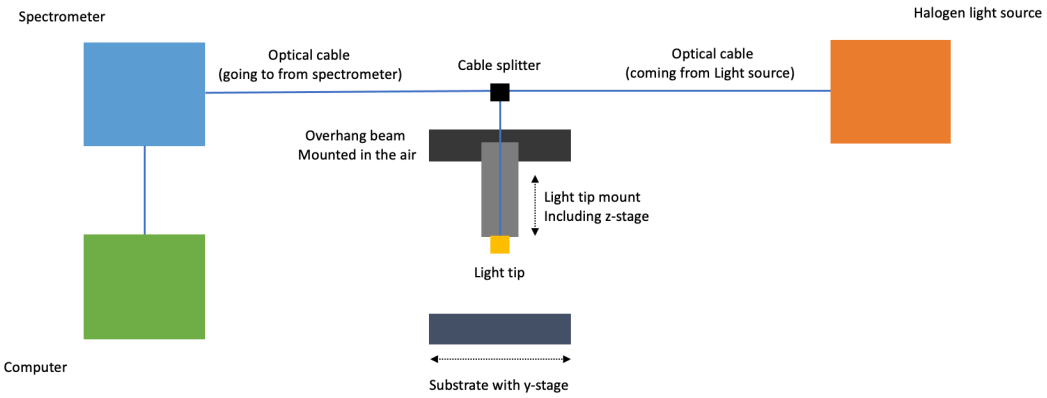

Figure 4.3: Schematic overview of the measurement setup highlighting the most important pieces of equipment.

The schematic in figure 4.3 shows where the individual pieces of equipment are located and how they are connected with each other. The overview show how an optical cable connects the lightsource with the spectrometer as well as the lightsource mount. This mount is positioned above the substrate. It also shows a USB cable that connects the computer with the spectrometer. Besides that, y- and z-stages are depicted that allow the user to change positioning of the lightsource and substrate. Finally in figure 4.4 the setup is shown. The first photo shows the setup in the lab (figure 4.4a). The second photo shows a zoomed in photo of the mount (figure 4.4b) that is used to keep the light tip in place above the substrate throughout the measurements.

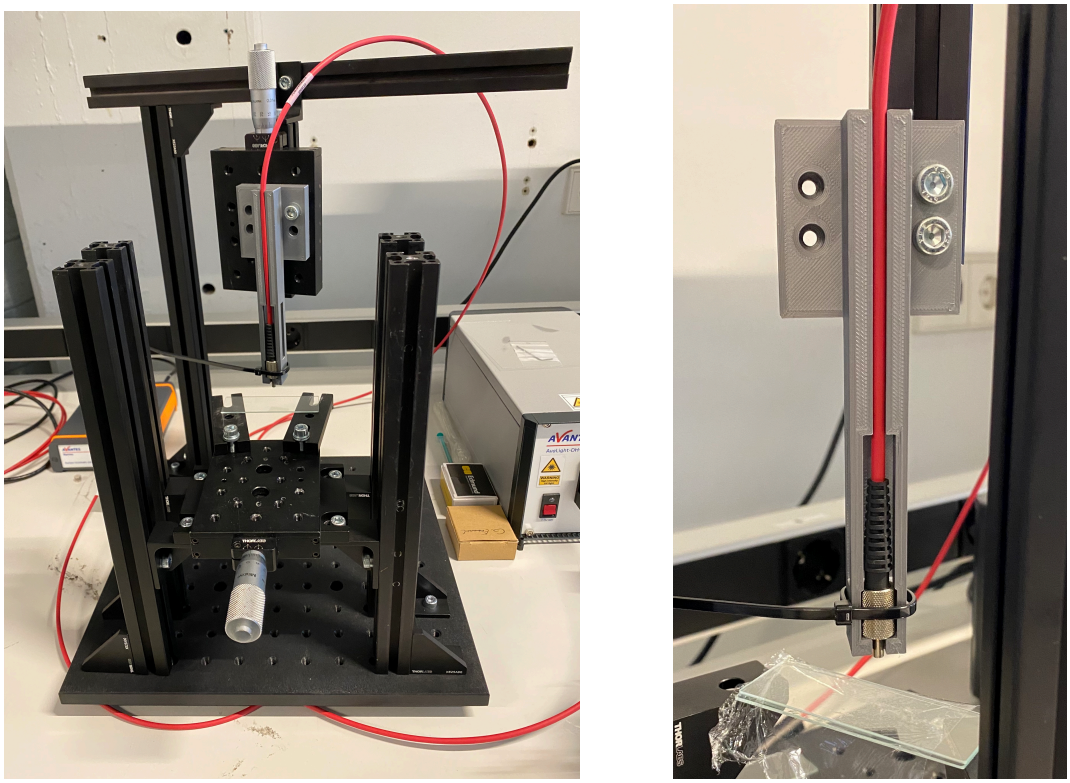

(a) (b)

Figure 4.4: The Avantes equipment implemented in the final setup that has been used to conduct the measurements.

4.2. Usage of equipment

4.2.1. Sample distance

Halogen light sources typically have diverging light rays. The degree of divergence is defined by the numerical aperture. The numerical aperture of the used light source is 0.22 NA (Appendix B). While this is defined as follows:

$$NA = n \cdot sin(\theta) \tag{4.1}$$

With NA being a dimensionless number that is given by the optical fiber, n being the refractive index of the medium that the light travels through and θ being the half the angle between the divergent light rays. Examples of different numerical apertures are shown in the figure below (figure 4.5).

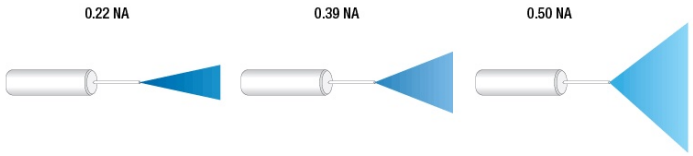

Figure 4.5: Different numerical apertures and visualization of how the divergent ligth rays look [30].

Since the numerical aperture is known, it is possible to determine the spotsize of the light onto the substrate, which essentially is the measurement spotsize. This can be calculated by using the distance between the tip where the light leaves the cable and the substrate you are measuring. From here on this distance will be referred to distance z (see figure 4.6). The z distance can be adjusted according to the desired measurement spotsize. The measurement spotsize can be increased by increasing the z distance. This allows to measure bigger parts of the substrate at once. However, the downside of this is that once you increase the spotsize by increasing the distance, the light intensity decreases. There is a limit in increasing the distance. This limit is reached once the light intensity of the signal is of the same order of magnitude as the noise in the signal. Differently said, once the signal to noise ratio is nearing 1 the z distance is too large.

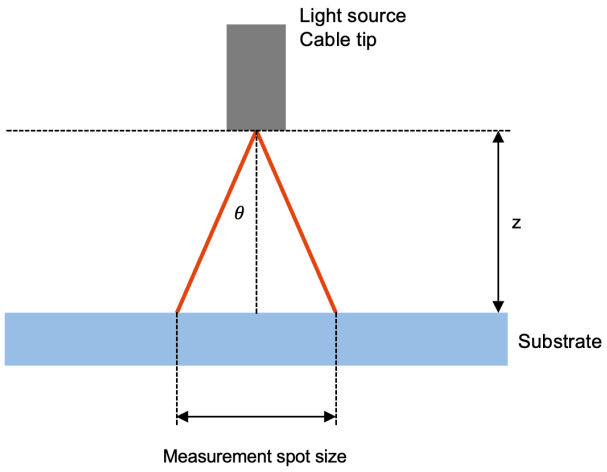

Figure 4.6: Spotsize determination by setting the distance between the tip of the light cable and the substrate.

If for a certain reason one wants the z distance to be larger than the allowable z distance due to the noise restriction, it is possible to work with a collimator. A collimator bends the light rays in a way that cause the light rays to travel parallel instead of divergent. This allows the light intensity to be more dense at a further distance from the cable tip.

As discussed, when increasing the distance between the light tip and the substrate, the reflected light intensity is expected to decrease. In order to find out what the relation is between the light intensity and the z-distance a practical measurement has been conducted. This is a reflectance measurement on a single thin film of foil stretched while surrounded by air. As a starting position the light tip has been positioned roughly at the foil which is said to be z equal to 0mm. By gradually increasing the z-distance multiple reflectance spectra have been measured. These reflectance spectra of the different z-distances have been combined in a single figure (see figure 4.7a).

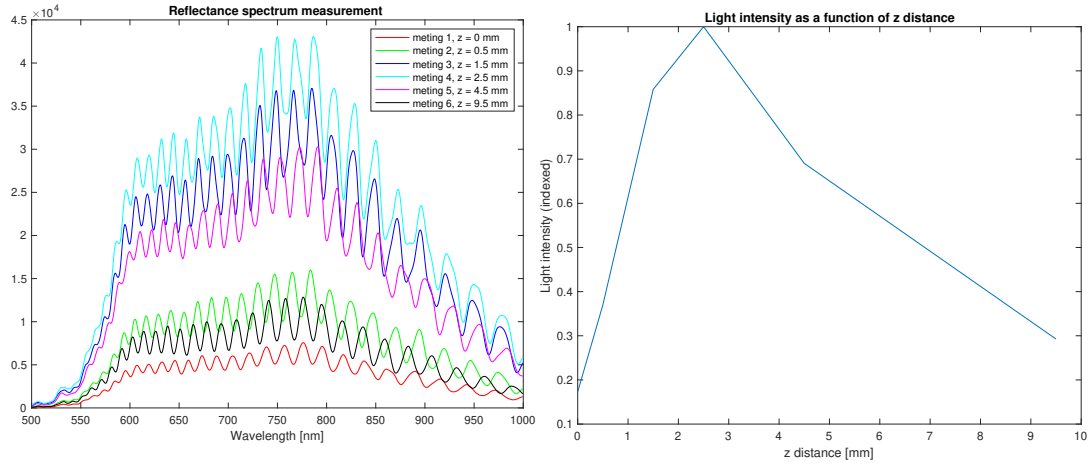

(a) Reflectance spectra for different z-distances.

(b) Relation between light intensity and z-distance.

Figure 4.7: Measurements have been done to find out what the relation is between the light intensity and the z distance.

It is clear to see that each signal contains the same frequency content but with different light intensities. It can be seen that the signal with the lowest intensity is the signal where z is equal to 0 mm (red line). By increasing the z distance with 0.5 mm the corresponding reflectance spectrum (green line) shows that the light intensity actually increases rather than decreases. By further increasing the z distance with 1 mm, to 1.5 mm (dark blue line) away from the foil, results again in a higher light intensity signal. The next increase in z-distance of 1mm to 2.5mm (light blue), makes the light intensity again go up rather than down. Additional z distance is added, this time by adding 2mm to the total z-distance which means 4.5 mm (pink line). With this step, one finally starts seeing the intensity of the signal decreasing. The next step in increasing the z distance, which now means that the distance between the foil and the tip is 9.5 mm (black line), has a logical result again with a lowered intensity. It can be said that initially the light intensity increases by increasing the z-distance and only after reaching a certain distance, the light intensity starts to decrease with an increasing z-distance (see figure 4.7b).

When dealing with light rays coming out of a light probe, the light rays first travel through the so called near-field region which is a region defined as being close to the light probe. In this near-field region, the light rays have not yet spread out or fully propagated, it means that the light wavefront has not been correctly formed as 'normal' yet. After the light rays have travelled a certain distance away from the probe they enter the far-field region. This is the region where the light rays are fully propagated. The initial increasing intensity occurs in this near-field region. While the expected relationship occurs in the far-field region.

4.2.2. Sample time

The influence of the z-distance in relation to the intensity of the signal has just been discussed. Another factor to take into account is the sample time of the measurement. One can adjust the sample time of the signal and hereby influence the intensity of the signal similar to the effect of the z-distance.

When the sample time changes, what actually happens is that the amount of time that the substrate is exposed to the light is either increased or decreased. For longer sample times we therefore logically expect that the reflectance signal intensity increases while the intensity is expected to decrease for shorter sample times. An example of a reflectance spectrum is shown in figure 4.8, where the reflection of light on a single thin film of foil is captured by the spectrometer. For this measurement, a sample time of 50 ms has been used which results in a peak intensity of roughly $2.4x10^4$.

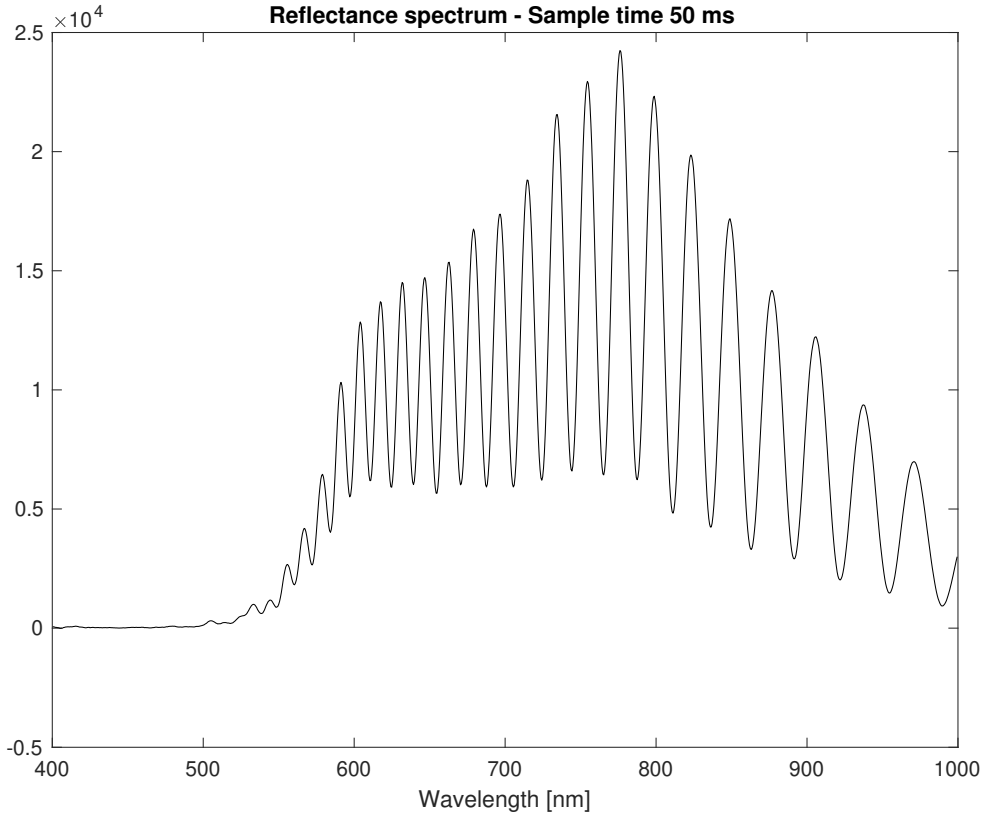

Figure 4.8: Reflectance spectrum while using 50 ms as the sample time.

Now that we can use the 50 ms reflectance spectrum as our reference spectrum, let us investigate what the influence of the sample time is by both increasing and decreasing the sample time as shown in figure 4.9. Figure 4.9a and 4.9b show the same reflectance spectra but now for sample times of 0.1 and 0.01 ms, respectively. As can be seen, the maximum intensity of the signal decreases as sample time decreases. A problem occurs once the sample time is decreased below a certain number. As a result of using such low sample times, the maximum light intensity of the signal comes close to the noise of the signal. Similar to the z-distance, this becomes a problem when signal to noise ratio nears 1. It describes the lower limit of the sample time.

On the other hand, see figure 4.9c and 4.9d which again show the same reflectance spectra but now for 200 and 300 ms, respectively. While the sample time is increased in two steps, it can be seen that there seems to be a maximum allowable light intensity that the spectrometer can measure. Every light intensity above a certain level is not measurable. The maximum intensity is found to be around roughly $6.5x10^4$. As one continues to increase the sample time, more and more of the signal is unreadable. One needs to make sure that no important data is missing from the signal by keeping the peak signal intensity well below this saturation intensity of the spectrometer.

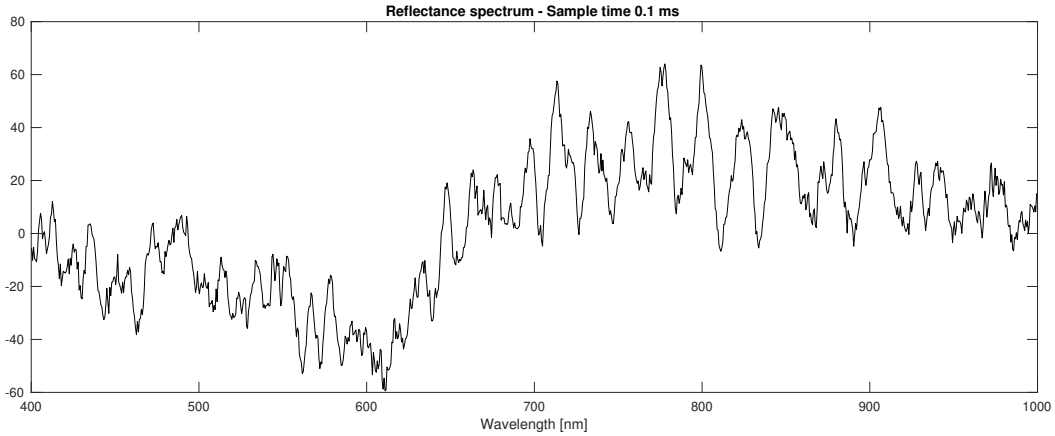

(a) Sample time of 1 ms

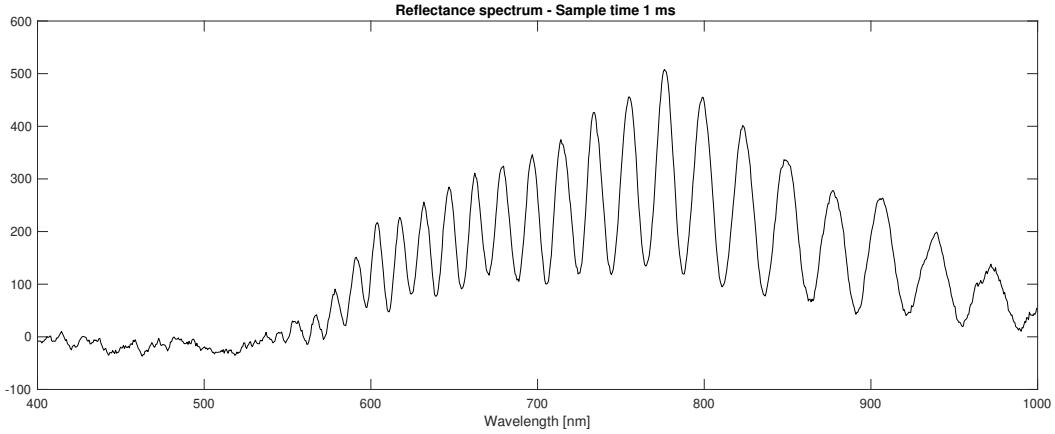

(b) Sample time of 0.1 ms

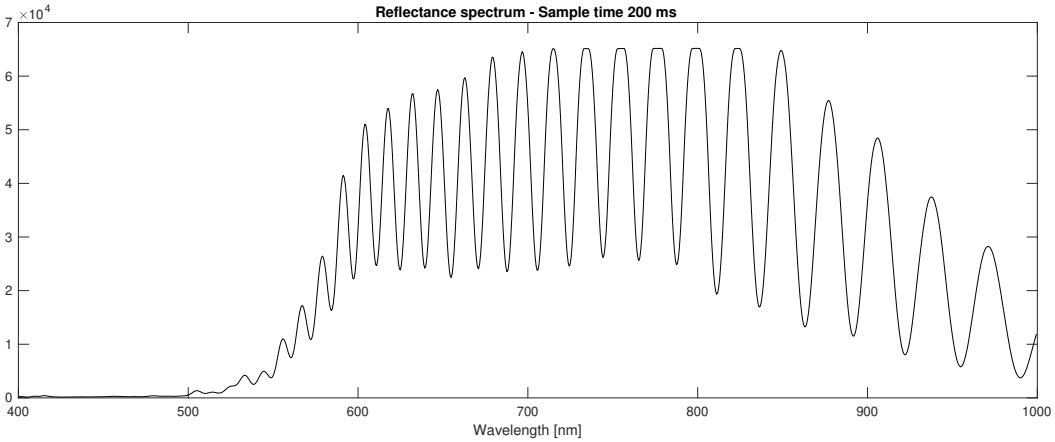

(c) Sample time of 200 ms

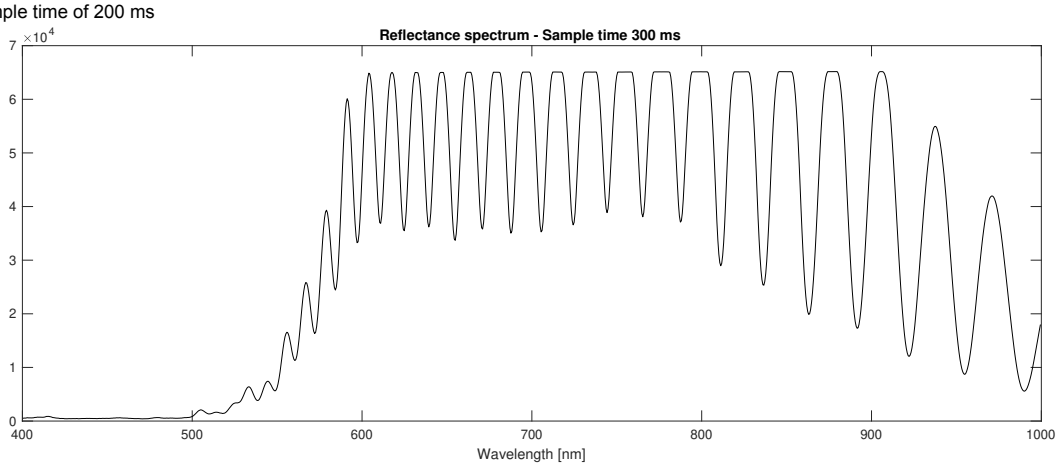

(d) Sample time of 300 ms

Figure 4.9: (a) Reflectance spectrum while using 1 ms as the sample time (b) The same reflectance spectrum but now while using 0.1 ms as the sample time. (c) The same reflectance spectrum but now while using 200 ms as the sample time. (d) The same reflectance spectrum but now while using 300 ms as the sample time.

If the upper limit of signal intensity is not taken into account, the maximum light intensity in the signal can go beyond the saturation limit of the spectrometer. As a consequence, the spectrometer will not be able to measure the signal correctly. An example of this is shown in figure 4.10. It shows that the majority of the signal is not measured correctly at all causing crucial information of the signal not to be displayed.

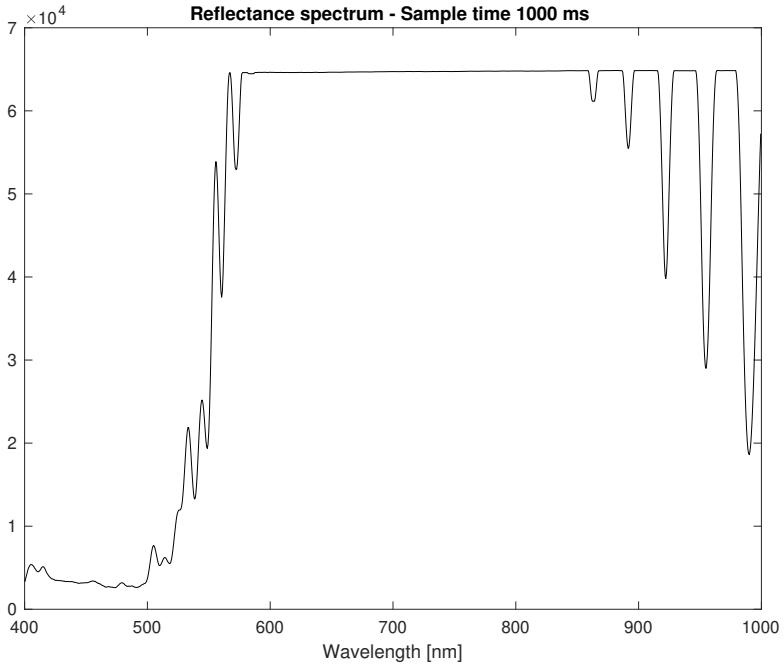

Figure 4.10: Reflectance spectrum while using 1000 ms as the sample time.

4.2.3. Software

When performing a thin film thickness measurement with the spectral reflectance measurement technique it is important to first do a couple of steps before the actual measurement can be conducted. The first step is to make a reference signal of the noise surrounding the light source. This allows the user to filter out for example noise from ambient light. Besides this you have to take a dark measurement before you start a measurement. These reference measurements can all be used when post processing of the measurement data takes place. Figure 4.11 shows an overview of what the used software from Avantes looks like. More information on how to use this specific software can be found in the manual from Avantes [2].

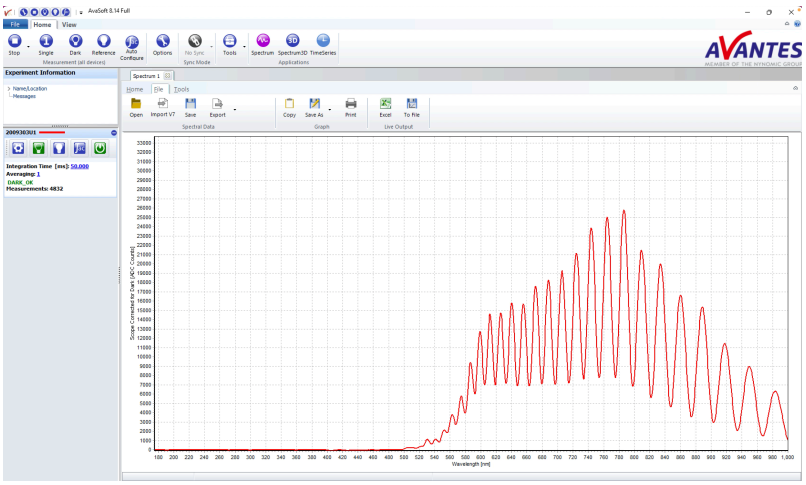

Figure 4.11: A view on the software from Avantes while performing a thin film reflectance measurement.

5

Results

In order to show that the measurement technique that has been studied throughout this research can be used to non-destructively measure a thin film within a multilayer is shown by using a measurement setup. The measurement results that followed from conducting a wide range of measurements with this setup will be shown in this chapter including the reasoning on the measurement uncertainty. Starting with a calibration of the measurement technique, followed by the measurement of single thin film measurements and finally by measuring multilayer including the relevant thin films. All the measurement results have been created with the help of measurement data from the practical reflectance setup and are then used in the model presented in Appendix G.3.

5.1. Calibration of measurement technique

5.1.1. Reference thickness comparison

In order to quantify the measurement uncertainty of the measurement technique, different measurements have been performed and compared to reference measurements and reference thicknesses. Two different reference thickness methods have been used to evaluate the performance of the spectral reflectance measurement technique. The additional steps that have been taken [13, 14, 20] before the desired reference thickness measurements were achieved can be found in Appendix E.

One method that has been used is a thin film reference measurement with an alternative measurement technique. This has been done with a cured acrylic based thin film on top of a relatively thick glass substrate, see figure 5.1. The reference measurement works by scratching into the cured thin film. This scratches through the acrylic thin film until the glass is reached. By using a confocal microscope thickness measurement technique, the height from a surface to the microscope can measured. On both the cured acrylic material and the part where the cured acrylic is scratched, a line measurement is performed to measure the height. Followed by a height difference determination between the cured acrylic thin film and the scratch. The height difference is an accurate determination of the cured acrylic local thin film thickness.

Two samples have been made with the use of a resin and equipment from Morphotonics. The samples consist of a cured acrylic-based thin film on top of a glass substrate of thickness 500 µm. Figure 5.2 shows the structure of the two layers for both samples including the thicknesses, materials and refractive indices, where the thickness of the thin film is measured with both the reference method as well as the spectral reflectance setup. Those reference measurements are done with the confocal microscope method at Morphotonics. Two different measurements have been performed per sample on the locations indicated with the yellow circles (A, B, C and D in figure 5.1).

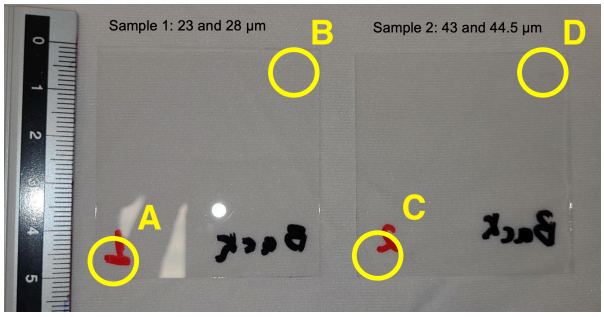

Figure 5.1: Samples of cured acrylic-based thin film on top of a glass substrate that have been used to do the calibration measurement.

Figure 5.2: Structure of the two layers from the samples.

This gives four different reference thicknesses which can be compared to measurements of the spectral reflectance measurement technique. The measurement results from the confocal microscope can be seen in figure 5.3. The figure shows the height difference results measured between the scratched part and the cured acrylic-based thin film for the four different locations. On the left side of the figure one can see the scratches and the line measurements. On the right side of the figure the resulting height differences are shown.

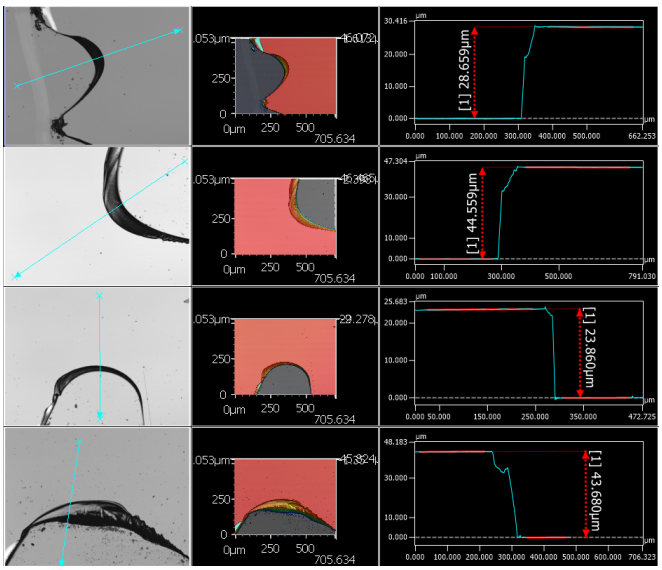

Figure 5.3: Thickness measurement results from the confocal reference measurement technique [15].

These reference measurements can now be used to see what the performance of the spectral reflectance measurement is. This is done by using the setup shown in Chapter 4 (See figure 4.4). The measurements have been done on the four different locations on the two samples as indicated in figure 5.1. In order to get proper and realistically comparable results, the light source has to shine close to the scratch as that is where the reference thickness is measured. This is necessary since it is known that there is a thickness variation across the surface of the samples.

Table 5.1: Measurement calibration with alternative measurement method

Measurement Location	**Confocal measurement** [µm]	**Expected thickness uncertainty (±2.00%)** [µm]	**Reflectance measurement** [µm]	**Measured uncertainty** (±) [µm]
A	28.66	0.57	29.23	0.337
B	23.86	0.48	25.41	0.248
C	43.68	0.87	44.43	1.160
D	44.56	0.89	44.37	0.610

Measurement results from both the reference measurement as well as the results from the spectral reflectance measurement technique are shown in table 5.1. Where the confocal measurement is the expected thickness of the sample, and the reflectance measurement is the measured thickness. Both methods have an uncertainty. The confocal measurement technique has a 2.00% accuracy which is defined by the manufacturer [15]. The uncertainty of the spectral reflectance measurement is a standard deviation which is calculated based on five point measurements around each scratch at the four different positions on the two samples. The resulting reflectance spectra and FFT can be found in Appendix D. The average measured uncertainty is 1.53%. This is calculated by dividing the measured uncertainty by the thickness measured with the spectral reflectance measurement technique and taking the average of the four locations.

The second reference measurement is with a liquid thin film. This film is created with the use of a thick and round optical flat with a surface area of 506.7 mm^2. On top of this optical flat, a water droplet with a volume of 4.40 µl is deposited. The water droplet has a known volume since a precise pipette that can be adjusted based on preference has been used. A glass substrate with a larger surface area than the optical flat is put on top of the water droplet. This result is that the water is smeared out over the surface of the optical flat. With this method, a thin film of water between the two glasses is created. The glass substrate has a thickness of 500 µm and the optical flat is 12.70 mm thick which means that both layers can be assumed to be incoherently thick. The optical flat is from a different type of glass (zerodur [11]) which has a slightly different refractive index compared to SiO_2. See figure 5.4 for more details on the structure of the multilayer. Since both the area of the optical flat and the volume of the droplet are known, one can get a rather accurate thickness determination of the water film. The results of this thickness determination as well as the film thickness measurement results from the spectral reflectance setup are shown in table 5.2.

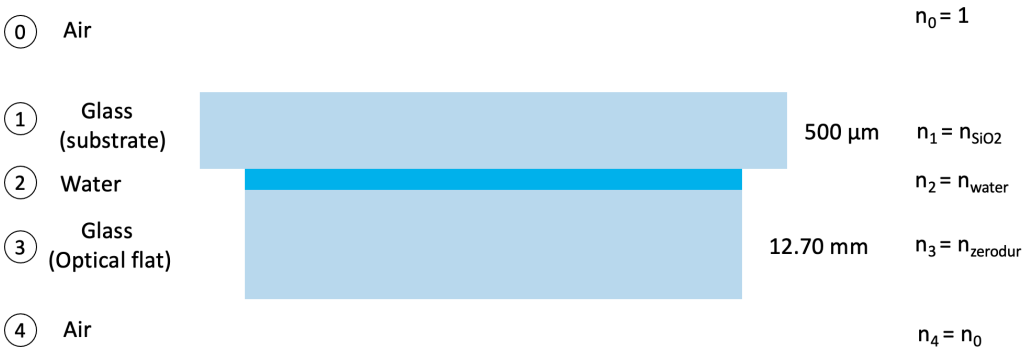

Figure 5.4: Structure of the multilayer used for water thin film reference measurement.

Measurement results from both the reference measurement as well as the results from the spectral reflectance measurement technique are shown in table 5.2. Where the pipette reference thickness determination is the expected thickness of the water film, and the reflectance measurement is the measured thickness. Both methods have an uncertainty. The pipette method has an uncertainty of 1.55% which is an average error for micro-pipettes [8]. The uncertainty of the spectral reflectance measurement is a standard deviation which is calculated based on six point measurements in the middle of the optical flat for six individual situations with the same volume. The resulting reflectance spectra and FFT can be found in Appendix D. The average measured uncertainty is 7%. This is calculated by dividing the measured uncertainty by the thickness measured with the spectral reflectance measurement technique.

Table 5.2: Measurement calibration with thin film of predetermined thickness

Thickness determination [µm]	**Expected thickness uncertainty (±1.55%)** [µm]	**Reflectance measurement** [µm]	**Measured uncertainty** (±) [µm]
10.07	0.16	9.29	0.65

With both calibration methods, a thin film is measured with the spectral reflectance measurement technique, and then compared with either a known thickness or alternative reference measurement technique. In both cases thick glass is used in the spectral reflectance measurements as those layers can be assumed to be incoherently thick with the used resolution of the spectrometer as previously discussed.

The performance of the reflectance measurement method is measured by uncertainty levels. When verifying the performance of a measurement method, it is necessary to verify the uncertainty of the measurement method one is looking into. Besides this, it is also important to verify the uncertainty of the reference measurement method that one is comparing it to. This means that on the one hand, there will be an uncertainty that originates from the spectral reflectance measurement technique. On the other hand, there will be an uncertainty that results from the expected thickness which in this case comes from two different reference measurement methods. Five different thicknesses including both the measured and expected uncertainties that resulted from the two reference methods have been visualized in figure 5.5. Where the uncertainties are used that have been discussed and are shown in table 5.1 and table 5.2.

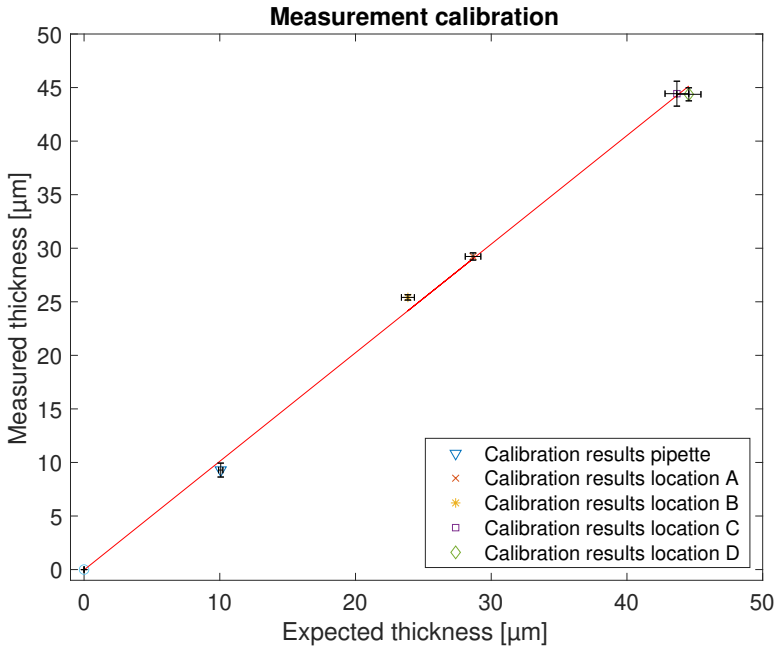

Figure 5.5: Performance determination for measurement technique of measured against expected reference thickness.

In this part it will be discussed what needs to be considered in order to deal with the uncertainty of the confocal measurement method. Which is the first reference method that measures the height difference between two surfaces after scratching into a surface. The measurement technique has an accuracy of $\pm$ 2% according to the manufacturer [15]. This accuracy is used to calculate the error on the measured thicknesses in table 5.1.

The next uncertainty to consider is the uncertainty from the second reference method. This is the reference method used for the water thin film created with a pipette. For this method, multiple contributions have to be taken into account to come to the total uncertainty of the expected thickness. The individual contributions are:

1. **Uncertainty pipette:**
   The pipette has an uncertainty of 2.00% which is specified by the manufacturer [8]. This contributions is rather straightforward and applies to all measurements done with the pipette.
2. **Tilted water film due to center of mass glass substrate:**
   This contribution has the potential to cause errors in the measurement. The reference thickness is created with a larger glass substrate. This substrate must be larger than the optical flat to make sure that the entire surface of the optical flat will be covered with water. This means that when the water thin film is measured, one has to put the center of mass of the larger glass substrate precisely in the middle of the optical flat in order to create a flat thin film of water. In reality this will not work perfectly when done manually. In reality, the water film is tilted with a certain angle dependent on where the center of mass of the glass substrate is. However, while the angle is considered to be there (see figure 5.6), when the reflectance measurement is performed in the middle of the optical flat, the average thickness should be measured. This would exactly be inline with the desired thickness. For the reference measurements with the water thin films, it is assumed that the angle is relatively small. Besides this, it is assumed that the measurement are performed in the middle of the optical flat. Therefore the second contribution to the total error is neglected.
3. **Rounded edges optical flat:**
   The optical flat has rounded edges. The water droplet spreads out over the surface of the optical flat due to the gravitational force of the glass substrate. Part of the water can be located in the rounded edges. However, the weight of the glass substrate is relatively small. Besides this, relatively small volumes of water are used in the measurements and the weight of the glass substrate is also small. When larger volumes are used or heavier substrates, this contribution becomes significant. Therefore, this contribution is neglected in the measurement results.
4. **Evaporation time water thin film:**
   As the measurement is done with a small volume (micro liters) evaporation time of the water can start playing a role. This influences the total volume over time. However, for the used volumes of water, the evaporation time does not play a role as long as the measurement do not take too much time. When measurements are done within a span of 5 minutes, the evaporation time can be neglected. This is the case for all measurements in this research [16].

This means that from the four individual contributions, only the uncertainty of the pipette will be taken into account when using the water thin film thickness.

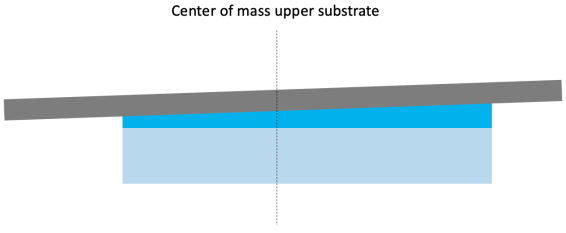

Figure 5.6: As the center of mass of the upper substrate is not in the middle of the optical flat, the substrate is positioned slightly inclined affecting the water thin film thickness (exaggerated effect here).

Lastly, one needs to think about the uncertainty originating from the spectral reflectance measurement method. This uncertainty has been calculated by measuring the same or comparable points multiple times. From these measurements, the average is taken. The standard deviation that follows from the multiple measurements is then used as the uncertainty. For the water thin film, six different measurements have been performed in the middle of the optical flat. For the two samples with a cured acrylic thin film, five measurements have been performed on four different location with four different thicknesses.

The uncertainty of the spectral reflectance measurement technique can be caused by multiple factors. The factors that potentially play a roll are listed and discussed below:

1. **Surface roughness:**
   One factor could be that surface roughness is not taken into account. Light that hits an interface with a certain surface roughness causes light scattering and therefore results in a loss of light intensity. This intensity loss can impact the accuracy of the thickness determination.

2. **Absorption:**
   Another loss of light intensity can be caused by absorption. However, since non-absorbing materials ($\kappa = 0$) have been used only, meaning that refractive indices only exist of real parts, this is a negligible factor.

3. **FFT - spectral leakage:**
   When a reflectance spectrum of a single thin film is taken, a certain frequency is visible. Depending on where the reflectance spectrum starts and ends in the oscillation, a symmetrical peak will or will not show up in the FFT result. In some cases, there may not even be a peak at all. In order to get the most accurate result, the FFT must begin and end measuring at the same point in the oscillation so that only complete periods are measured which creates a symmetrical peak. A symmetrical peak is desired as it ensures the smallest possible error due to this problem which is referred to as spectral leakage [22]. When the FFT begins the measurement at the bottom of an oscillation and ends at the top of an oscillation, an error occurs due to the peak being tilted towards either the left or right side meaning that there will no longer be a symmetrical peak. This leakage problem can be minimized by windowing the reflectance data which has been done manually to achieve the smallest possible leakage error contribution in the results for the remainder of this research.

4. **FFT - oscillation with few periods**
   Another source of error can be due to the fact that the wavelength range is limited. Again in simulating there is not really any limit since any arbitrary large wavelength range can be used. While in reality one often has to deal with a light source that has a fixed wavelength range or a spectrometer that can only measure a part of that wavelength range. FFT is often used in engineering applications where a time signal is plotted versus displacement. In these examples, frequencies are measured with relatively great amount of periods compared to the optical application in this research. The higher the number of periods in a signal, the sharper the peak will be. If the number of periods in a signal is limited, the error will be larger.

5. **FFT - average refractive index**
   A final contribution to the error of the FFT can be due to the fact that an average value of the refractive index is used to translate the optical thickness result from the FFT into a geometrical thickness. When the refractive index has a huge slope in the measure wavelength range, the average refractive index may not be an accurate way to determine the geometrical thickness.

This research has not focused on determining to what extend the contribution of these individual factors play a role. For the results in this research, only a single uncertainty has been specified for the spectral reflectance measurements.

5.1.2. Post processing of data

By now it is clear what to expect and consider in the reflectance spectrum when simulating thin films. This section covers measurement results from the practical setup where a light source is used with a non constant intensity over the wavelength range. A single thin film measurement result from the spectral reflectance setup is shown in figure 5.7. For the measurement of a single thin film, there should be a single frequency in the signal which is clearly seen. However, there seems to be another pattern in the overall signal. This larger pattern originates from the light source. This is due to the fact that the used halogen light source does not have a constant intensity over the measured wavelength range. The light source intensity pattern shifts the signal in the reflectance spectrum away from the zero intensity line. This structure shows up in every measurement that is done with this light source. When the FFT of this structure is taken, the result is certain noise between 0 and 5 µm and also converges towards a high number at zero. This makes it difficult to measure thin films with thicknesses in that range.

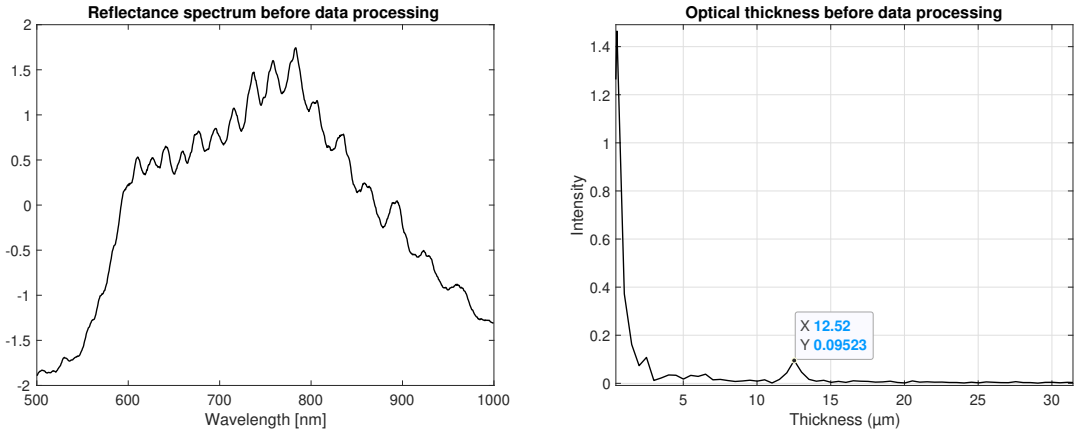

Figure 5.7: Reflectance spectrum and FFT result followed from a single thin film.

The intensity pattern of the light source can be determined by connecting the light source directly to the spectrometer, see figure 5.8. On the left, the reflectance spectrum of the light source is shown and at the right the noise that it creates in the FFT. In order to filter out the light source noise one needs to normalize the reflectance data of the light source as well as the reflectance data from a thin film measurement. The measurement as shown in figure 5.7 is used to illustrate what this looks like. By normalizing both this signal and the light source reflectance and then subtracting the light source from the thin film measurement, one can filter out the light source data, see figure 5.9.

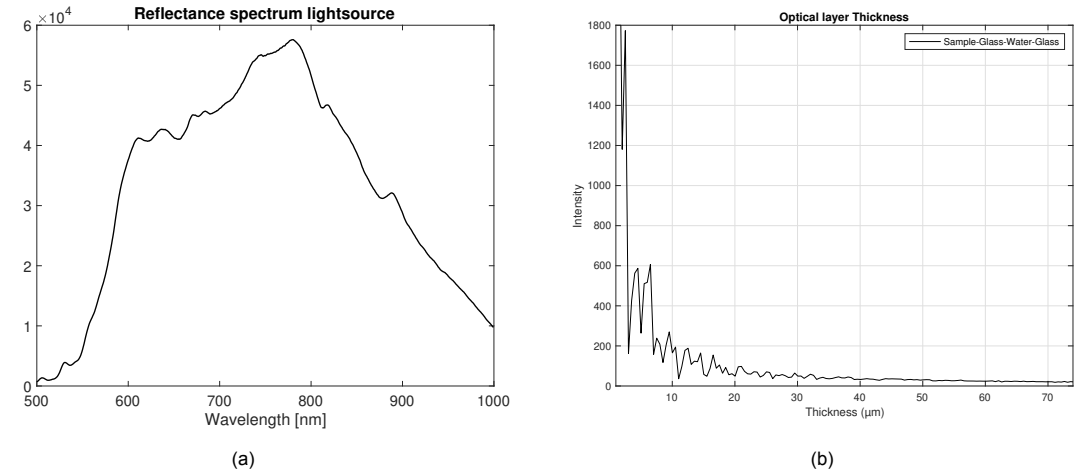

Figure 5.8: Reflectance spectrum and FFT result followed from connecting the light source directly to the spectrometer.

The desired result is here, the light source pattern has disappeared and only the frequency of thin film and including ambient light noise is present in the remaining reflectance spectrum. While the noise in the FFT has certainly decreased (the peak at zero also significantly lower), it is still not entirely removed. One can attempt to further adjust and improve the reflectance spectrum to precisely make it oscillate around the zero intensity axis to create the best result. However, for this research, the current version of the reflectance spectrum will be enough.

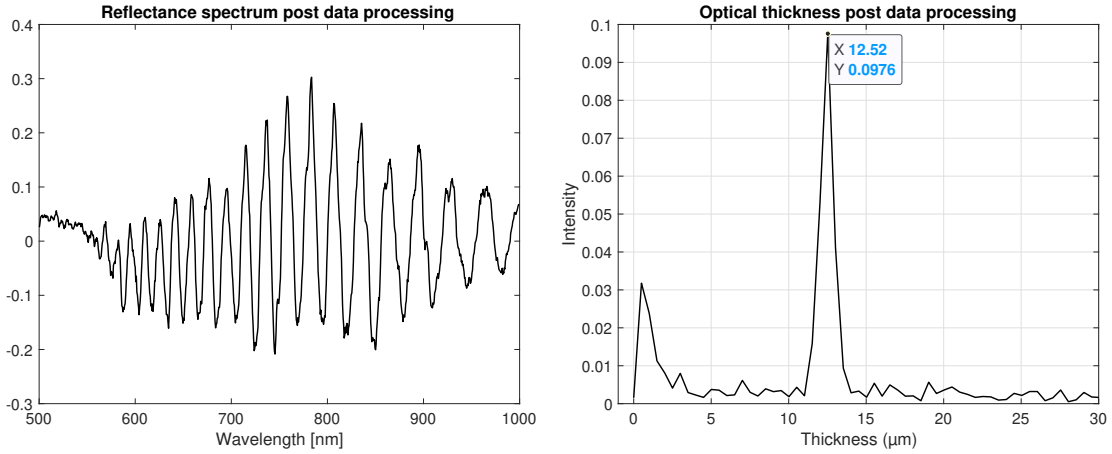

(a) (b)

Figure 5.9: Reflectance spectrum and FFT result of the thin film corrected for the light source.

The FFT now no longer converges towards a high number but goes to zero intensity for a frequency of zero. In the remainder of this research, measurement results from the spectral reflectance setup will be shown with already filtered out reflectance spectra to create the best results.

5.2. Measurement results

5.2.1. Sample measurements

In the previous section, the spectral reflectance measurement technique was calibrated with two different reference thickness measurements and compared to these thickness determinations. Now that reasonably good comparison measurements and the related uncertainties have been put into context, the next steps are towards measuring the desired multilayer consisting of four layers.

For the multilayer measurements, the two samples with relatively thick glass substrates that have a cured acrylic based thin film on them will be used again. In the previous section it has been proven that measurements from the reflectance setup are reliable for measurements on this sample. From here on, measurements on that same sample at different spots on the samples can said to be accurate with the same uncertainty that has been found in the calibration step. As discussed it is already known that there is a relatively big thickness variation between the two reference measurement points on both samples. In order to use the samples for the multilayer measurements a grid of points has been drawn on the samples (see figure 5.10). The thickness slightly above these points has been measured. The thickness measurement results can be found in table 5.3. Besides this, also the reflectance spectra and FFT results will be shown including the steps to go from optical to geometrical thickness. As expected was similar thickness variation found on the grid.

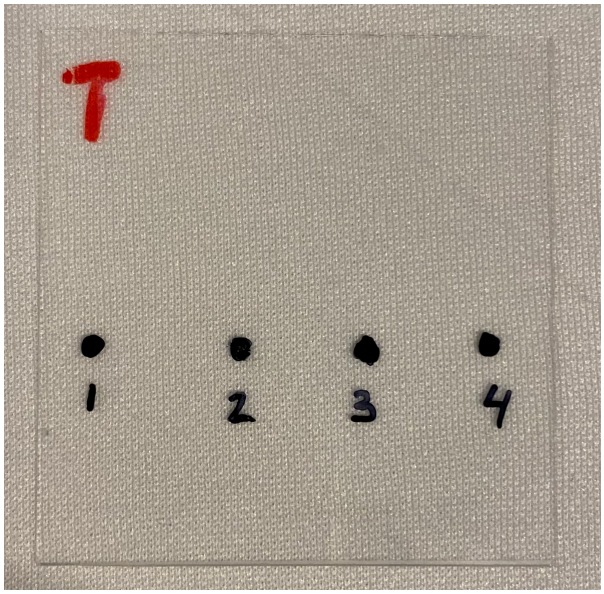

Figure 5.10: Grid of four dots on the sample with the scratches used for the reference thickness measurement.

Now that the thickness at the gird on the sample is known, the sample can be used in the desired final multilayer measurement. For this measurement we are not bounded by the reference thickness at the scratches but the grid measurement can also be used since the thickness has been accurately determined there as described. The next section will continue with multilayer measurements.

Table 5.3: Measurement of cured acrylic thin film thickness on a grid

Measurement Location	**Spectral Reflectance thickness measurement** [µm]
Point 1	26.34
Point 2	30.84
Point 3	33.24
Point 4	34.88

The resulting reflectance spectra and FFT that has been used to determine the geometrical layer thickness for the four measurements are shown below. Where the reflectance spectra have been corrected for the light source.

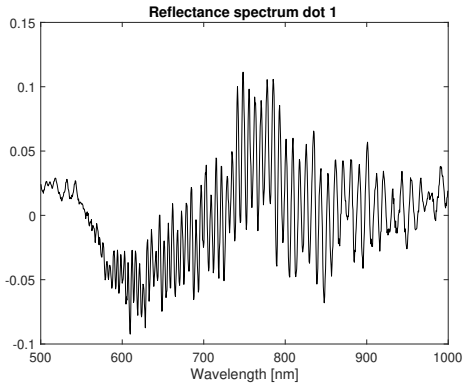

(a) Reflectance spectrum

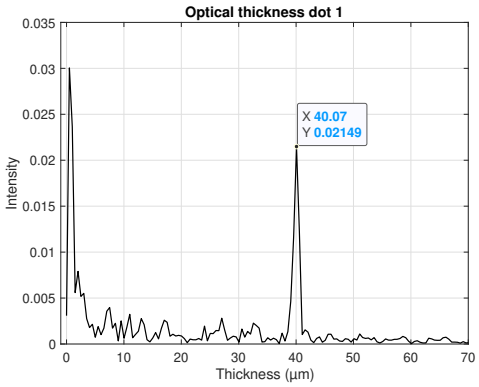

(b) Thickness determination (FFT).

Figure 5.11: The measurement results from thin film cured acrylic on top of a incoherently thick glass substrate showing both Reflectance spectrum and FFT for dot number one on the grid.

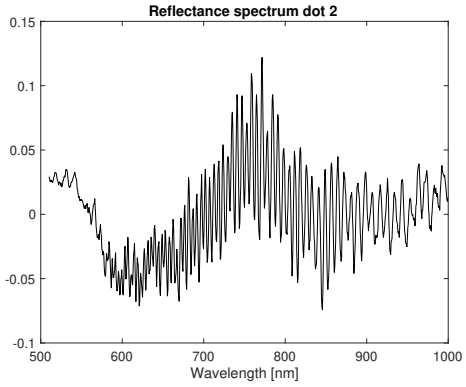

(a) Reflectance spectrum

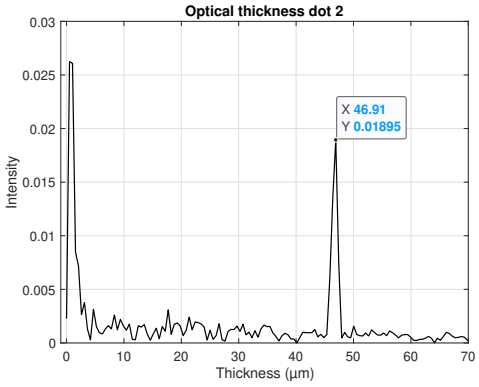

(b) Thickness determination (FFT).

Figure 5.12: The measurement results from thin film cured acrylic on top of a incoherently thick glass substrate showing both Reflectance spectrum and FFT for dot number two on the grid.

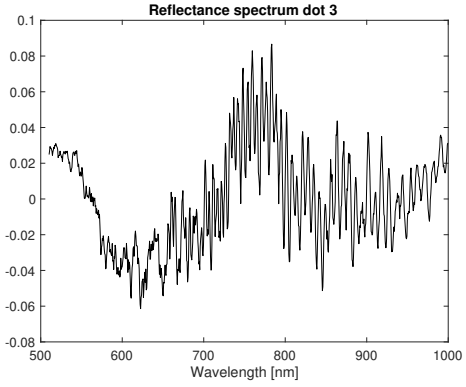

(a) Reflectance spectrum

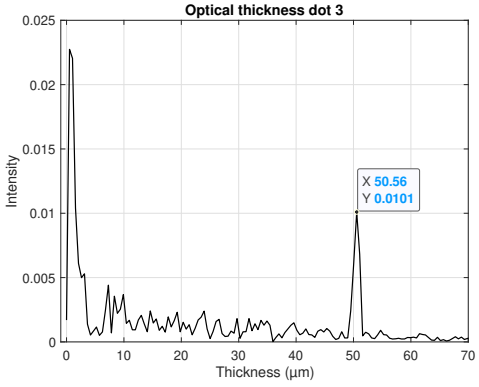

(b) Thickness determination (FFT).

Figure 5.13: The measurement results from thin film cured acrylic on top of a incoherently thick glass substrate showing both Reflectance spectrum and FFT for dot number three on the grid.

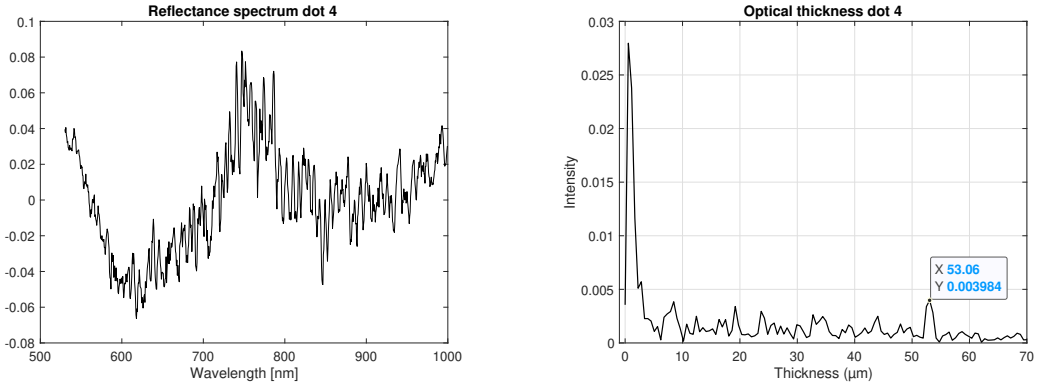

(a) Reflectance spectrum

(b) Thickness determination (FFT).

Figure 5.14: The measurement results from thin film cured acrylic on top of a incoherently thick glass substrate showing both Reflectance spectrum and FFT for dot number four on the grid.

The cured acrylic material has a refractive index as a function of the wavelength which can be seen in figure 5.15. The optical thicknesses of the four dots on the grid are shown in the FFT results above and are 40.07, 46.91, 50.56 and 53.06 µm for dot 1, 2, 3 and 4 respectively. The average refractive index of the material over the measured wavelength range is determined from figure 5.15 and is 1.521. This means that the geometrical thicknesses for dot 1, 2, 3 and 4 are 26.34, 30.84, 33.24 and 34.88 µm respectively. See table 5.3. Note that from the data used to create the reflectance spectra, the light source has been filtered out by normalizing both the signal and the light reference signal as described before.

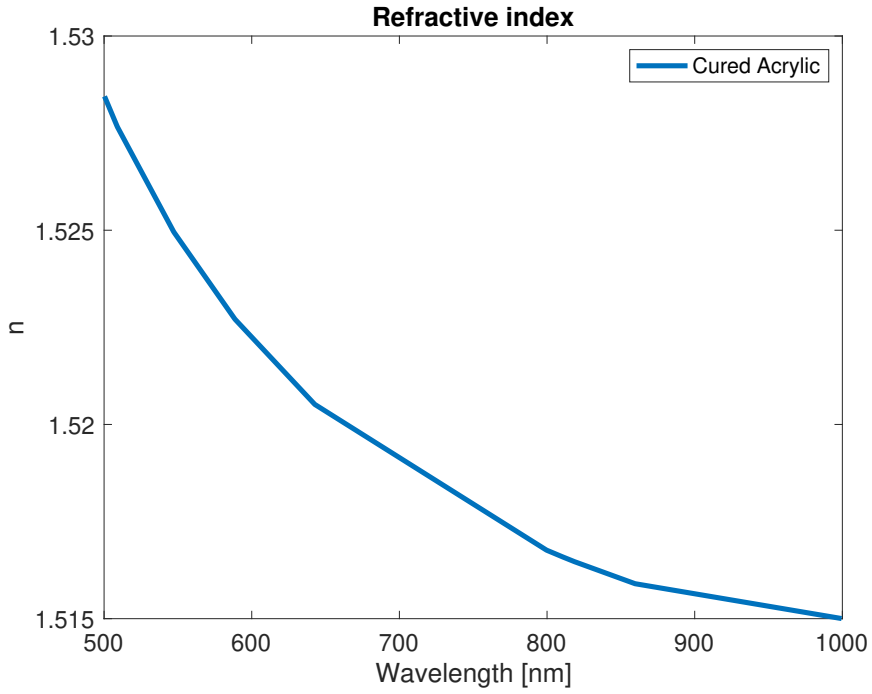

Figure 5.15: Refractive index of cured acrylic (resulting from measurement data by Morphotonics).

5.2.2. Multilayer measurement result

For the final multilayer measurement that this research has been working towards the following multilayer has been created, see figure 5.16. The top two layers consists of the sample with the cured acrylic thin film fixed to it. The bottom two layers consist of a thin film of water and an optical flat. The thin film of water is created by depositing a droplet of water measured with a pipette on the optical flat. The water is smeared out over the surface of the optical flat once the sample is deposited on top of it. An optical flat is a rounded piece of glass which is often used in optical experiments because it has been well calibrated in for example the surface roughness. The benefit of using a round optical flat in this case is that the water can easily smear out over the surface since it will not need to be pushed into any corners. This means that the water is automatically smeared out over the round surface when one deposits the sample on top of it without the need of any additional force.

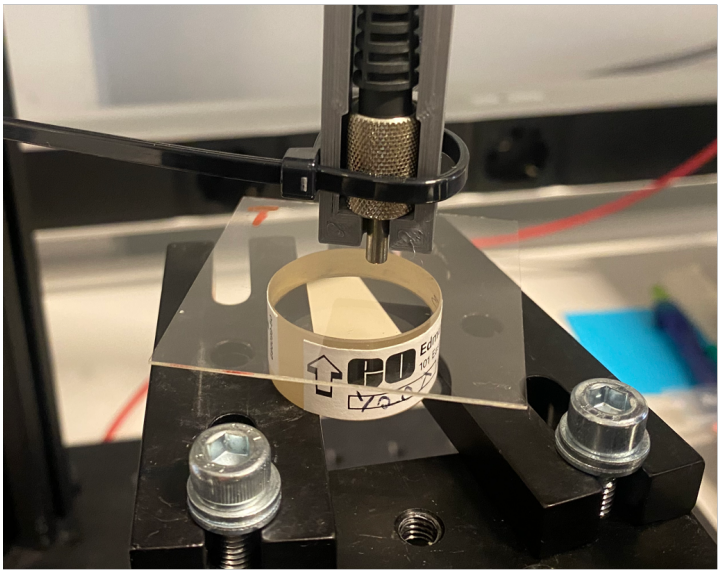

Figure 5.16: Overview of the multilayer measurement in the Optics Lab.

The water thin film has been created with the use of the same pipette that has been used for the calibration measurements. The used volume for this measurement is 5.1 µl while an optical flat with diameter of 1 inch was used. This means that the area of the optical flat is 506.7 mm^2. Using both the area of the optical flat and the volume of the droplet, the thickness is determined to be roughly 10.06 µm. The sample is measured in the middle which is in between point 2 and 3 of the grid that has been measured in the previous section and comes down to a thickness between 30.84 and 33.24 µm (see table 5.3). The resulting reflectance spectrum and FFT of the measurement can be found in figure 5.18. A sketch of the structure of the multilayer is shown in figure 5.17 including the expected thicknesses.

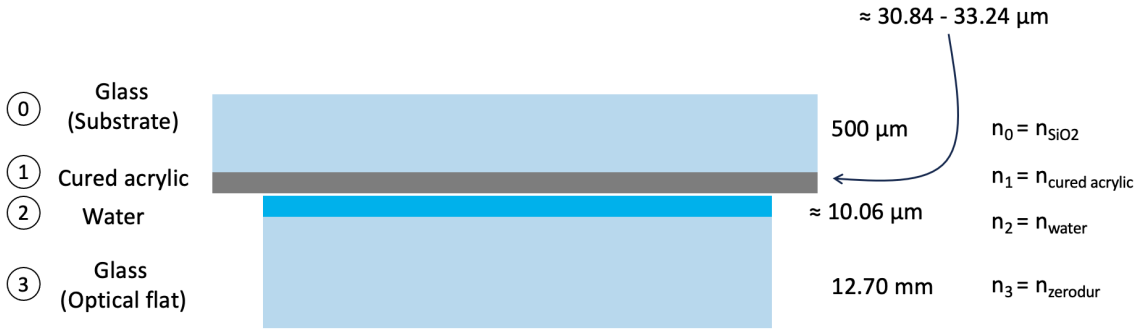

Figure 5.17: The multilayer structure as used in the measurement.

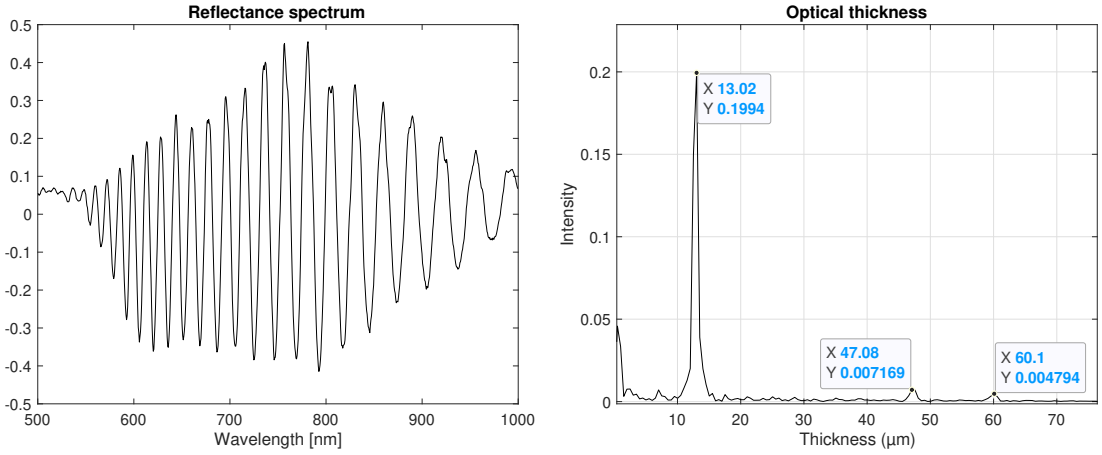

(a) Reflectance spectrum

(b) Resulting FFT

Figure 5.18: Reflectance spectrum and FFT result followed from the final multilayer measurement consisting of the materials: Glass (substrate) - Cured Acrylic - Water - Glass (optical flat).

The measured multilayer includes four layers of which two layers, the top and bottom, are incoherently thick layers of two types of glass in combination with the used resolution of the spectrometer. This means that the glass layers will not contribute to the frequency content of the reflectance spectrum of the multilayer measurement and will therefore not show in the FFT. However, since the glass layers are essentially the surrounding materials, they do influence the amplitude of the signal for both layers. The refractive indices of the four different materials are shown in figure 5.19.

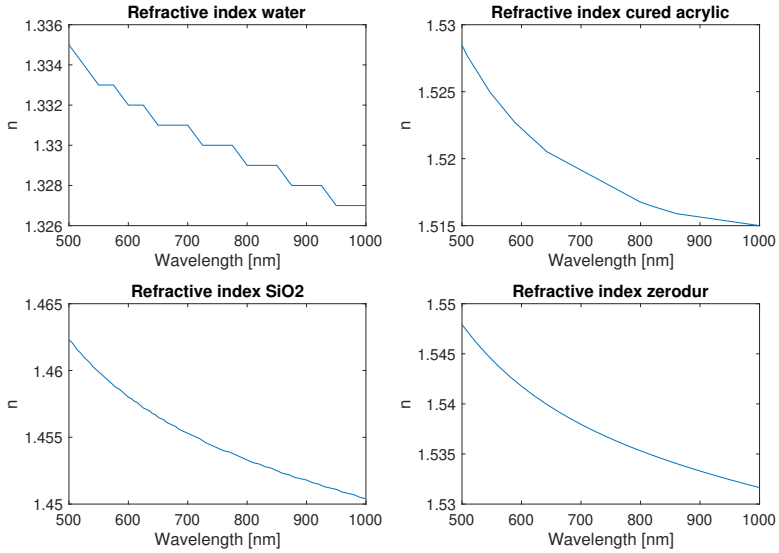

Figure 5.19: Refractive indices of water and cured acrylic [12, 27].

Besides the remaining noise of the light source, the FFT (figure 5.18b) shows three peaks, one for each individual coherent layer and one for the combination of those two. Optical thickness peaks of the layers result from the FFT and are t_{water} = 13.02 µm and $t_{\text{curedacrylic}}$ = 47.08 µm. The average refractive indices over the measured wavelength range are n_{water} = 1.331 and $n_{\text{curedacrylic}}$ = 1.522. This means that the geometrical thickness of the layers are d_{water} = 9.78 µm and $d_{\text{curedacrylic}}$ = 31.26 µm according to the spectral reflectance multilayer thickness measurement.

In figure 5.20 the FFT results for both the practical measurement as well as for the theoretical simulation of a comparable situation is shown. The situation in the simulation is for a 9.78 µm thin film of water and a 31.26 µm thin film of cured acrylic, surrounded by incoherently thick glass similar to the thicknesses expected and measured during the practical measurement. This means that in both situations there are two coherent thin films surrounded by two thick, incoherent glass layers simulated with the same resolution. This make it identical situations, one practical measurement and one theoretical simulation. It can be seen that the first peak, which is the peak of the water has the largest amplitude. This is due to the fact that the refractive indices between the water layer and its surrounding materials is the largest. Where as the cured acrylic peak is significantly smaller followed by the combined optical peak of the two layers as explained in section 3.2.

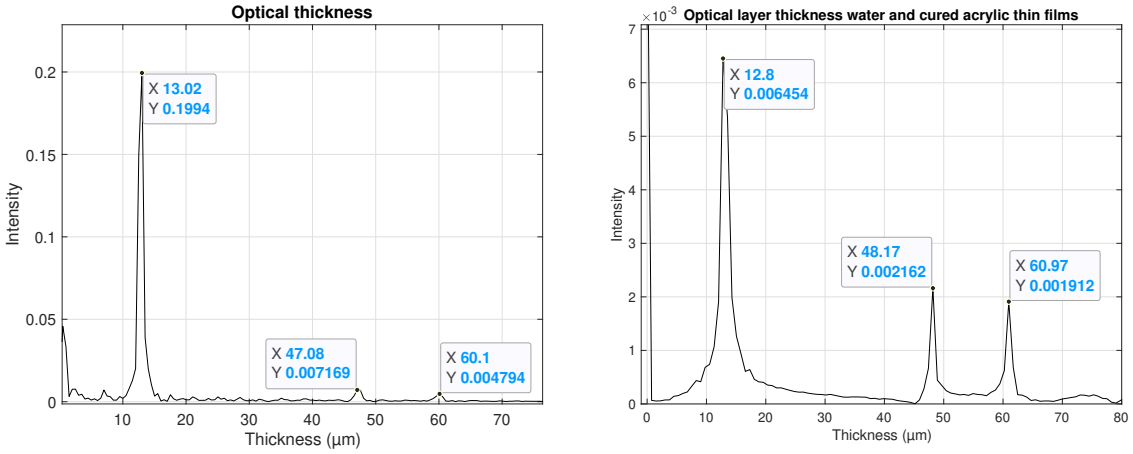

(a) Multilayer FFT measurement

(b) Multilayer FFT simulation

Figure 5.20: The FFT result for both the practical measurement and the theoretical simulation for the multilayer: Glass (substrate) - Cured Acrylic - Water - Glass (optical flat).

6

Discussion

To briefly recap, in this research a multilayer thickness measurement technology has been investigated. It has been investigated to test what the possibilities are in terms of measuring thickness of a liquid thin film that is situated between multiple other layers of both thicker layers and another thin film. A simulation model was created to predict the reflectance coming from both single thin films and multilayers when shining a light beam perpendicular to the layers. The simulation model has been used to estimate the required specifications of light source and spectrometer to measure the desired thin film thickness. An experimental setup was built to perform measurements on a multilayer especially for this research. This multilayer consists of comparable characteristics as the multilayer that is seen in the process of Morphotonics. This resulted in thickness measurements of the individual layers as has been shown in chapter 5. While useful and logical measurement results were found, the results have to be critically reviewed to see whether requirements of the measurement technique stated in the introduction were met.

Evaluation of the measurement requirements:
First an evaluation of the measurement requirements, as stated in the introduction, is done to see whether the requirements are met.

- **Non destructive:**
  The measurement method is an optical technique that uses reflection of light and therefore prevents damage to the multilayer, which means that this condition is met.

- **Measuring liquid thin films of 10 µm:**
  The measurement technique is able to measure liquid thin films with thicknesses of 10 µm, depending on the available wavelength range and spectrometer resolution. Meaning that this requirement is also met. With the measurement of thicknesses between 1 and 5 µm issues can arise with the spectral reflectance measurement method. This is because the FFT of the measurements contains noise within that range. The consequence is that thickness peaks can be overlapped with this noise. Another issue is that thicknesses of 1 µm and thinner can become a problem since not enough or no periods at all of the oscillation are visible within the reflectance spectrum.

- **Measure a thin film within a stack of layers (multilayer):**
  The measurement technique that is used to build a measurement setup is able to measure through multiple layers. Besides this, the method is able to determine thicknesses of more than just the one desired layer within a stack of layers depending on the chosen light source wavelength range and spectrometer resolution. One issue may arise due to the fact that the thick layers within the process are not thick enough such as the stamp and the glass substrate. In most cases, 500 µm thick substrates are used which can be assumed to be incoherently thick without problems. However, the stamp might not be thick enough and can therefore influence the frequency content of the measurement. This means that the process needs certain adjustments to make sure the stamp can be assumed to be incoherently thick. Another option would be to realize that the frequency content of the stamp will be visible in the reflectance spectrum. This will add another

layer to the FFT result but it will still be possible to measure the thin films. It means that this requirement is also met.

- **Accuracy:**
  Morphotonics currently only has a thickness measurement technique available that is able to measure single thin films. In addition, the measurement technique requires the user to remove the thin film from the machine and is therefore not an inline measurement technique. This means that there is no other multilayer measurement technique available to measure a thin film in a multilayer. Therefore it was desired to find a measurement method without any specific accuracy requirements.

- **Implementable within Morphotonics process:**
  The measurement technique consists out of a light cable tip, light source, spectrometer and optical cable. The equipment apart from the light cable tip can be positioned next to the equipment of the process so that will not be an issue. The light cable tip has to be positioned close enough to the multilayer that has to be measured. In case this is not an option, a collimator can be used allowing to increase the distance from the cable tip to the multilayer. Therefore, the measurement method promising to inline measure the thickness of the thin films within multilayers which means this requirement is also met.

Limitations of the measurement method: The measurement technique with the simulation model and the experimental setup have some limitations which are listed below:

- **Accuracy comparison with reference thicknesses:**
  When creating a measurement technique one of the most important subjects is to find reliable and proper reference data. This reference data has to be used to verify that the new measurement method measures logical and correct information. In order to make a perfect measurement technique, one needs a reference measurement which contains no uncertainty. This is clearly not a realistic expectation. In fact, finding good reference layers of which the thickness is in the same range as the desired thin films from the multilayer, turned out to be one of the toughest parts of this research (see Appendix E for a summary). Several attempts have been made with multiple methods to create reference thin films with the desired thickness. This includes a lot of iterations and improvements of these reference thin films. Finally, two methods have been found and used to verify the performance of the spectral reflectance measurement technique. While these reference layers were working relatively well, they still contain an uncertainty.

- **Thickness determination uncertainty:**
  A mathematical model is used to translate the frequency content that can be found in the reflection signal due to interference of light at different interfaces. This mathematical model uses the fast Fourier transform and is able to translate this frequency into an optical thickness. This optical thickness can in another step, be translated into a geometrical thickness with the use of the materials refractive index. The mathematical method used to translate this signal into geometrical thickness includes slight errors which are already noticed during simulation. An approach that can be considered to improve this is to look into the regression analysis instead.

- **Transparent and non absorbing materials:**
  The simulation model assumes that the materials used in the multilayer have zero losses due to absorption and therefore the measurement method is limited in the sense that only a specific range of materials can be used. Besides this, the assumption that the materials are non absorbing might also not be entirely true. Some of the materials used have extremely low absorption coefficients but not a coefficient of exactly zero. Perhaps this causes an additional loss of light intensity in reflectance spectra for the measurements. However this error is most likely negligible since the coefficients will be extremely small if not zero.

- **Effect of surface roughness:**
  The simulation model in this research assumes that thin and thick films which are simulated have flat surfaces and do not include surface roughness. Quinten mentions the Rayleigh criterion [25] that can be used to distinguish rough surfaces from smooth surfaces. Surface roughness can

be neglected below this limit and allows one to use the equations in the model described in this research. Once surface roughness is above this limit, the effects can no longer be neglected. Surface in this research have been those of an optical flat, substrates, both with calibrated surfaces, cured acrylic and water thin films between or on top of these surfaces. Even though surfaces are relatively flat in this research, surface roughness still plays a role in the uncertainty. Further research is necessary to verify to what extend this impacts the performance of the measurement method. Once textures are introduced in future research, the impact of Surface roughness on the thickness determination increases. According to Quinten it 'causes incident electromagnetic radiation to be scattered at this interface, resulting in the loss of intensity of light collected by the detector' [25]. This causes an additional loss of total reflected intensity.

- **Peak recognition:**
  When simulating one or two layers, it is relatively simple to identify which optical thickness peak is related to which film thickness in the multilayer from the FFT result. For a single layer, a single peak in the reflectance spectrum can be seen. For a two layer multilayer, there will be three peaks, one for each layer and one for the combination of the two layers. For a three layer multilayer, there will already by seven peaks in the FFT. This makes it more tedious to identify which peak belongs to which layer since the FFT shows optical thicknesses. Since the FFT deals with optical peaks, peaks from different layer thicknesses with different refractive indices can overlap in certain situations.

Side note:
It is desired to measure the thickness of the thin film while it is still a liquid which is during phase two. After phase two the curing fo the liquid acrylic thin film with UV light begins. However, it is important to realize that there will be a transitioning stage between phase two and three. This means that the the acrylic thin film will not be a perfect liquid resin at one point, and then slightly after that instantly a cured resin. Instead, it will slowly go from a liquid to a cured thin film. This is something to keep in mind when attempts are made to incorporate a measurement technology like spectral reflectance in the R2P NIL process. This may create an uncertainty in the thickness measurement of the liquid thin film. The uncertainty would in this case be caused by the fact that the refractive index and thickness may slightly vary during the transitioning stage of the layer where the layer is partly cured and partly liquid. Besides a thickness measurement uncertainty, it may also become less convenient to tune the process and change the layer thickness since it has already been partly cured.

7

Conclusion

In this thesis a study has been conducted to find out how spectral reflectance can be used to measure the thickness of a liquid thin film. Where the liquid thin film is between two surrounding thick layers together with a second thin film. In this chapter, the conclusions that followed from the results of this thesis will be presented.

The spectral reflectance measurement technique has been proven to be useful in measuring thicknesses of thin films within a multilayer under specific conditions. The thin films can be surrounded by incoherently thick layers which can then be assumed as incident and rear media. Besides this, the technique can be used to measure the thin film thicknesses of a coherent thin films in a multilayer if all the layers can be assumed to be non-absorbing and transparent. The incoherently thick surrounding layers should also be non-absorbing and transparent.

The Spectral reflectance measurement method is preferably used on a stack of two or three coherent thin films. The measurement method can be used on a stack with more than three layers however as more layers are added, the peak recognition becomes rather difficult, especially if there is no thickness information available of any layer within the multilayer. This is due to the fact that the amount of peaks in the measurement result increase significantly as more thin films are added.

The surrounding relatively thick layers can be included while measuring the thicknesses of the coherent stack of thin films as long as the thick layers can be assumed incoherent. This assumption is dependent on a combination of the thickness of the layer, the resolution of the spectrometer and the measured wavelength range of the light source. This means that as the thin films become thicker and come closer to the thick layers, a higher resolution is needed to measure the thin films. This is due to the fact that thicker layers cause a higher frequency in the reflectance spectrum. At some point the resolution is not low enough anymore to assume that the thick layers are incoherent.

The measurement technique includes an uncertainty which has been verified. The technique is verified to be able to measure thin film thicknesses of two layers at the same time. According to the spectral reflectance measurement, one of the layers in the multilayer was a thin film of water with thickness of 9.78 µm and the other layer was a thin film of cured acrylic with thickness of 31.26 µm. During the measurement, the thin films were surrounded by a 500 µm thick glass substrate and a 12.70 mm thick optical flat. Both thin films have different uncertainties that originates from the thickness measured by the spectral reflectance technique. The uncertainty for the water film is 7% and 1.53% for the cured acrylic thin film. The uncertainties are based on the findings from the calibration measurements. It is important to realize that there is also an uncertainty on the expected thickness. For the water film this is an uncertainty of 1.55% due to the pipette. For the cured acrylic thin film it is an uncertainty of 2.00% due to the alternative measurement technique that has been used.

When measuring thin film thickness with spectral reflectance, the oscillation in the reflectance spectrum is used to determine the thickness. The amplitude of this oscillation is dependent on the difference between the refractive index of the layer that is measured, and the refractive index of the layers that are surrounding the layer that is measured. One can use materials with a small refractive index difference and even lower the difference in refractive index by using any combination of materials. However, at a certain point, as the difference between the refractive indices becomes smaller, the amplitude of the oscillation becomes of equal size as the noise in the signal. At this point the difference in refractive index is too small and as a consequence it will no longer be possible to determine the layer thickness.

8

Recommendations

When researching literature one can find multiple topics for future research to increase the performance and measurement possibilities of the spectral reflectance measurement technique. Future research recommendations on the measurement technique that followed from this research will be listed and explained below. Besides that, recommendations for the company Morphotonics are given who might wish to implement a thickness measurement technique into their process.

Future research recommendations:

- To further improve the performance of the spectral reflectance measurement method for multilayers a future research topic can be on the influence of absorption. For this research, only materials of which the absorption coefficient is equal to zero were used meaning that there is no additional phase shift due to absorption. ($\hat{n} = n + i\kappa$ where $\kappa = 0$).
- Another topic can be on taking into account a phase shift due to surface roughness. Or even a step further and develop a simulation model for the total reflection when a thin film includes a texture like the imprints that are done at Morphotonics. One could start with a relatively simple imprint texture such as a step structure and then gradually work towards the more complicated textures.
- Another research direction could be on increasing the number of layers and including incoherent layers in between the multilayer rather than only using incoherent layers as surrounding materials. This will no longer allow one to use the simplified model since the thick layers can no longer be seen as incident and rear media.
- A last recommendation for future research would be to focus on the accuracy of the thickness determination. This can be approached either by looking at the FFT accuracy or by switching to a regression analysis method that tries to simulate reflection of thin films to recreate a measured reflectance spectrum.

Recommendations for Morphotonics:

- Since Morphotonics uses a glass substrate in their process or other thick substrates and relatively thick layer for the stamp, a recommendation would be to make the thick layers thick enough so that those can be treated as an incoherent layers. This is determined by a combination between resolution of the used spectrometer and thickness of the thick layers (see section 3.1.2).
- Another recommendation in the case that the light source has to be placed further away from the multilayer that has to be measured would be to include a collimator (see section 4.2.1).
- The last recommendation would be to prevent optical thicknesses of different layers from overlapping either by making adjustments in thickness or in materials since this is due to a combination of refractive indices and thicknesses. Especially when measuring multiple layers at the same time it can be a tedious task to identify which peak belongs to what layer.

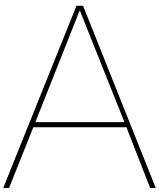

Appendix Literature study

Delft University of Technology

Master Thesis Literature Review

Research into the state-of-the-art multilayer liquid thin film thickness measurement methods

Author:
Julian Bleeker

April 7, 2022

Contents

Abstract

Morphotonics is a company focused on the imprinting of nanostructures in thin films on substrates called nanoimprint lithography. When substrates contain non-uniformities, the imprinting of uniform thickness structures in thin films becomes substantially harder in comparison to imprinting on uniform substrates. Knowing the thickness of the thin film throughout the process allows the user of the imprinting machines to influence parameters in the process to create more uniform imprints. Within this process, one is dealing with a multilayer including an initially liquid layer which is meant for the imprint of the nanostructures. To know the thin film thickness of this specific layer, a nondestructive, noncontact, multilayer liquid thin film thickness measurement technique is required. This literature study will contain a study on the state-of-the-art measurement techniques for thin film thickness measurements and will eventually compare three different techniques. In the end, the study will reason towards spectral reflectance as being the most suitable technique for the given problem. Spectral reflectance does not require any moving parts since it only looks at the reflectance spectrum over a specific wavelength range for a fixed angle of incidence. A spectral reflectance measurement setup requires relatively simple parts such as a light source, spectrometer and an optical cable which makes building a setup feasible within the duration of the master thesis.

1 Introduction

Nanoimprint lithography

As Chou et all mentions in their work [1], nanoimprint lithography (NIL) is a technique for producing micro or nano-scale features and patterns over a large area, with high throughput and for a low cost. It is a technology that works based on a mechanical deformation of a resist. NIL works with a mold that transfers an inverse geometry in a resist onto a desired surface. The best part about this technique is that it allows for the mold to be reused and therefore enables for a long-life cycle. This comes down to a large area, high throughput, low-cost micro/nanoimprint application suitable for a large range of industries. Back in 1995 Chou et all were the first to publish about the concept of nanoimprinting [2]. The mentioned paper from 1995 is the first ever published attempt of imprinting sub-25 nm structures with high aspect ratios into polymers.

As Lan presents in his work [3] one can divide NIL into two main categories. The full wafer NIL and the roller type NIL [4]. Full wafer, also known as plate to plate (P2P). It works by pressing a flat plate which can be seen as a mold or stamp into a resist layer which lays on a rigid substrate see figure 2. This creates full surface contact of two plates which results in high imprint and demolding forces.

To further improve the development of NIL, the issues concerning P2P had to be described. Four important issues had been identified:

1. Achieving uniform pressure distribution across the full wafer
2. Ensuring entirely conformal contact on the imprint full field
3. Avoiding trapped air bubble defects
4. Reducing imprinting forces

While roller type NIL was invented to increase imprint surfaces and throughput of the process it also gave solutions for the mentioned issues. The main difference between full wafer NIL and roller type NIL is that the roller type works with a line contact rather than full surface contact. This highly reduces the imprint and demolding forces. This line contact also reduces the trapped air bubbles effect and variation in thickness. Besides this, the roller type NIL can imprint continuously whereas the full wafer technique can imprint one substrate at the time.

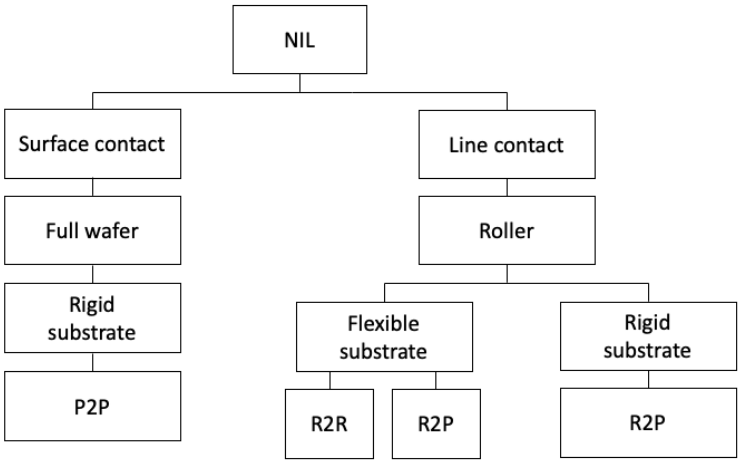

Figure 1: Nanoimprint lithography (NIL) categorization

The roller type NIL can be further divided into two subcategories, roll to roll (R2R) and roll to plate (R2P) as can be seen in figure 1. R2P works with a flexible stamp wrapped around one or multiple rollers and a flat rigid substrate. Instead of a flexible stamp wrapped around rollers one often uses a textured roller. This rigid substrate is supported on top of different rollers in such a way that it can be pushed through the rollers with the flexible stamp. This creates a line contact between the flexible stamp and the rigid substrate which has a resist deposited onto it.

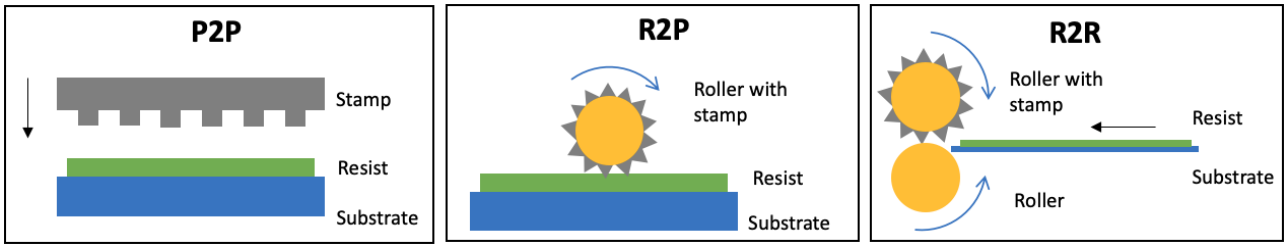

Figure 2: Illustration of the different NIL methods.

Since R2P works with this line contact it has great advantages over the conventional P2P method. However, the R2P still has some problems in realizing an imprint process that works continuously. Especially when dealing with a substrate that has surface non-uniformity issues such as waviness. Figure 2 shows an schematic of both methods where sizes of structures are not shown with proper ratios.

The R2R method uses a flexible stamp around a roller to transfer a nano or micro-structure. With this method a flexible substrate is used to imprint structures on which is generally done in a continuous process of longer substrates. While the R2P method enables you to imprint structures on both flexible as well as rigid substrates but uses relatively shorter substrates compared to R2R.

With all three of the previously described nanoimprint methods initially a fluid resist is used. The molds imprint the structures while the resist stays a fluid. An important step is the curing of the resist. This is done by either of the two fundamental types, either with UV NIL or with thermal NIL [4] Where thermal NIL [5, 6] works with imprinting onto a thermally softened thermoplastic polymer resist, UV NIL [7, 8] makes use of a liquid photopolymer resist that cures by exposure to ultra violet light.

Applications

Nano textures have been an important research area for some time in the high-tech industry now. Different nano textures are applied to improve the performance from a wide range of applications such as the brightness of LEDs, improved efficiency solar panels, high density storage to high clearness (HD) display.

Since large-area NIL is the most cost-efficient way to do this, it is already used to create micro/nanostructures and features for multiple applications in nanoelectronics optoelectronics, optical components, nanostructured glass, biological applications. Multiple dimensional micro- and nanostructures are used to enhance performance of these applications. Figure 3 shows the representative industrial applications and products that fit into the different NIL categories as given by H. Lan [3]. For the roller type NIL category the application are AR films, solar cells, patterning of flexible films, architectural glass, TV with AR structures, flexible electronics, HD displays and OLED. While full wafer NIL is utilized mainly for LEDs but also for HDD and micro lenses.

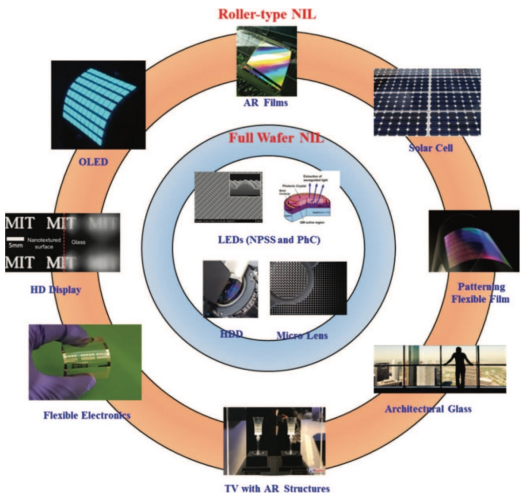

Figure 3: Large area NIL applications per category

Research Motivation

The process of Morphotonics can be divided into five separate phases. These phases take place inside the Portis NIL600 machine from Morphotonics see figure 4a. The five different phases are listed and explained next:

1. Lamination phase

In this phase the mold gets laminated over the substrate. At the same time, the dispensed droplets are spread out over the surface during the lamination and since the roller ensures a continuous line contact, air bubbles are eliminated. Important in this phase is also that textures in the flexible stamp are now filled with the resist.

2. Liquid film phase

In this phase we are dealing with a liquid film which is in between the substrate and the flexible stamp.

3. UV curing phase

In this part of the process, the thin film is cured by UV light. This phase can be seen as a transitioning phase from liquid to solid imprinted textures.

4. Cured film phase

In this phase the thin film is completely cured but is still under the stamp.

5. Delamination phase

The last phase is the delamination phase which is where the flexible mold comes off the imprint and where we have the cured thin film on a substrate. This gives the final result of the imprint process. This result can be a flat thin film or a thin film with texture. Where the objective of this process is to create a uniform texture in a thin film on top of the substrate. See figure 4b for a schematic of these phases.

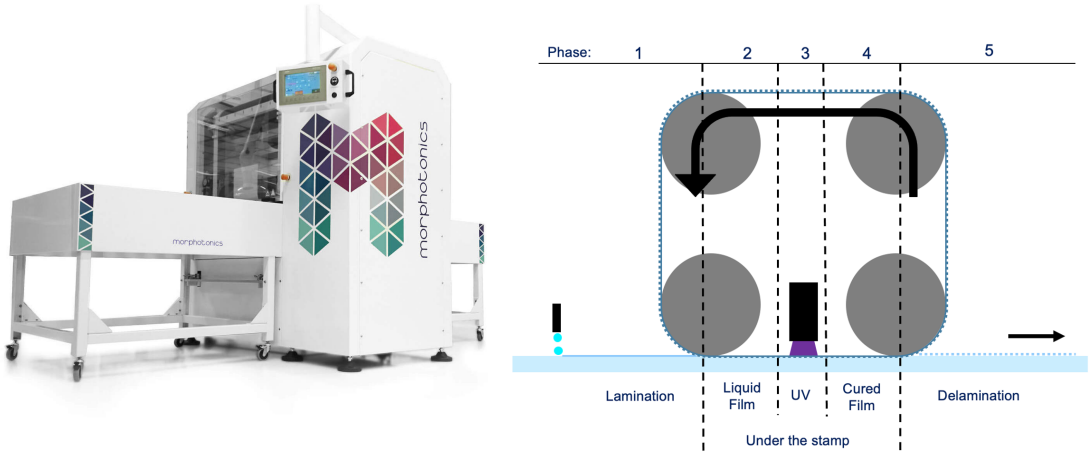

(a) Portis NIL600 from Morphotonics. [9] (b) A representation of the phases in the process.

Figure 4

The described process works well whenever there is a flat substrate. Morphotonics has realized that the process of imprinting a uniform texture becomes significantly more challenging whenever the substrate contains non-uniformities such as being slightly curved. Due to such non-uniformities the imprint pressure will not be uniformly distributed over the surface of the substrate. This results in non-uniform residual layers. This problem often occurs when imprints need to be made on solar panels. Multiple attempts have been made by Morphotonics to solve this problem. For example, initially depositing an excess volume of resist onto the substrate. Also, changing the formation of droplet deposition. Besides this there is also a certain pressure on the flexible stamp. Different pressures have been used to try and change the result of the process.

In the end there is an input, depositing droplets on the substrate. Which leads to a result, a cured thin film. But when you look at what happens to the resin in phase two, three and four one can conclude that these phases can, to some extend still be seen as a black box.

To come closer to a solution for this problem, one needs to have a better understanding of what happens to the resin inside the black box. One of these steps is to measure the thickness of the thin film in each of the individual phases. A first step would be to measure the film thickness of the thin film in phase two where the thin film is still a liquid. It is important to measure the liquid at this point in the process (phase 2) since we are not yet dealing with a cured layer which means that one can still have an impact on this layer. It will not be possible or at least significantly more challenging to make adjustments to the layer in phase three or four once it is cured.

This thesis will focus on measuring the thickness of this thin film in phase two of the process. Knowing the thickness at the individual phases allows the user of the machine to influence different parameters in the process to adjust the layer thickness more precisely. It is also important be able to measure the thicknesses at the individual phases to see what the impact of the different phases is to the thickness. There may be factors that have an impact on the layer which are currently unknown. Measuring the thickness differences at the individual layers gives meaningful information on where to look for these unknown factors.

2 Layer characterisation and thickness measurement

At Morphotonics there are machines available to imprint nano textures onto a surface with the use of nano-imprint lithography (NIL) that is focused on the technique roll-to-plate (R2P). To get a sense of the outcome of this imprint process, Morphotonics currently performs thickness measurements of the cured imprinted layer after the process is completed and the substrate has been taken out of the machine. For this research it is desired to get more information of what happens with the thickness of the imprint during the process. Earlier, this process has been divided up into five different phases, lamination, liquid film, UV hardening, cured film and the delamination phase. As a first step, the focus of this research will be on phase two where the deposited resin on the substrate is still a liquid and is still covered by the stamp.

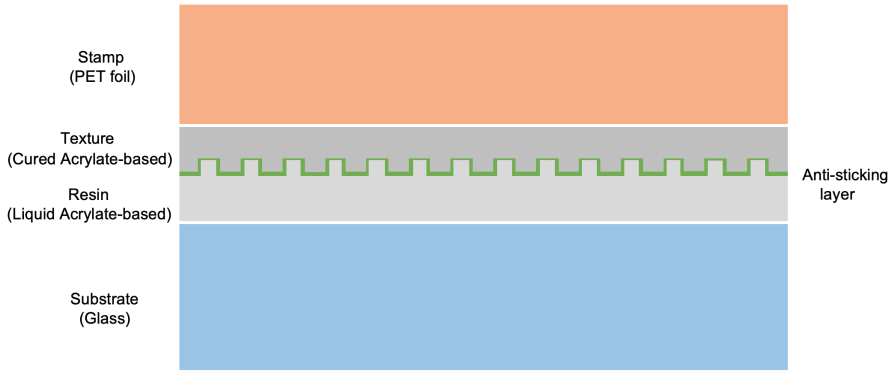

Figure 5: Different layers in the process at Morphotonics

Multiple layers of different material can be identified within this phase of the process. The different layers starting from the bottom are, the substrate, a liquid resin, an anti-sticking layer, a cured resin and the stamp (see figure 5). Generally, the substrate is made from thin glass (eagle glass), the liquid resin layer is the in phase one deposited acrylate-based layer, the anti-sticking layer is a layer that prevents the cured resin layer to stick to the liquid resin layer, the cured resin layer is an acrylate-based layer that consists of the inverse texture that should be imprinted and the stamp is a flexible polyester foil. The liquid resin layer has similar material properties as the cured texture resin layer. This is why an anti-sticking layer is applied to prevent these two layers from sticking to each other.

At this point the different layers during the process in phase two have been identified. Information about some of these layers is known. The thickness of the substrate is determined by choice of eagle glass type. The thickness of flexible stamp is also given while the cured texture resin is a predetermined thickness containing the inverse of the desired imprint texture. This texture resin can contain thickness steps whereas the substrate and the flexible stamp are relatively flat. The thickness of the anti-sticking layer is not known but it is known that this layer has an extremely small thickness compared to the thickness of the texture resin layer. Apart from these layers we are left with the deposited liquid resin layer. This is the layer that should be measured. It is known that part of this layer is used to imprint the inverse texture of the cured resin layer and that a part of this layer is excess liquid called the residual layer. Morphotonics uses two ranges of thicknesses for this layer. A thicker and thinner range. See table 2 for more details of these individual thicknesses.

Table 1: Thickness ranges of the different layers in the process at Morphotonics

Layer	**Thickness range(s)**
Substrate	300 µm–500 µm
Resin	Thick: 1 µm–10 µm Thin: 100 nm–150 nm
Anti-sticking	$\ll$ Thickness liquid resin
Texture	Comparable to liquid resin (differences in residual layer)
Stamp	250 µm

The goal is to measure the thickness of the liquid layer at phase two. This means that the measurement must go through multiple layers. From this perspective you could say that it concerns a multilayer measurement. Either from above meaning it must measure through the stamp, cured resin and anti-sticking layer, or from below which then means that it must measure through the substrate. But since the only thickness that we are really interested in is from the liquid resin layer one could argue that it is rather a single thin film measurement problem. This thesis will look at this problem as a multilayer measurement going forward.

Morphotonics has a department that uses imprints with a flat stamp as tool to get more information on layer thickness uniformity within the imprinting process and preferably improve on this matter. In order to keep the tool relatively simple, it is done by applying exactly the same process as mentioned above in figure 5 but then with the texture layer being replaced by a flat stamp. This is done because the influence of textures are then eliminated at first. This information is the first step towards getting a better uniformity in layer thickness with imprinting textures in the future.

This process results in the multilayer stack as can be seen in figure 6. Their goal is to make this layer uniform over the entire surface. Measuring the thickness will help them with this objective. Besides this, the NIL research group is also interested in knowing more about the possibilities of measuring thin film thicknesses.

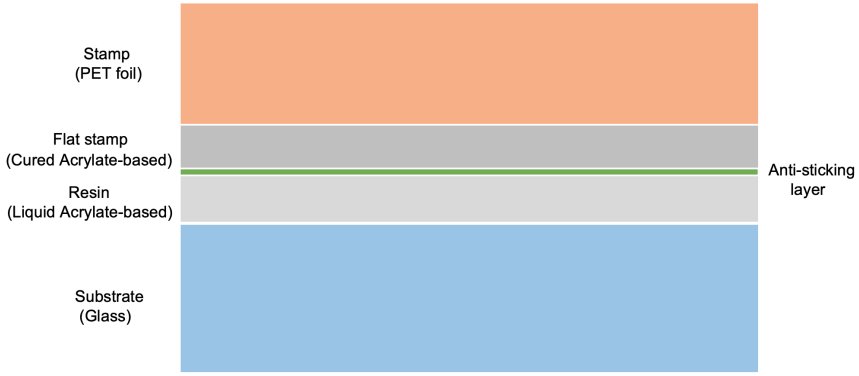

Figure 6: The different layers in this case with a flat stamp.

For this research the goal is to find a measurement technique that can measure the thickness of the liquid resin layer inside the multilayer. At this point it is known what layers the multilayer consist of in the process of Morphotonics both with regular and flat stamp. For this measurement, a certain technique will be necessary. Let us look at the different requirements for this measurement technique.

First of all, the technique should be able to measure two thickness ranges, thick and thin, see table 2. Besides this it will not be possible to get into contact with the resin layer since the layer will be a fluid that is kept in position by the other layers around it. Therefore the measurement technique should be a contact-less method which can measure through the layers. To preserve the imprinted structure for the final application, it is also important to work with a non-destructive measurement technique. The measurement method must be able to make a distinction between the different layers present. Lastly, a desire is there to make the thickness measurement an inline measurement. This would theoretically allow for adjustments on the volume of resin that has been deposited to match the needed quantity. This brings certain size limitation since it will become an inline measurement in the machine from Morphotonics. The step to making this an inline measurement is out of scope for this master thesis and therefore these size limitations will not be part of the requirements of the measurement system.

- Thickness ranges: Thick and thin
- Contact-less and non-destructive
- Distinction between different layers in the multilayer
- Liquid layer measurement

3 State of the art measurement techniques

In this chapter, the literature of the state of the art thin film thickness measurement techniques will be presented. This chapter will start by showing the different measurement techniques that have been found broken down into the different physics they belong in. After that, an attempt to further characterize the individual measurement techniques will be shown.

Literature has been gathered with the use of Google scholar, mainly to get an idea of the existing measurement techniques for thin film thickness. When searching different words have been used including synonyms or different formulations. The search started with different combinations of "thin film thickness measurements" and gave a couple of overviews with different techniques [10, 11, 12]. This gave the first idea to separate the measurement techniques into different physics. Then by using the words "multi-layer", "thin film stack", "wet film thickness measurement", "coating measurement", "surface measurement", "lubrication thickness measurement", "lubricant layer", "non destructive", "non contact" it became clear that optics and ultrasonic where two important areas of research. Focusing on these areas important keywords were, "reflectance", "transmission", "spectral reflectance", "multi-layer optical", "ellipsometry", "spectral ellipsometry", "multi wavelength reflectance", "interferometry", "ultrasound", "time-of-flight", "resonant frequency ultrasound", "overlapping reflections". After it was clear that spectral reflectance was important, papers found were screened for references. Two important aspects to look for were determined to be the measurement range limits and the ability to measure non destructively over multilayered stacks.

3.1 Mechanical

3.1.1 Stylus profilometer

Stylus profilometry is a contact and destructive method that is mostly used to measure surface roughness but can also be used to measure thicknesses. It works with a stylus which is a sharp tip, that is put into contact with the substrate that has the to be measured surface positioned on it. The substrate is moved underneath the stylus and the deflection of the stylus is measured. With this deflection, the thickness of the surface can be determined. There should be a step between the substrate and the film as discussed in the work by Piegari [12] which make the stylus vertically displace as the substrate is pushed further underneath the stylus.

3.1.2 Liquid film gauge tool

The liquid film tool is a contact and destructive technique made to measure liquid film thickness. It is used by simply pressing the tool onto the liquid film and then look for the value that is not covered by substance of the layer [13].

Figure 7: Example of a liquid film gauge tool made from stainless steel.

3.2 Electrical

3.2.1 Capacitive comparison

The capacitance measurement technique is a non-contact technique that can be used to measure thickness of conductive materials and works by comparison. It is used by measuring a film with known thickness and measuring the capacitance through it. By comparing this to a film with unknown thickness but from the same material one can determine the thickness since capacitance response curves are highly linear [14]. This is possible since the output of a capacitance sensors is proportional to the distance to the object. The capacitance method requires access to the substrate from both sides and is not suitable for measuring multilayered stacks [11].

3.3 Optics

When it comes to measuring surface roughness and thickness, optical methods have been a well established research area. The great thing about optical techniques is the fact that they are non-destructive and most of the times do not require any surface treatment while giving reliable measurement results.

An initial breakdown of optical measurements techniques for thin film measurements has been as shown in figure 8.

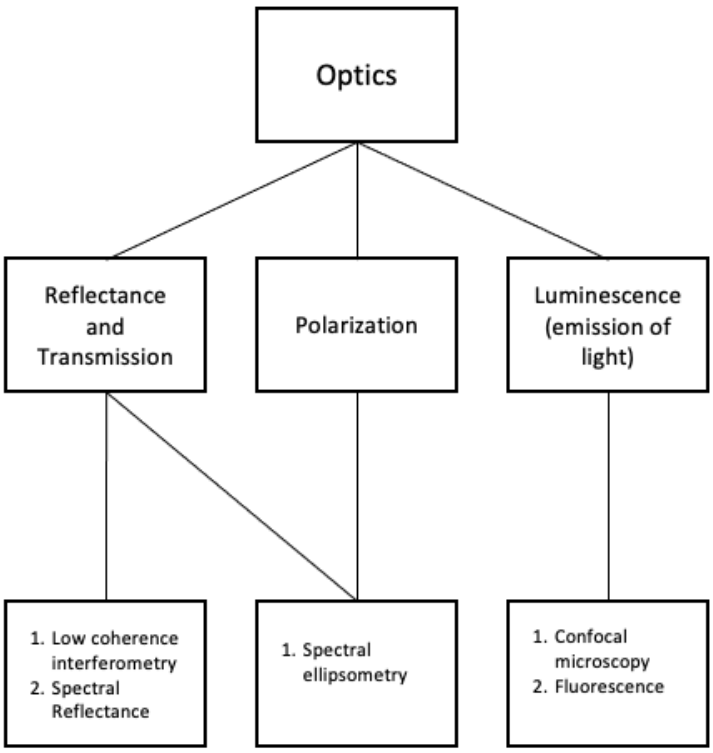

Figure 8: Breakdown of different optical techniques

3.3.1 Spectral reflectance

The measurement technique used to measure thin film thicknesses that looks at interference between reflected/transmitted light rays is called spectral reflectance (SR). Measurements give a reflection spectrum as output and from these spectra optical parameters can be determined. Often used to measure a single film thicknesses for example as El-Naggar et al. did [15] among others [16, 17, 18]. Besides this it is also used in the literature for multilayer films thickness measurements [19, 20, 21].

Let us have a look at the case with a single layer, a light source is sending out light onto the substrate see figure 9. Part of the light reflects (B1) and the remainder transmits through the first interface it runs into which is the top of this layer. The part of the light that transmits through then reflects on the next interface which is the bottom of this layer (B2). Again the remainder transmits (B3) through the bottom interface of this layer. This reflection then transmits through the top interface and interference takes place with the rays that reflected at the first interface at the top surface (B1 and B2). The interference between these different reflections is measured in a reflection spectrum for different wavelengths of the light. From this reflection spectrum thin film optical parameters such as refractive index, absorption coefficient, extinction coefficient and thickness can be retrieved.

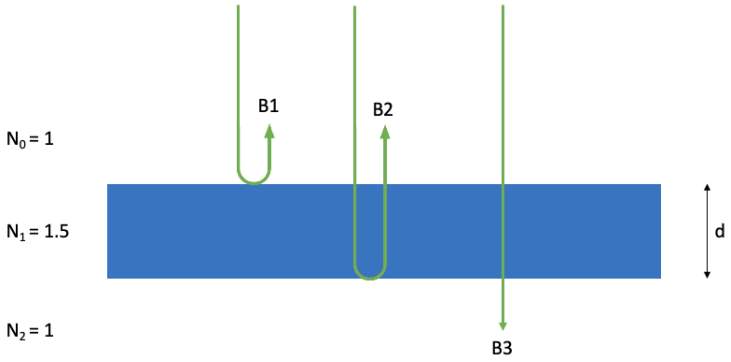

Figure 9: Light reflects and transmits on/through the interfaces.

Reflectance is measured at different wavelengths of light with this measurement technique. There are a few possibilities in creating different wavelengths. One way to create a situation with multiple wavelengths is with the use of an LED that has a distribution of wavelengths. In figure 10, three different Gaussian distributed LEDs are shown. These are Light emmitting diodes that have a distribution of wavelengths with the highest wavelength in the middle of the light and a decreasing wavelength towards the outer circles of the light. So in fact the wavelength is not changed during the measurement but since these LEDs include different wavelengths it can be seen as such. The figure shows a Gaussian distributed LED but this could work with any sort of wavelength distributed LED. A different way of conducting this measurement would be with the use of a single wavelength light and changing this wavelength over time so that a similar outcome for the reflectance spectrum can be measured. This can for example be done with a scanning laser. The spectrum will then have a different shape.

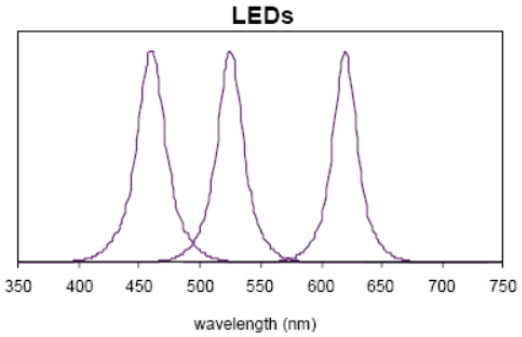

Figure 10: LEDs with a Gaussian distribution of wavelengths [22]

An example of a reflectance spectrum can be seen in the upper part of figure 11. One can clearly see how an LED with a Gaussian distribution of wavelengths was used for this measurement. Also an interference pattern is formed around this Gaussian distribution. This is a pattern formed by constructive and destructive interference of light between rays B1 and B2 (see figure 9). You can see the different maxima and minima with a certain frequency.

The frequency of this spectrum can be translated into a optical thickness with the use of a Fast Fourier Transform (FFT). One determines the geometrical thickness by dividing the optical thickness by the refractive index. In the example a substrate with refractive index of 1.5042 was used which gives a geometrical thickness of 750 divided by 1.5042 equals 498.6 mm while a 500 mm thickness substrate was used for this measurement. When multiple layers are measured, one will notice that these frequencies overlap each other in this graph. Is is especially at that point that the FFT comes in useful to extract the different frequencies [23].

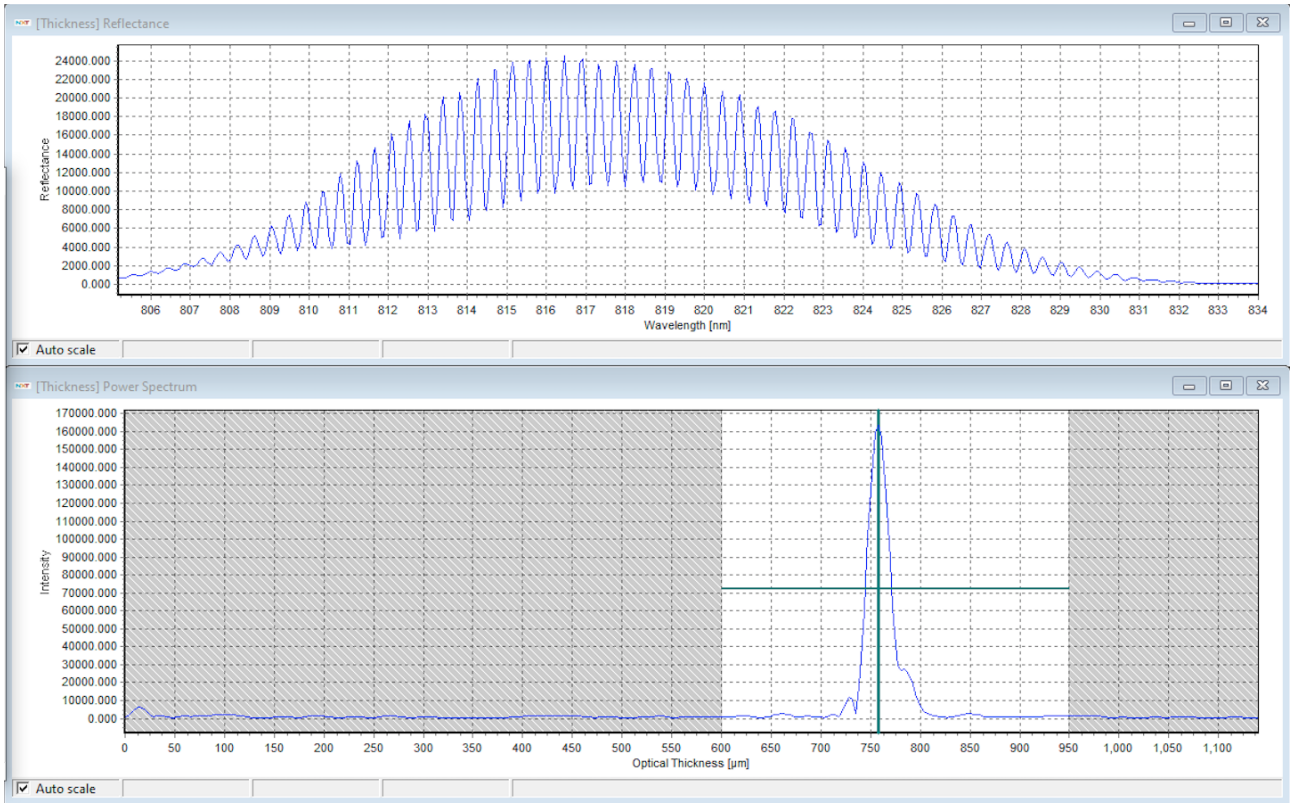

Figure 11: Reflectance spectrum measurement result for single layer of glass substrate.

We know that B2 travels two times the thickness d of the substrate more than B1. Multiplying this geometrical distance by the refractive index gives us the optical path length difference (PLD) between B1 and B2. This can be used to calculate the amount of wavelengths of the light that fit into this optical path length. This gives us the following equation:

$$m \cdot \lambda = 2 \cdot d \cdot n \tag{1}$$

Where m is the amount of wavelengths thus an integer number, λ is the wavelength, d is the film thickness and n is the refractive index of the film material. Besides this we are looking for the constructive interference points in the spectrum. Constructive interference occurs when waves have a PLD of λ or a multiple of λ. This should be equal to the difference in wavelength of the individual peaks in the spectrum multiplied by the amount of wavelengths.

$$m \cdot \delta\lambda = \lambda \tag{2}$$

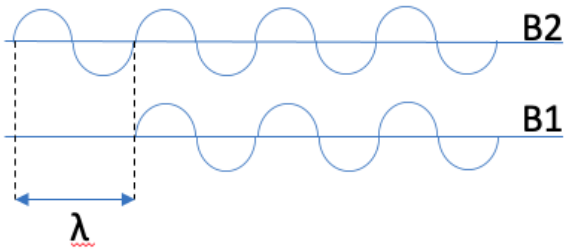

Figure 12: Constructive and destructive interference for certain path length differences between waves.

3.3.2 Spectral ellipsometry

Assume a thin film that is too small for interference bands to appear in the reflection spectrum. The consequence will be that the use of SR for thickness measurements is not feasible. In this case where the thin film thickness is too small one usually makes use of ellipsometry methods [24].

Spectroscopic Ellipsometry (SE) not only looks at reflection of light but also at the polarization of the light before and after this reflection [25]. Light from a light source is send out with an angle of incidence and is first linearly polarized before it reflects from the substrate. The polarization changes are measured as well as the reflection. The polarization change adds another known variable besides the reflection data and makes it a more powerful technique. This also means that it is a more complex technique with longer measurement times which ultimately means that it is a more expensive method compared to SR. With SE one looks at the ratio of outgoing to incoming orthogonal electric fields. These are measured at a wide spectral range of wavelengths. More wavelength gives more information of the layers. With this information, more unknowns are involved as the complex refractive index (n - ik) for each individual material changes with the wavelength. Doing this measurement from different angles of incidence gives more known variables in this problem. It is important to note that SE is not directly measuring film properties. These film properties are later extracted from data analysis by comparing the measurements with theoretical calculations based on model description of the sample structure.

When you are looking for information of a multilayer stack it is recommended to acquire information of a more feasible sample first according to to N. Hilfiker et al. [26]. For example start with only two layers or even a single layer. Two different approaches have been looked at. Imagine it is desired to measure the thickness of a 4 layered stack including the substrate. The first approach that is recommended first measures substrate with layer A, then substrate with layer B followed by the substrate with layer C and at last a combination of layer A,B,C and the substrate. Besides this research one can also start with the substrate and layer A and then step by step add another layer. These individual steps will help with data processing later on.

3.3.3 Low coherence interferometry

Low coherence interferometry (LCI), also known as white light interferometry (WLI) aims to measure the path length difference between light beams reflecting from the test substrate and beams reflecting from a reference mirror. This is done by producing a short coherence interferogram as shown by kim et al [27]. LCI has been used a lot to make multi-dimensional surface maps. Several difference techniques have been developed but most of them allow for a precision of nanometer resolution in surface mapping of opaque surfaces. With LCI one can not only measure thickness of a thin film but an entire volumetric map can be created. At this point (1999) the technique was still looking at single layers. Multiple reflections theory is an important piece of this technique which looks at reflection from the top and bottom interfaces of the layer similar to the spectral reflectance technique.

Reflectometry (spectral reflectance) can be used to measure the reflectance of a layer and calculate the thickness from it while being limited by a single point as Jo et al [28] mentions. White light scanning interferometry on the other hand, can be used to measure 3 dimensional profile of a transparent surface and therefore also the thickness. By combining a spectrometer in an interferometry system, which essentially means combining reflectometry and white light interferometry, it allowed for higher resolution and less ambiguity in detecting the height of the surface caused by the thin film effect. This makes LCI or WLI a more powerful but more complex and expensive method compared to spectral reflectance.

Table 1. Comparison results with a commercial instrument of ellipsometer.

Sampling Position		Ellipsometer	(mean ± σ)
SiN Layer (1st Layer)	P1	581.7 nm	594.3 ± 0.25 nm
	P2	1004.3 nm	1011.5 ± 1.55 nm
SiO_2 Layer (2nd Layer)	P1	1246.9 nm	1255.2 ± 0.75 nm
	P2	1563.9 nm	1568.0 ± 2.52 nm
SiON Layer (3rd Layer)	P1	1312.1 nm	1294.1 ± 2.06 nm
	P2	641.5 nm	642.6 ± 0.27 nm

Figure 13: Results of multilayer measurement compared to commercial ellipsometer.

Later on Ghim et al [29] proposed a spectrally-resolved white-light phase shifted interferometer technique that focuses on measuring phase and reflectance over a wide range of wavelengths and thereby achieving volumetric measurements of multilayer structures.

3.3.4 Fluorescence

Fluorescence is a non-contact, non-destructive thickness measurement technique for single layers. The technique works with a light source that brings excitation energy of the light towards the to be measured layer which should contain fluorescent dye. This excitation energy of the light excites the fluorescent particles towards a different energy state. While these particles are in this higher energy state in the order of nano-seconds they dissipate part of that energy. The energy level of the particles will now be lower when they return to their ground state. They will be emitting light of a wavelength that is higher than the wavelength of the light source [30].

Different colours of fluorescent light will be emitted and through that the thickness can be measured see figure 14. The important part of fluorescence is that it shines light on the entire substrate which means that it is not just a single point measurement but rather a surface measurement.

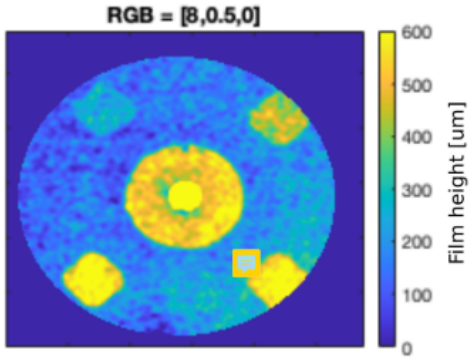

Figure 14: Example of thickness measurement with fluorescent technique.

3.3.5 Confocal microscopy

Similar to fluorescence confocal microscopy makes use of shining a light and look at excitation energy of the light in dye that are included in the specimen. The main difference is that fluorescence methods do surface measurements which means the light is shining over the entire surface. While a light beam in confocal microscopy travels through a microscope which means that the light is focused on a small spot on the specimen. Namely, the focal point of that microscope. This significantly increases resolution of images from a confocal microscope when comparing to the regular fluorescence method. Combining individual point measurements into a grid then gives a surface measurement. With this method 3D images can be constructed. To learn more about this technique see the work by Nwaneshiudu et al [31].

3.4 Electromagnetics

3.4.1 X-Ray spectroscopy

X-Ray spectroscopy works by beaming the substrate with electron and looking at the electron beam energy required to penetrate the film. With this knowledge one can determine the film thickness of a layer. To learn more about this method see the work by Wei et al [32]. An important condition for this technique is that the measurement takes place in vacuum.

3.4.2 Auger electron spectroscopy

Measuring method that works with electron or photon excitation. Similar to X-Ray spectroscopy does this technique require to be in a vacuum. See the handbook of thin films by Frey and R. Khan for further details on this technique [10].

3.4.3 Eddy current

The eddy current method is a contactless method to measure layer thickness which works for conducting thin films. It works with an alternating primary magnetic field which induces electric currents. These currents are called eddy currents in an electrical conductor. The magnetic field is created with the use of a coil. Change of impedance can be used to determine the distance from the coil to the conducting layer. High frequency currents (100 kHz to a few MHz) are need for accurate measurements. In principle one can say that as frequency increases, so does the accuracy of this technique [10]. This technique is often refered to as magnetic induction [33].

3.4.4 Quartz Crystal monitor

Wajid did research on the topic of quartz crystals [34]. These crystals are oscillators used to have an impact on the deposition rate of the layer. This means that it is not a method used to measure a thickness after it has been deposited. The working principle of this method is that these quartz crystals have a certain resonant frequency which is impacted when weight is added on top of it. This frequency changes then gives the user the ability to adjust the deposition rate.

3.5 Chemical

3.5.1 Ink colour saturation

This measurement method works when measuring thickness of a liquid thin film by dissolving a small percentage of ink particles into the layer. With this method, layer thickness over an entire surface can be measured. As can be seen in figure 15, the darker the printed surface, the thicker the layer. This imagine is from a measurement performed at Morphotonics with ink particles dissolved in a thin film, it can clearly be seen that there is a distribution of colour over the surface indicating a thickness variation. Theoretically this colour distribution could be used to measure the thickness variation but literature does not show any performed research on this topic.

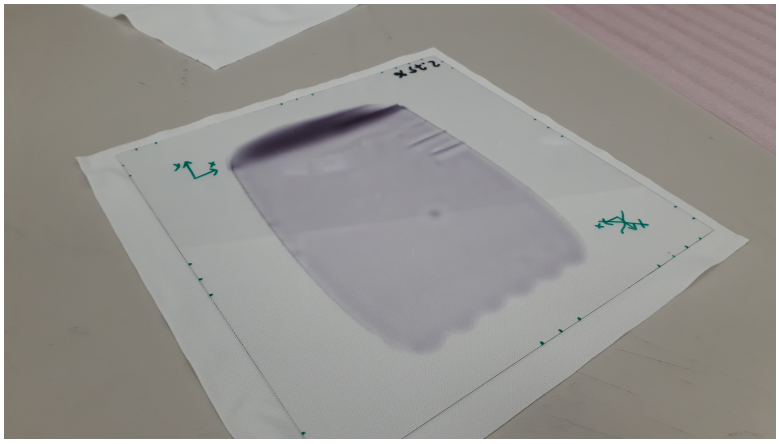

Figure 15: Thickness measurement result from the ink saturation method.

3.6 Acoustics

3.6.1 Ultrasound

To start with, ultrasonic measurements can be used to analyze not optically transparent films [10]. Just like certain optical measurement methods use transmission and reflection of light waves, does ultrasound use transmission and reflection of sound waves. Dwyer-Joyce et al. [35] have done a research to discover the possibilities of measuring lubricant-film thickness in bearing systems using ultrasound waves. This research concludes that there are three methods that can be used for ultrasonic measurements, time of flight (TOF) method, resonance method and the spring model. See figure 16 for the thickness ranges of these individual methods. The reflections of ultrasound waves are depending on the ultrasonic frequency, acoustic properties of the layer material and the layer thickness. Two scenarios are described. One where the wavelength is much greater than the film thickness, which means that the response is dictated by the stiffness of the layer. The other scenario is where the wavelength is similar to the film thickness. The interaction of the wave with the layer is then dictated by its resonant behaviour. Reflected sound pulses give a reflection coefficient spectrum as output. Combining this spectrum with either the layer stiffness or the resonant frequency the thickness is obtained. Measured film thickness values ranged from 50 nm − 100 nm.

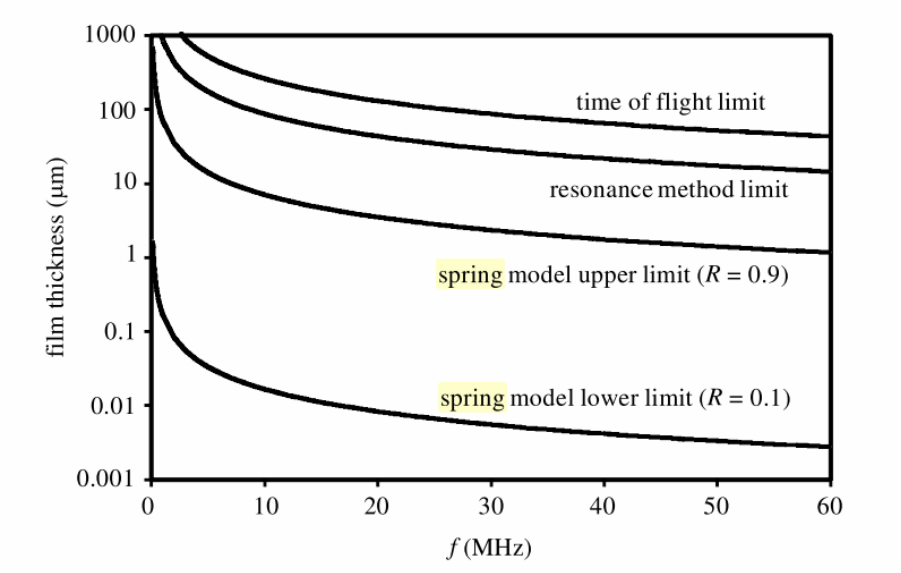

Figure 16: Film-thickness measurements limits for ultrasonic methods.

Al-Aufi et al [36] looked at the research done for a thin film between two stationary solid materials, so that he could get a better understanding for his research that included an gas/liquid annular flow where the liquid is flowing and has a different material on either side.

It all begins with a conventional method that is mentioned. The time of flight method (TOF). This works by sending out an ultrasound waves and measuring the time difference between transmitted and reflected pulses from the top and the bottom. With this information the thickness can be determined when the speed of sound through the medium is known. However, this technique only works whenever a film thicker than 50 µm. If a film is too thin, the reflected pulses overlap and it becomes impossible to distinguish the individual reflections. This technique is often used for corrosion monitoring and gauging of metallic components.

When layers become thinner, different reflected pulses can overlap which has to do with the wavelength of the pulse. This makes it hard to extract the right information from reflection coefficient spectra. Certain techniques are investigated and do come up with solutions for certain thickness ranges (figure 16).

4 Research loop

The aim of this thesis is to measure the thickness of a thin film inside a multilayer of thin films. An attempt will be made to do this with an advanced optical measurement technique. To validate the measurement results, a calibration system is necessary.

This means that there are two parts to this research:

- Contact-less, nondestructive measurement of thickness from a thin resin film within a multilayer of different materials.
- Realizing a calibration design that validates the realized measurement technique.

The focus will be to make a complete research loop that includes a first attempt of this measurement technique. A future thesis subject could be an in depth research on the optical side of this problem to get measurements with higher resolution or improving on other issues that may arise on the optical part.

5 Thesis proposal

5.1 Problem definition

Morphotonics desires to get more information about the different phases in the process of imprinting nanostructures. A step in the right direction would be to find out what the thickness of the thin resin film is during the process. At that point in the process the resin is still a liquid which means that one can influence the layer relatively easy compared to phase four where it has been cured. There are two parts to that problem as stated in the previous section:

- Contact-less, nondestructive measurement of thickness from a liquid thin film within a multilayer of different materials with spectral reflectance upto 5 layers and finding out what the limits are in terms of thickness range and minimal difference in refractive index between the different layers.
- Validating the measurement results.

In order to reach these objectives, the following research questions have been formulated. Some of these questions have already been discussed and answered within this literature study.

- What measurement technique can best be used to measure a thin film thickness within a multilayer of materials?
- What is the difference between measuring a solid or a liquid thin film?
- Will significant thickness differences between layers within a multilayer stack cause any problems in the measurement? So can you for example have a relatively thick layer together with a rather thin layer?
- What ranges need to be measured with the measurement technique?
- What type of light source is needed to perform the measurement? What wavelength ranges?
- What calibration method can be used to validate this measurement technique?
- What is the minimal difference of refractive index between different layers to get reflection of light at the interfaces between these layers?
- Can the measurement technique be implemented within a Morphotonics machine?
- Can individual layers be "turned off" by using a reflective layer?

5.2 Approach

In order to achieve the desired goal, which is the measurement of the liquid resin layer within a multilayer stack of five different layers, let us first look at how to divide this task up into simpler milestones.

It all begins with the theory behind the spectral reflectance measurement technique. Before a measurement setup can be build, a simulation should be performed to get an understanding of the measurement method and the assumptions that are made within this method. A simulation of the reflectance of light on single layer of thin film will be made. This will tell us more about aspects such as different light source inputs, the impact on internal reflection inside the thin film or about the differences between using a solid or a liquid material. Besides this, it could also show more about the impact of changing thickness of the thin film on the reflectance spectrum. When single layer reflectance simulation is successfully done, adjustments and additional inputs will be done to create a multilayer simulation.

After completing the simulation for single and multilayer reflectance it will be time to find the right materials and building blocks to build a spectral reflectance measurement setup. This setup will give reflectance as a function of wavelength as an output, in a so called reflectance spectrum. Within this setup, a light source, optical cable and spectrometer will be the most important parts. After this setup has been build, the first step would be to try and measure a single layer with known thickness. This could for example be a substrate since this has known dimensions. As soon as this works properly, one can start looking at a double layer measurement. This measurement will include some more difficulties in data processing because multiple peaks can overlap in the reflectance spectrum. The steps that follow are about adding the other layers to get closer towards the real scenario of five layers that is described in chapter two for the process at Morphotonics.

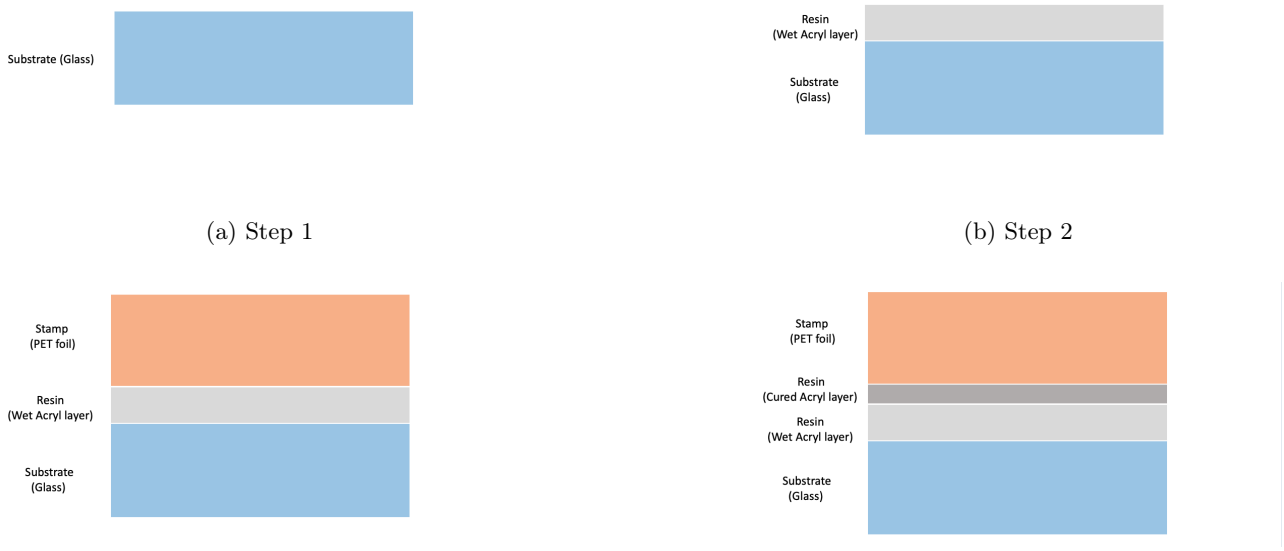

(a) Step 1

(b) Step 2

(c) Step 3

(d) Step 4

Figure 17: The different individual step in this research.

In summary these will be the steps of this research:

- Reflectance simulation
- Building measurement setup
- Measuring single layer - Substrate
- Developing calibration method
- Measuring double layer - Substrate + foil
- Measuring 3, 4 and 5 layers - Substrate + liquid resin + anti sticking layer + cured resin + foil

Simulation direction and sources
Within this simulation different light source inputs can be compared. One could for example think about using gaussian distributed light source. The question is whether the wavelength range of a single LED is wide enough for the measurements. If not, a combination of multiple LED's might be worth looking into. Alternatively, one could look at a different light source that allows you to have a wider range of wavelength.

Apart from this, the impact of internal reflection can be looked into. Each time light reflect or transmits at or through an interface, an extra factor is added to the light intensity. This can best be explained with the fresnel equations as shown by Stenzel [37]. In his book Stenzel also talks about the difference between light reflection and transmission in thin films versus big slabs and a combination of the two.

Another input for the model can be the reflectance calculator from Filmetrics [38]. This calculator allows you to see theoretical reflectance spectra for different settings concerning number of layers, thickness of layers and material of these layers. This calculator is based on the complex-matrix form of the Fresnel equations.

When looking at the theory behind multilayer thin films the paper by Byrnes can be useful [39]. Simulating a combination of thin and thick films is also sumarized there and is referred to as incoherent films. This paper also refers to a Python software package with calculations on the matter. Reflection or transmission through a single interface between two media can be described by the fresnel equations. When multiple interfaces exist which is the case in a single layer already, then the transfer matrix method can be used to describe the interference of internal reflection between two interfaces [40].

Apart from building the measurement setup and measuring multilayers two other aspects concerning the reflectance measurement technique should be looked at:

Minimum difference in refractive index
When measuring a double layer with the spectral reflectance technique another interface is added. In this measurement there is the top interface of the first layer, the bottom interface of the first layer (which is the top layer of the second layer) and the bottom interface of the second layer. In order to make a distinction between the individual layers, light should reflect at each of these interfaces (B1, B2 and B3, see figure 18). When the two layers have a clear difference in refractive index, this will not be an issue. But when those materials have similar refractive indices it could become an issue as light does not reflect at the interface in the middle anymore. Part of the measurements will include a study on the limits of these refractive index similarities. Morphotonics has multiple resins available that have slightly different refractive indices. If they allow usage of these resins, that could be the starting point for this topic. If smaller or bigger differences between different layers are required then a different solution needs to be found for this.

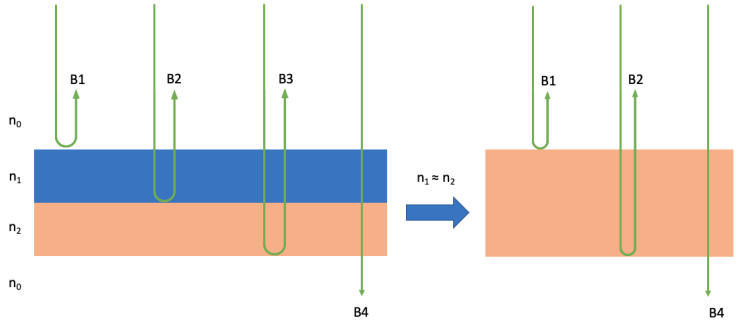

Figure 18: Finding out what the limits on the refractive index are between different layers.

Minimum film thickness
When a film is too thin interference patterns can not fully develop with this technique. Part of the measurements will include a study on the limits of the thickness for which the interference patterns are not useful anymore. When measuring the thickness of one layer within a stack of five layers becomes an issues for example due to significant thickness differences between the layers, a plan to fall back on can include the following while sticking to rather simplified situation that can be measured by the realized measurement setup:

Preventing light from entering certain layers
Let us look at the measurement of a multilayer consisting of an n number of thin films. When you are for example only interested in the thickness of the second layer within this multilayer it would be of great help to simplify the situation. This simplifying of the situation might be possible by eliminating certain layers in the measurement by restricting light from entering into these layers. This can perhaps be done by applying a reflective coating on a layer in the multilayer stack. This way one can arguably "turn off" certain layers.

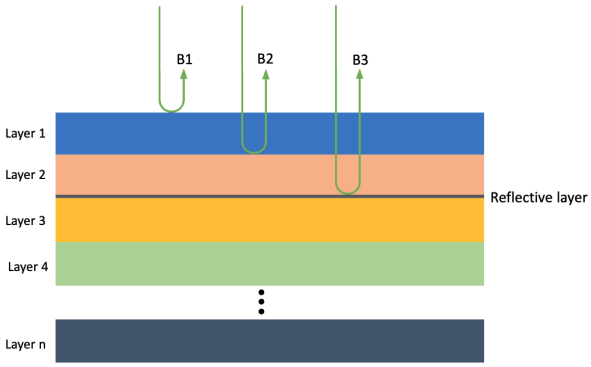

Figure 19: Way to eliminate layers from the reflection spectrum with the use of a reflection coating.

5.3 Planning

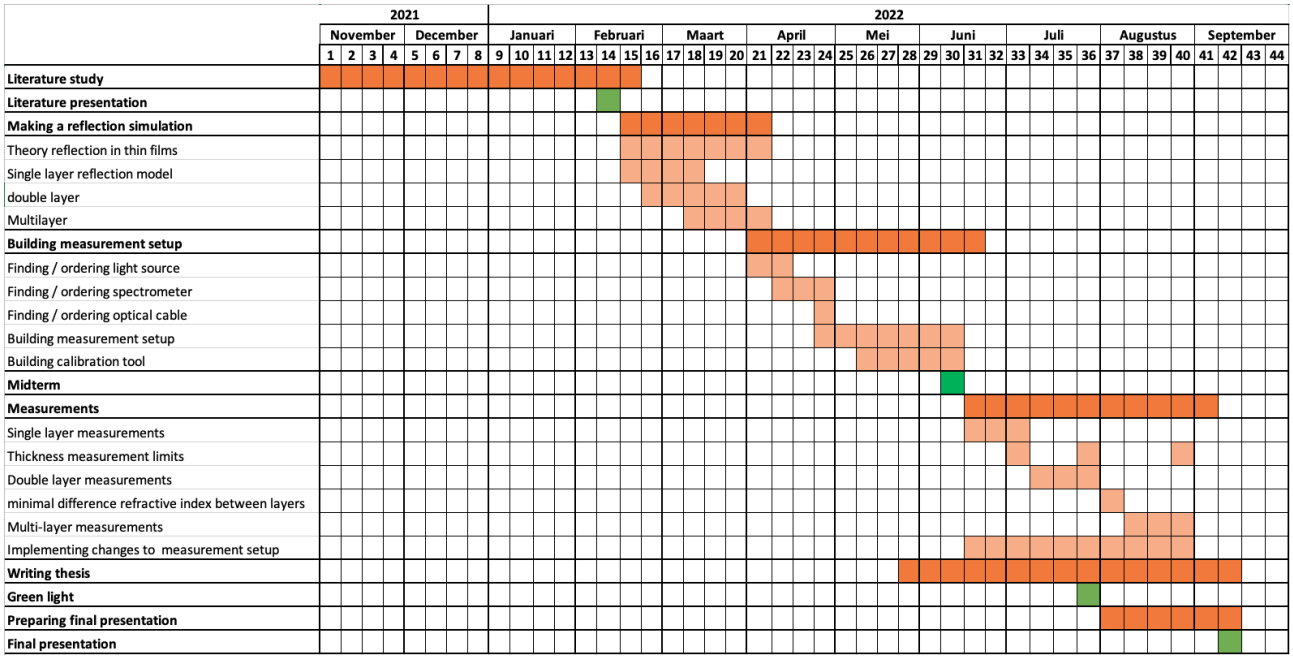

Figure 20: Research planning for the proposed thesis.

6 Discussion

In this literature study, state-of-the-art thin film thickness measurement technologies have been studied. The objective of the literature study was to find out which of the mentioned techniques is most suitable for measuring a multilayer stack of thin films including a liquid layer. While these layers have a comparable refractive index and layer thickness differences between layers can be large.

Of the techniques that have been discussed, ellipsometry, reflectance and ultrasound are the most suitable techniques. Ellipsometry is a very impactful technique with high resolution. This is because it looks at both reflectance and polarization at multiple wavelengths and with a varying angle of incidence. Due to this it requires moving parts and is therefore relatively complex in usage. Besides this, the data processing can become quite extensive due to this. A direct consequence of these things is that ellipsometry systems are much more expensive. Besides ellipsometry, ultrasound has been seen as a possibility for the multilayer measurement. One of the things that makes this technique rather costly is the ultrasonic transducer. Besides this, ultrasound measurements require an expensive control system. Therefore, mainly due to cost, this technique is not feasible for this master thesis. That leaves us with reflectance, more precisely, spectral reflectance. Out of the three techniques, spectral reflectance is the least complex method as it only looks at the reflection spectrum of light and does not need any moving parts. The challenge with this technique can be the data processing due to overlapping reflections in the reflectance spectrum once layers become too thin (See table 2) which is outside of the desired measurement range.

Table 2: Comparison of the measurement ranges for single layers of thin films from the suitable techniques [35, 41].

Technique	**Measurement range**
Ellipsometry	0.001 µm–1000 µm
Reflectance	0.001 µm–1000 µm
Ultrasound	0.05 µm–1000 µm

7 Conclusion

After completion of the literature study, a suitable technique was found to measure the thickness of different layers within a multilayer of thin films. The technique found is often referred to as spectral reflectance and works with a reflection spectrum over a wide range of wavelengths. The main advantage is that the technique is non-destructive, non-contact and can measure the interference between reflections from the different interfaces within a multilayer stack. The interference pattern is needed to determine optical parameters of the layers in the stack but can also determine layer thickness through calculations. A proposal was made to work towards measuring a liquid thin film within a stack of five different materials. While this stack included relatively thin and thicker layers. Successfully being able to measure such a thin film within a stack of layers will give Morphotonics more insights into their process and could help them influence certain parameters in the process whenever layer thickness is measured to be non-uniform. In order to perform these measurements, a measurement setup will be made. This setup will consist of a light source, optical cable and a spectrometer. It is important to figure out what the necessary wavelength range is needed for the combination of layers in the stack. Besides this, it will be necessary to find out what the resolution of the spectrometer should be.

References

[1] S. Y. Chou, P. R. Krauss, and P. J. Renstrom, "Nanoimprint lithography," *Journal of Vacuum Science & Technology B: Microelectronics and Nanometer Structures Processing, Measurement, and Phenomena*, vol. 14, no. 6, pp. 4129–4133, 1996.

[2] ——, "Imprint of sub-25 nm vias and trenches in polymers," *Applied physics letters*, vol. 67, no. 21, pp. 3114–3116, 1995.

[3] H. Lan, "Large-area nanoimprint lithography and applications," *Micro/Nanolithography-A heuristic aspect on the enduring technology*, pp. 43–68, 2018.

[4] N. Kooy, K. Mohamed, L. T. Pin, and O. S. Guan, "A review of roll-to-roll nanoimprint lithography," *Nanoscale research letters*, vol. 9, no. 1, pp. 1–13, 2014.

[5] V. Trabadelo, H. Schift, S. Merino, S. Bellini, and J. Gobrecht, "Measurement of demolding forces in full wafer thermal nanoimprint," *Microelectronic Engineering*, vol. 85, no. 5-6, pp. 907–909, 2008.

[6] A. Pandey, S. Tzadka, D. Yehuda, and M. Schvartzman, "Soft thermal nanoimprint with a 10 nm feature size," *Soft Matter*, vol. 15, no. 13, pp. 2897–2904, 2019.

[7] H. Lan and H. Liu, "Uv-nanoimprint lithography: structure, materials and fabrication of flexible molds," *Journal of nanoscience and nanotechnology*, vol. 13, no. 5, pp. 3145–3172, 2013.

[8] M. Bender, A. Fuchs, U. Plachetka, and H. Kurz, "Status and prospects of uv-nanoimprint technology," *Microelectronic Engineering*, vol. 83, no. 4-9, pp. 827–830, 2006.

[9] Morphotonics machines. [Online]. Available: https://www.morphotonics.com/nanoimprint-machines/

[10] H. Frey and H. R. Khan, *Handbook of thin film technology*. Springer, 2015.

[11] A. Robinson and R. Leach, "Overview of tomography techniques to measure wafer thickness in mems structures," 2008.

[12] A. Piegari and E. Masetti, "Thin film thickness measurement: a comparison of various techniques," *Thin solid films*, vol. 124, no. 3-4, pp. 249–257, 1985.

[13] Wet film thickness gauge. [Online]. Available: https://tqcsheen.com/en/product/wet-film-thickness-gauge-stainless-steel-en/

[14] Capacitance sensors. [Online]. Available: https://mtiinstruments.com/technology-principles/capacitance-based-measurement/

[15] A. El-Naggar, S. El-Zaiat, and S. M. Hassan, "Optical parameters of epitaxial gan thin film on si substrate from the reflection spectrum," *Optics & Laser Technology*, vol. 41, no. 3, pp. 334–338, 2009.

[16] T. Huen, "Reflectance of thinly oxidized silicon at normal incidence," *Applied optics*, vol. 18, no. 12, pp. 1927–1932, 1979.

[17] G. Amaratunga *et al.*, "Determination of the optical constants and thickness of thin films on slightly absorbing substrates," *Applied Optics*, vol. 34, no. 34, pp. 7914–7924, 1995.

[18] J. C. Martínez-Antón, "Determination of optical parameters in general film–substrate systems: A reformulation based on the concepts of envelope extremes and local magnitudes," *Applied optics*, vol. 39, no. 25, pp. 4557–4568, 2000.

[19] J. Bae, J. Park, H. Ahn, and J. Jin, "Optical method for simultaneous thickness measurements of two layers with a significant thickness difference," *Optics Express*, vol. 29, no. 20, pp. 31 615–31 631, 2021.

[20] M. Ylilammi and T. Ranta-aho, "Optical determination of the film thicknesses in multilayer thin film structures," *Thin Solid Films*, vol. 232, no. 1, pp. 56–62, 1993.

[21] P. Hauge, "Polycrystalline silicon film thickness measurement from analysis of visible reflectance spectra," *JOSA*, vol. 69, no. 8, pp. 1143–1152, 1979.

[22] Led with gaussian distribution. [Online]. Available: https://spie.org/publications/fg11_p26_light_emitting_diodes?SSO=1

[23] M. Quinten, "On the use of fast fourier transform for optical layer thickness determination," *SN Applied Sciences*, vol. 1, no. 8, pp. 1–12, 2019.

[24] V. P. Kutavichus, V. V. Filippov, and V. H. Huzouski, "Determination of optical parameters and thickness of weakly absorbing thin films from reflectance and transmittance spectra," *Applied optics*, vol. 45, no. 19, pp. 4547–4553, 2006.

[25] W. Giurlani, E. Berretti, M. Innocenti, and A. Lavacchi, "Measuring the thickness of metal films: A selection guide to the most suitable technique," in *Materials Proceedings*, vol. 2, no. 1. Multidisciplinary Digital Publishing Institute, 2020, p. 12.

[26] J. N. Hilfiker, G. K. Pribil, R. Synowicki, A. C. Martin, and J. S. Hale, "Spectroscopic ellipsometry characterization of multilayer optical coatings," *Surface and Coatings Technology*, vol. 357, pp. 114–121, 2019.

[27] S.-W. Kim and G.-H. Kim, "Thickness-profile measurement of transparent thin-film layers by white-light scanning interferometry," *Applied Optics*, vol. 38, no. 28, pp. 5968–5973, 1999.

[28] T. Jo, K. Kim, S. Kim, and H. Pahk, "Thickness and surface measurement of transparent thin-film layers using white light scanning interferometry combined with reflectometry," *Journal of the Optical Society of Korea*, vol. 18, no. 3, pp. 236–243, 2014.

[29] Y.-S. Ghim and H.-G. Rhee, "Spectrally-resolved white-light phase-shifted interferometry for 3d measurements of multilayer films," in *Optical Measurement Systems for Industrial Inspection XI*, vol. 11056. International Society for Optics and Photonics, 2019, p. 1105631.

[30] R. A. v. O. Sebas J. Siers, Joep P.A. Nijssen, "Development and implementation of a film height measurement approach for deforming hydrostatic bearings," 2020, unpublished.

[31] A. Nwaneshiudu, C. Kuschal, F. H. Sakamoto, R. R. Anderson, K. Schwarzenberger, and R. C. Young, "Introduction to confocal microscopy," *Journal of Investigative Dermatology*, vol. 132, no. 12, pp. 1–5, 2012.

[32] F. Ng, J. Wei, F. Lai, and K. Goh, "Metallic thin film depth measurements by x-ray microanalysis," *Applied surface science*, vol. 252, no. 11, pp. 3972–3976, 2006.

[33] H. Griffiths, "Magnetic induction tomography," *Measurement science and technology*, vol. 12, no. 8, p. 1126, 2001.

[34] A. Wajid, "On the accuracy of the quartz-crystal microbalance (qcm) in thin-film depositions," *Sensors and Actuators A: Physical*, vol. 63, no. 1, pp. 41–46, 1997.

[35] R. Dwyer-Joyce, B. Drinkwater, and C. Donohoe, "The measurement of lubricant–film thickness using ultrasound," *Proceedings of the Royal Society of London. Series A: Mathematical, Physical and Engineering Sciences*, vol. 459, no. 2032, pp. 957–976, 2003.

[36] Y. Al-Aufi, B. Hewakandamby, G. Dimitrakis, M. Holmes, A. Hasan, and N. Watson, "Thin film thickness measurements in two phase annular flows using ultrasonic pulse echo techniques," *Flow Measurement and Instrumentation*, vol. 66, pp. 67–78, 2019.

[37] O. Stenzel *et al.*, *The physics of thin film optical spectra*. Springer, 2015.

[38] Filmetrics reflectance calculator. [Online]. Available: https://www.filmetrics.com/reflectance-calculator

[39] S. J. Byrnes, "Multilayer optical calculations," *arXiv preprint arXiv:1603.02720*, 2016.

[40] Transfer-matrix method (optics). [Online]. Available: https://en.formulasearchengine.com/wiki/Transfer-matrix_method_(optics)

[41] Ellipsometry and spectral reflectance. [Online]. Available: https://www.filmetrics.com/ellipsometry

B

Appendix Light Source specifications

AvaLight-DH-S-BAL Balanced Power

AvaLight-DH-S-BAL

The AvaLight-DH-S is a powerful deuterium halogen source, but like any unbalanced deuterium halogen source it does have a very dominant alpha peak at 656 nm. This is why Avantes developed the DH-S-BAL, in which this peak is drastically reduced by a dichroic filter. This means less power, but an increase in the dynamic range of a factor 20. A comparison spectrum, which is taken with a standard AvaSpec-ULS2048CL, is shown on the next page.

The light source delivers a continuous spectrum with high efficiency. The highest stability is in the ultraviolet, visible and near infrared range, from 215 to 2500 nm. An integrated TTL-shutter and filter holder for filters of up to 50x50x5.0 mm are included. The TTL-shutter can be controlled from any AvaSpec spectrometer, which means the auto-save dark-option in AvaSoft software can be used (please note: IC-DB26-2 cable needed).

Connection to the fiber is done through an SMA-905 connector, which features an adjustable focusing lens assembly. This ensures you getting the maximum possible power into your fiber. For all deuterium light sources solarization resistant fibers are recommended. The output of the AvaLight-DH-S-BAL is optimized for fibers or bundles up to 600 µm.

The filter holder can be easily replaced by a direct-attach cuvette holder CUV-DA-DHS (see section accessories) useful for fluorescence or absorbance measurements.

- Balanced light source
- Wide spectrum: 215-2500 nm
- Integrated TTL shutter
- High efficiency
- Increased dynamic range

Technical Data

	Balanced Deuterium (Standard)	Balanced Halogen Lamp
Wavelength Range	215-500 nm	500-2500 nm
Warm-up Time	30 min.	20 min.
Lamp Power	78 W / 0.75 A	5 W / 0.5 A
Lamp Lifetime	2000 hrs	1000 hrs
Noise (AU)	$2x\ 10^{-5}$	10^{-4}
Max. drift	± 0.5%/hr	±0.1%/hr
Color Temperature	-	3000 K
Optical Power in 200 µm fiber	6 µW	17 µW
Optical Power in 600 µm fiber	33 µW	160 µW
Optical Power in 1000 µm fiber	90 µW	448 µW
Power consumption	90 Watt (190 Watt for heating D-Lamp 4-5 sec.)	
Power Requirements	100-240VAC 50/60 Hz	
Dimensions / Weight	315 x 165 x 140 mm / ca 5 kg.	
Lifetime shutter	1,000,000 cycles (typical)	

For a table of separate 50x50 mm filters to install in AvaLight-D(H)-S see AvaLight-HAL.

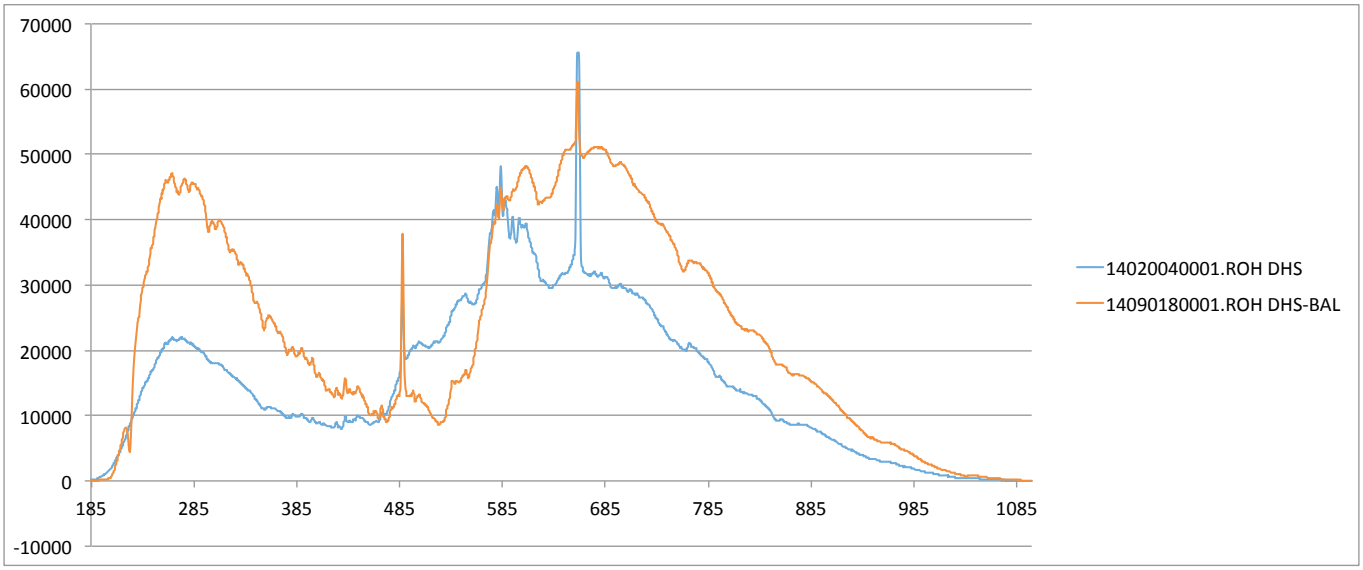

Figure 11 Spectral output AvaLight-DH-S-BAL (red) vs. AvaLight-DH-S (blue). (RAW data)

Ordering Information

AvaLight-D-S-BAL	• Balanced Deuterium light source, 215-500nm, incl. TTL shutter, -SR fibers needed
AvaLight-DH-S-BAL	• Balanced Deuterium-Halogen light source, 215-2500 nm, incl. TTL shutter, -SR fibers needed
IC-DB26-2	• Interface cable AvaSpec-USB2/EVO platform to AvaLight-D(H)S-BAL
AvaLight-D-B	• Replacement deuterium bulb for AvaLight-D/AvaLight DH-BAL light source
AvaLight-DH-B	• Replacement halogen bulb for AvaLight-DH-BAL light source
CUV-DA-DHS	• Direct-attach cuvette holder for AvaLight-D(H)S-BAL

C

Appendix Spectrometer specifications

EVO Series, with CMOS detector: StarLine AvaSpec-ULS2048CL-EVO Spectrometer

Using CMOS technology instead of the conventional CCD technology, this spectrometer offers you the latest technology.
New technologies like CMOS have evolved and become a suitable alternative.

In combination with our latest AS-7010 electronics it offers you a versatile device including USB3.0 communication with 10x higher speed compared to USB2, and a second communication port which offers Gigabit Ethernet for integration in your company network and possibility for long distance communication.

Besides the high speed communication options, the EVO also offers a fast microprocessor and 50x more memory which can help you to store more spectra onboard and realise more functionality.

Options include a detector collection lens to enhance sensitivity in the 200-1100 nm range and order-sorting filter to reduce 2nd order effects. Furthermore,the AvaSpec-2048CL is available with a wide range of slit sizes, gratings and fiber-optic entrance connectors.
It comes complete with AvaSoft-Basic software, USB cable and an extensive manual.

The AvaSpec-ULS2048CL-EVO is also available as OEM unit, Bench only or Rackmount version.

AvaSpec-ULS2048CL

Technical Data

Optical Bench	ULS Symmetrical Czerny-Turner, 75 mm focal length
Wavelength range	200-1100 nm
Resolution	0.06 –20 nm, depending on configuration (see table)
Stray-light	0.19-1.0%, depending on the grating
Sensitivity	375,000 counts/µW per ms integration time
Detector	CMOS linear Image Sensor
Signal/Noise	300:1
AD converter	16-bit, 6 MHz
Integration time	9 µs – 59s
Interface	USB 3.0 high-speed, 5 Gbps Gigabit Ethernet 1 Gbps
Sample speed with on-board averaging	0.38 ms /scan
Data transfer speed	0.38 ms/scan (USB3), 1.0 ms (ETH)
Digital IO	HD-26 connector, 2 Analog in, 2 Analog out, 13 Digital bidirectional, trigger, sync., strobe, laser
Power supply	Default USB3 power, 500 mA Or 12VDC, 300 mA

Ordering Information

AvaSpec-ULS2048CL-EVO	• Fiber-optic Spectrometer, 75 mm AvaBench, 2048 pixel CMOS detector 14 x 200 µm, USB powered, high-speed USB 3.0 and ETH interface, incl. AvaSoft-Basic, USB interface cable. Specify grating, wavelength range and options.

Grating Selection Table for AvaSpec-ULS2048CL-EVO

Use	Useable range (nm)	Spectral range (nm)	Lines/mm	Blaze (nm)	Order code
UV/VIS/NIR	200-1100**	891**	300	300	UA
UV/VIS/NIR	200-1100**	891**	300	300/1000	UNA-DB
UV/VIS	200-850	515	600	300	UB
UV	200-750	247-218*	1200	250	UC
UV	200-650	163-143*	1800	UV	UD
UV	200-580	113-69*	2400	UV	UE
UV	200-400	69-45*	3600	UV	UF
UV/VIS	250-850	515	600	400	BB
VIS/NIR	300-1100**	792**	300	500	VA
VIS	360-1000	495	600	500	VB
VIS	300-800	247-218*	1200	500	VC
VIS	350-750	142-89*	1800	500	VD
VIS	350-640	74-49*	2400	VIS	VE
NIR	500-1050	495	600	750	NB
NIR	500-1050	218-148*	1200	750	NC
NIR	600-1100	346-297	830	800	SI
NIR	600-1100**	495**	300	1000	IA
NIR	600-1100	495	600	1000	IB

* depends on the starting wavelength of the grating; the higher the wavelength, the bigger the dispersion and the smaller the range to select.
** please note that not all 2048 pixels will be used for the useable range

Resolution Table (FWHM in nm) for AvaSpec-ULS2048CL-EVO

	Slit size (µm)					
Grating (lines/mm)	**10**	**25**	**50**	**100**	**200**	**500**
300	1.0	1.4	2.5	4.8	9.2	21.3
600	0.40-0.53*	0.7	1.2	2.4	4.6	10.8
830	0.32	0.48	0.93	1.7	3.4	8.5
1200	0.20-0.28*	0.27-0.38*	0.52-0.66*	1.1	2.3	5.4
1800	0.10-0.18*	0.20-0.29*	0.34-0.42*	0.8	1.6	3.6
2400	0.09-0.13*	0.13-0.17*	0.26-0.34*	0.44-0.64*	1.1	2.7
3600	0.06-0.08*	0.10	0.19	0.4	0.8	1.8

* depends on the starting wavelength of the grating; the higher the wavelength, the bigger the dispersion and the better the resolution

Options

-RS	• Replaceable slit
DCL-UV/VIS-200	• Quartz Detector Collection Lens (200-1100 nm)
SLIT-XX	• Slit size, please specify XX = 10, 25, 50, 100, 200 or 500 µm
SLIT-XX-RS	• Replaceable slit with SMA connector , specify slit size XX=25, 50, 100, 200 or 500 µm. Only in combination with AvaSpec-ULS2048CL-EVO-RS
SLIT-XX-RS-FCPC	• as SLIT-XX-RS, but with FC/PC connector
OSF-YYY	• Order-sorting filter for reduction of 2nd order effects please specify YYY= 305, 395, 475, 515, 550 or 600 nm
OSC	• Order-sorting coating with 600 nm long-pass filter for BB (>350 nm) and VB gratings, recommended with OSF-305
OSC-UA	• Order-sorting coating Linear Variable Filter for UA, VA gratings
OSC-UB	• Order-sorting coating with 350 and 600 nm long-pass filter for UB or BB (<350 nm) gratings
-FCPC	• FC/PC fiber-optic connector

D

Measurement results

D.1. Standard deviation measurements around scratches

D.1.1. Sample 1 - location A

Below five measurements in the form of a reflectance spectrum and the result of the FFT for sample 1 close to the scratch at location A are shown.

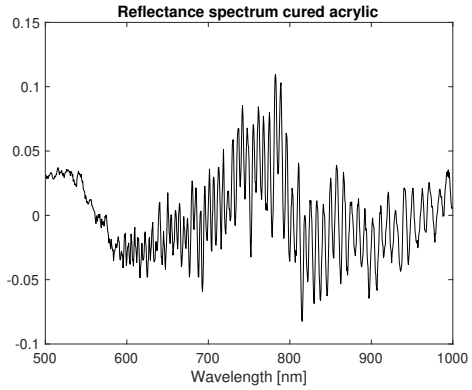

(a) Reflectance spectrum

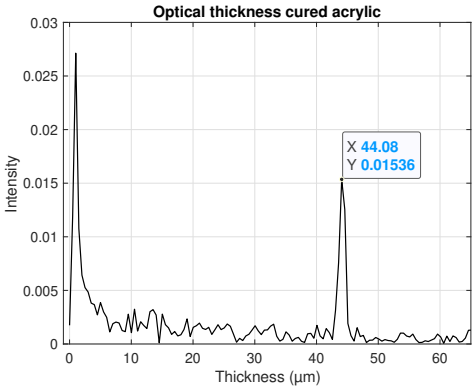

(b) Thickness determination (FFT).

Figure D.1: The measurement results from thin film cured acrylic on top of a incoherently thick glass substrate showing both Reflectance spectrum and FFT measured at location A, first measurement.

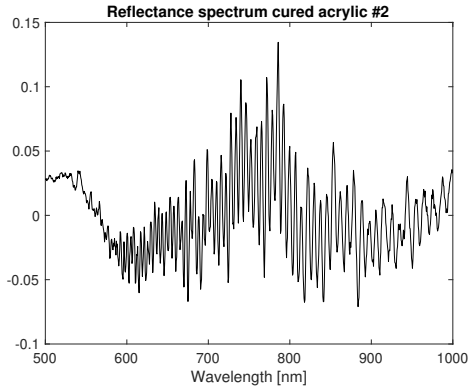

(a) Reflectance spectrum

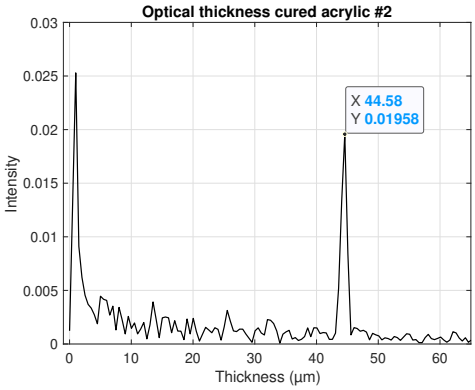

(b) Thickness determination (FFT).

Figure D.2: The measurement results from thin film cured acrylic on top of a incoherently thick glass substrate showing both Reflectance spectrum and FFT measured at location A, second measurement.

.

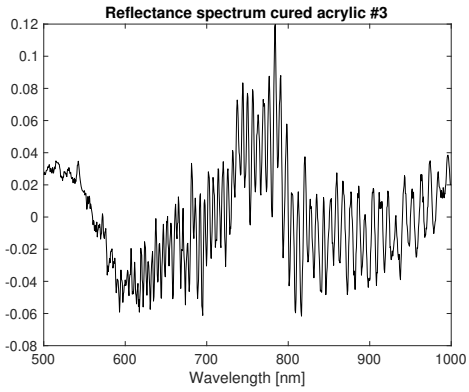

(a) Reflectance spectrum

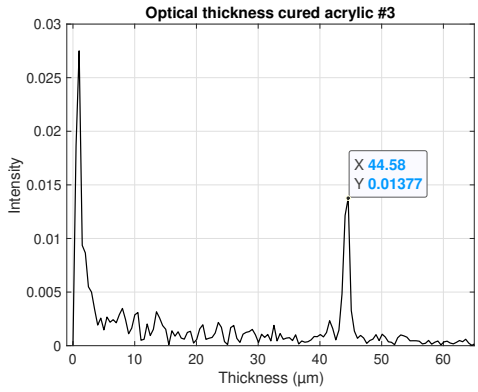

(b) Thickness determination (FFT).

Figure D.3: The measurement results from thin film cured acrylic on top of a incoherently thick glass substrate showing both Reflectance spectrum and FFT measured at location A, third measurement.

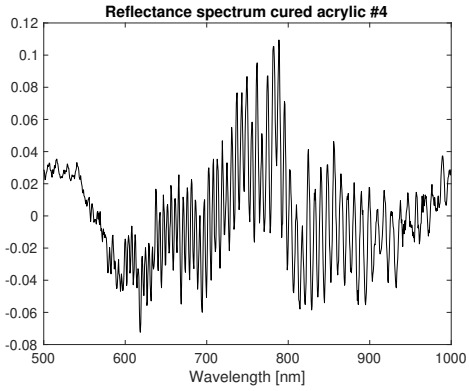

(a) Reflectance spectrum

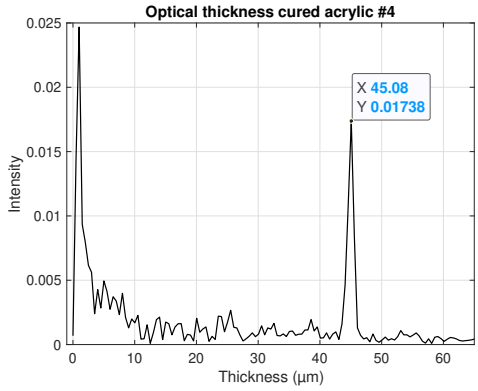

(b) Thickness determination (FFT).

Figure D.4: The measurement results from thin film cured acrylic on top of a incoherently thick glass substrate showing both Reflectance spectrum and FFT measured at location A, fourth measurement.

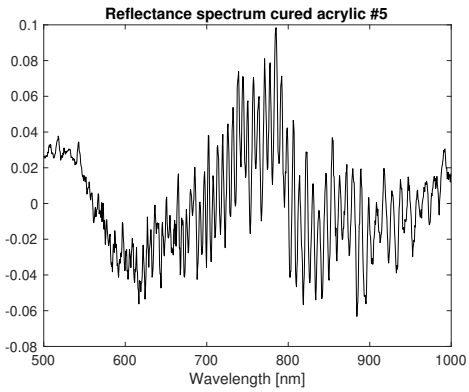

(a) Reflectance spectrum

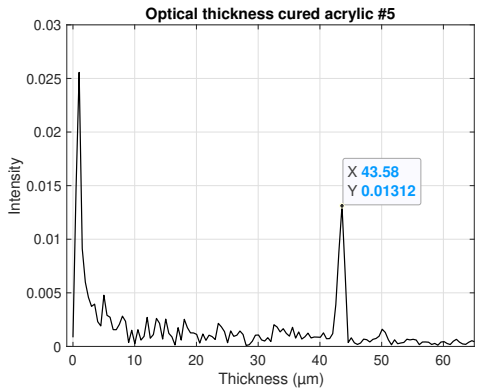

(b) Thickness determination (FFT).

Figure D.5: The measurement results from thin film cured acrylic on top of a incoherently thick glass substrate showing both Reflectance spectrum and FFT measured at location A, fifth measurement.

D.1.2. Sample 1 - location B

Below five measurements in the form of a reflectance spectrum and the result of the FFT for sample 1 close to the scratch at location B are shown.

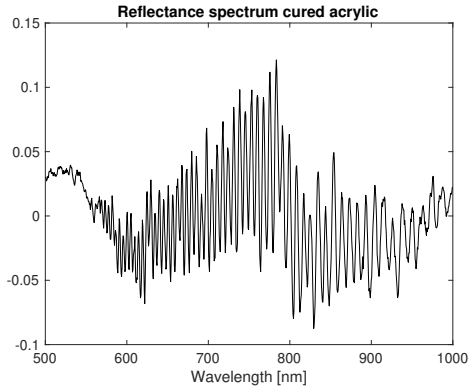

(a) Reflectance spectrum

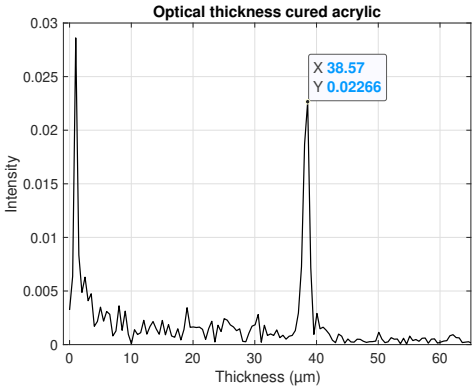

(b) Thickness determination (FFT).

Figure D.6: The measurement results from thin film cured acrylic on top of a incoherently thick glass substrate showing both Reflectance spectrum and FFT measured at location B, first measurement.

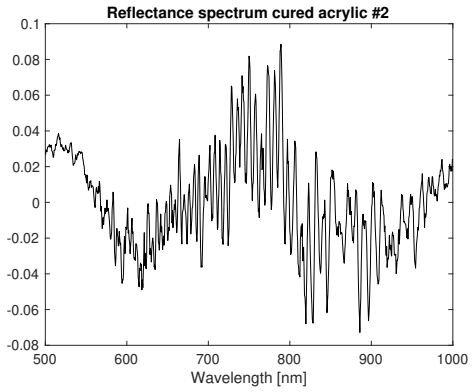

(a) Reflectance spectrum

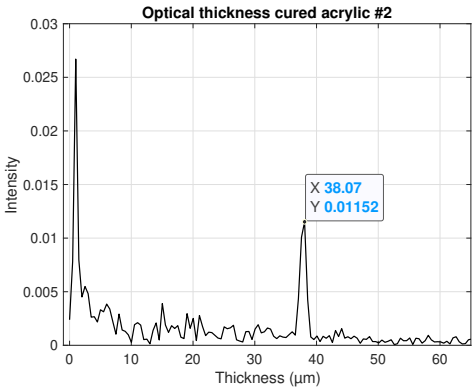

(b) Thickness determination (FFT).

Figure D.7: The measurement results from thin film cured acrylic on top of a incoherently thick glass substrate showing both Reflectance spectrum and FFT measured at location B, second measurement.

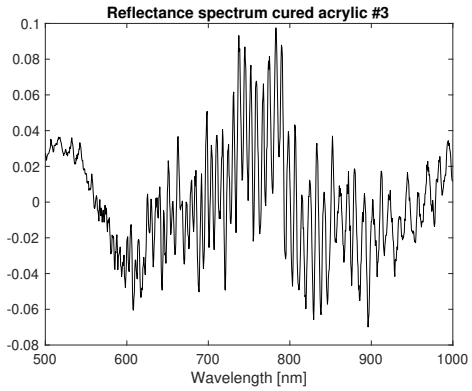

(a) Reflectance spectrum

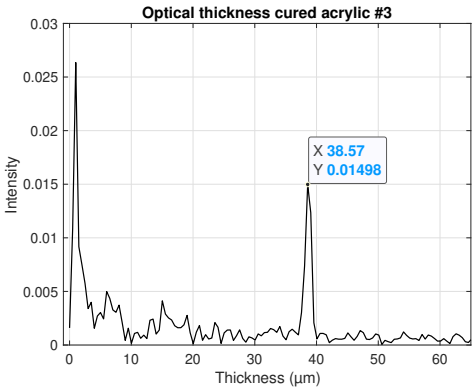

(b) Thickness determination (FFT).

Figure D.8: The measurement results from thin film cured acrylic on top of a incoherently thick glass substrate showing both Reflectance spectrum and FFT measured at location B, third measurement.

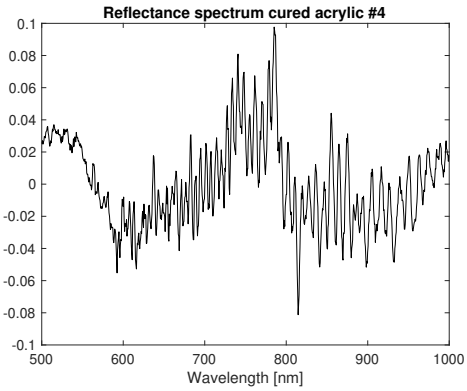

(a) Reflectance spectrum

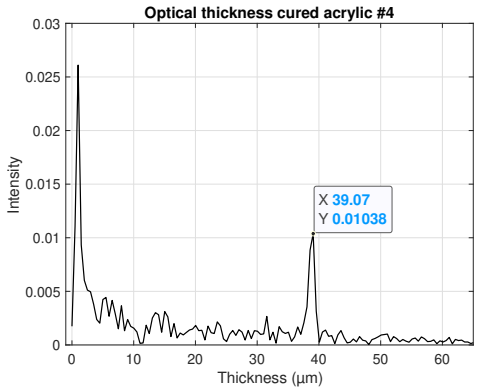

(b) Thickness determination (FFT).

Figure D.9: The measurement results from thin film cured acrylic on top of a incoherently thick glass substrate showing both Reflectance spectrum and FFT measured at location B, fourth measurement.

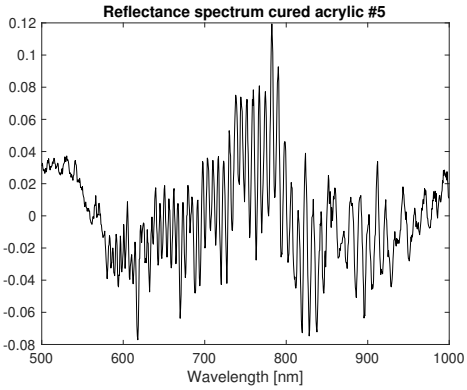

(a) Reflectance spectrum

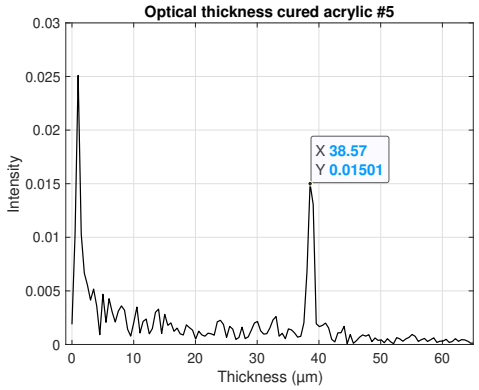

(b) Thickness determination (FFT).

Figure D.10: The measurement results from thin film cured acrylic on top of a incoherently thick glass substrate showing both Reflectance spectrum and FFT measured at location B, fifth measurement.

D.1.3. Sample 2 - location C

Below five measurements in the form of a reflectance spectrum and the result of the FFT for sample 2 close to the scratch at the location C are shown.

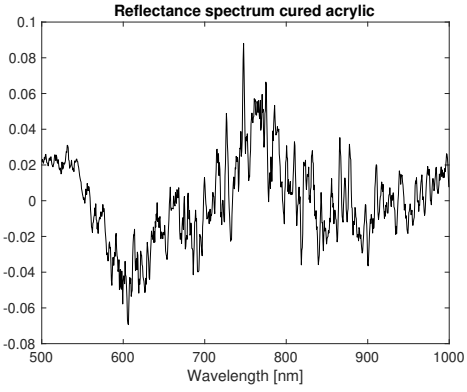

(a) Reflectance spectrum

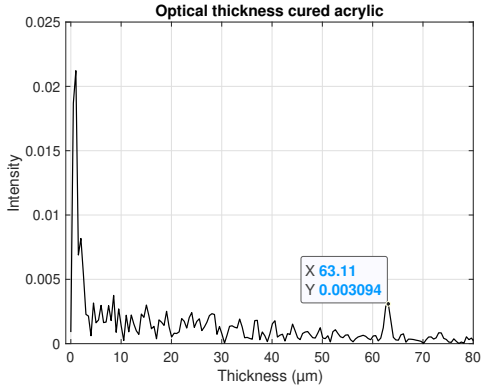

(b) Thickness determination (FFT).

Figure D.11: The measurement results from thin film cured acrylic on top of a incoherently thick glass substrate showing both Reflectance spectrum and FFT measured at location C, first measurement.

.

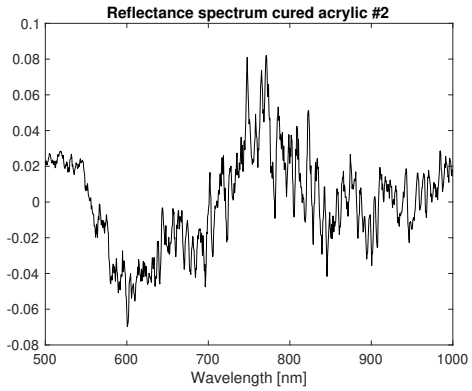

(a) Reflectance spectrum

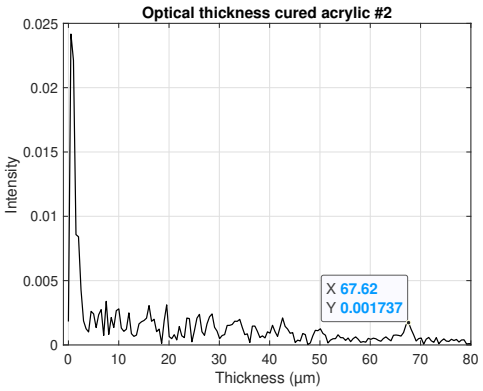

(b) Thickness determination (FFT).

Figure D.12: The measurement results from thin film cured acrylic on top of a incoherently thick glass substrate showing both Reflectance spectrum and FFT measured at location C, second measurement.

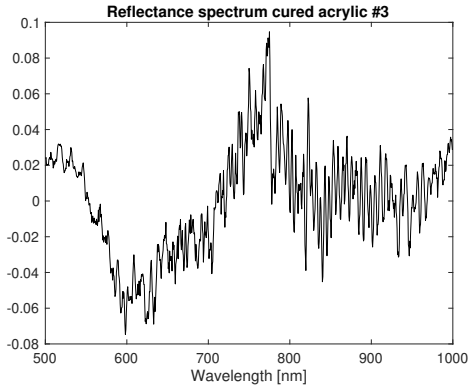

(a) Reflectance spectrum

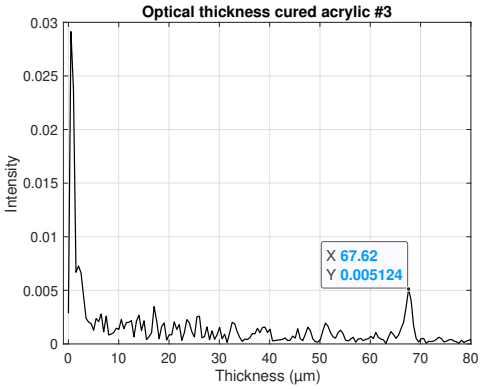

(b) Thickness determination (FFT).

Figure D.13: The measurement results from thin film cured acrylic on top of a incoherently thick glass substrate showing both Reflectance spectrum and FFT measured at location C, third measurement.

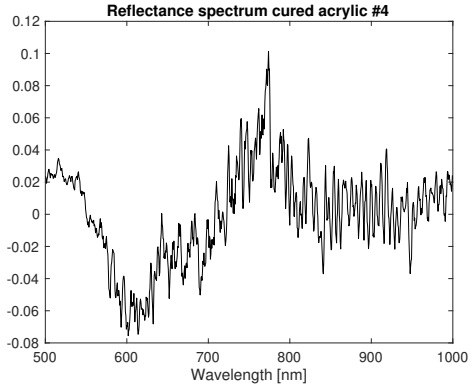

(a) Reflectance spectrum

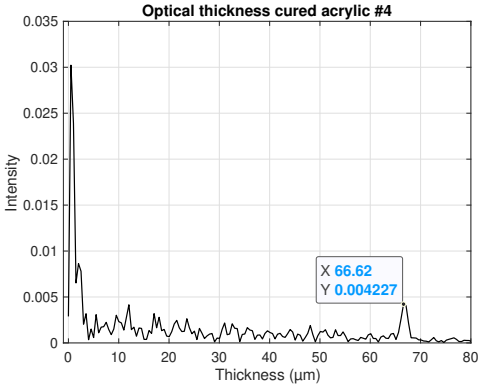

(b) Thickness determination (FFT).

Figure D.14: The measurement results from thin film cured acrylic on top of a incoherently thick glass substrate showing both Reflectance spectrum and FFT measured at location C, fourth measurement.

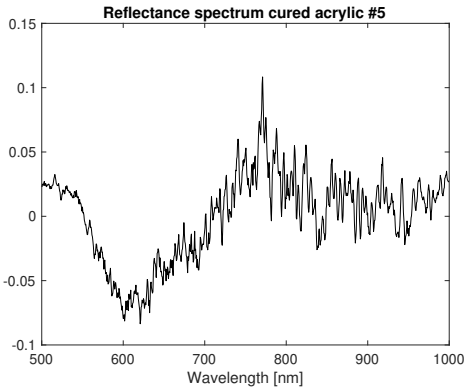

(a) Reflectance spectrum

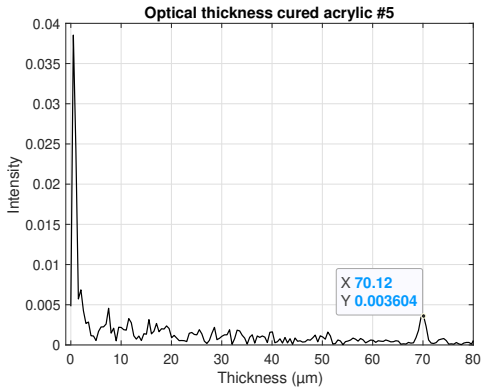

(b) Thickness determination (FFT).

Figure D.15: The measurement results from thin film cured acrylic on top of a incoherently thick glass substrate showing both Reflectance spectrum and FFT measured at location C, fifth measurement.

D.1.4. Sample 2 - location D

Below five measurements in the form of a reflectance spectrum and the result of the FFT for sample 2 close to the scratch a location D are shown.

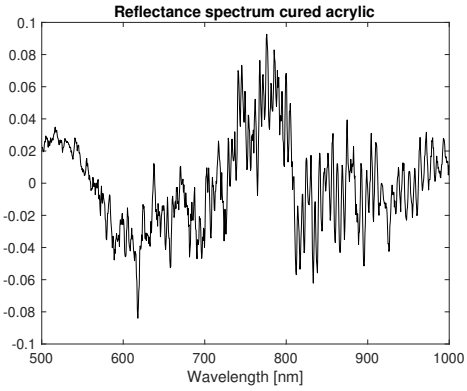

(a) Reflectance spectrum

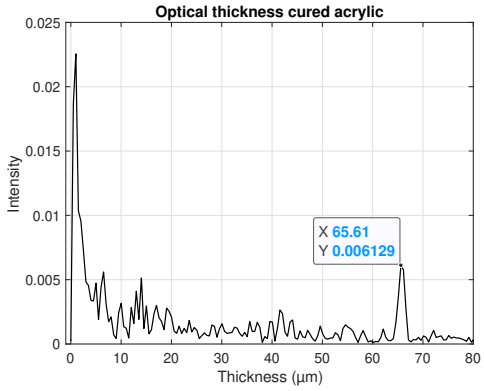

(b) Thickness determination (FFT).

Figure D.16: The measurement results from thin film cured acrylic on top of a incoherently thick glass substrate showing both Reflectance spectrum and FFT measured at location D, first measurement.

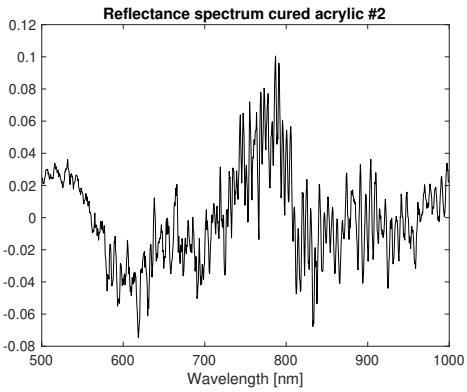

(a) Reflectance spectrum

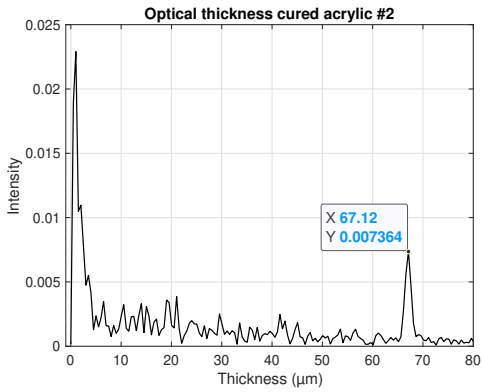

(b) Thickness determination (FFT).

Figure D.17: The measurement results from thin film cured acrylic on top of a incoherently thick glass substrate showing both Reflectance spectrum and FFT measured at location D, second measurement.

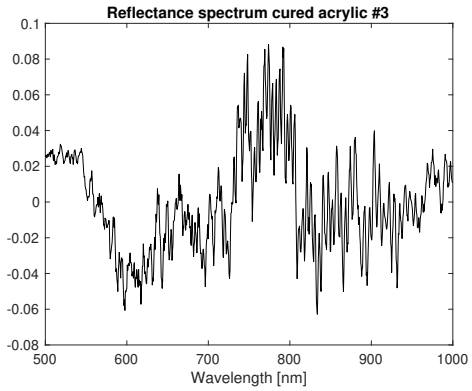

(a) Reflectance spectrum

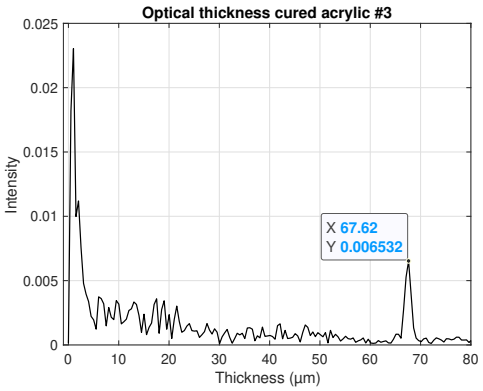

(b) Thickness determination (FFT).

Figure D.18: The measurement results from thin film cured acrylic on top of a incoherently thick glass substrate showing both Reflectance spectrum and FFT measured at location D, third measurement.

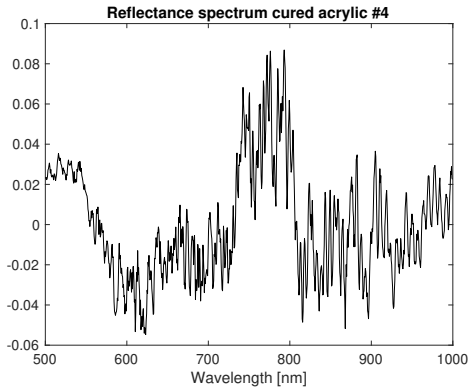

(a) Reflectance spectrum

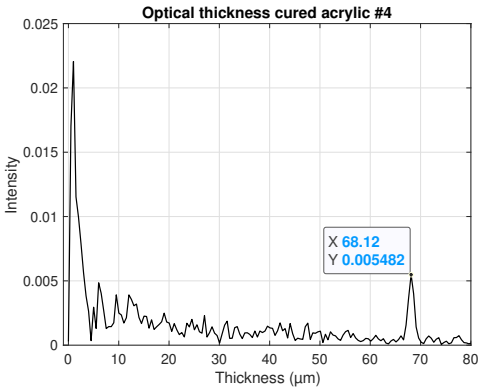

(b) Thickness determination (FFT).

Figure D.19: The measurement results from thin film cured acrylic on top of a incoherently thick glass substrate showing both Reflectance spectrum and FFT measured at location D, fourth measurement.

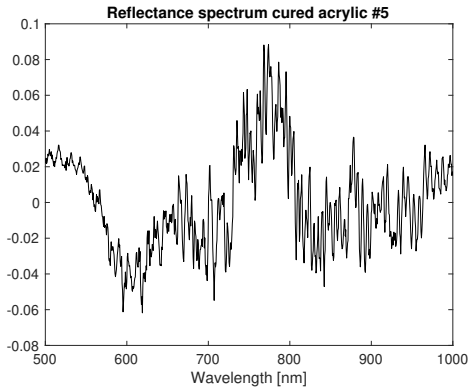

(a) Reflectance spectrum

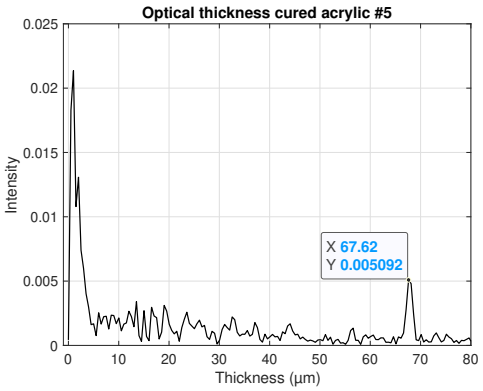

(b) Thickness determination (FFT).

Figure D.20: The measurement results from thin film cured acrylic on top of a incoherently thick glass substrate showing both Reflectance spectrum and FFT measured at location D, fifth measurement.

.

D.2. Standard deviation measurements with pipette

D.2.1. Water thin film

Below six measurements in the form of a reflectance spectrum and the result of the FFT for a thin film of water between two relatively thick pieces of glass. All measurements have been done in the middle of the optical flat.

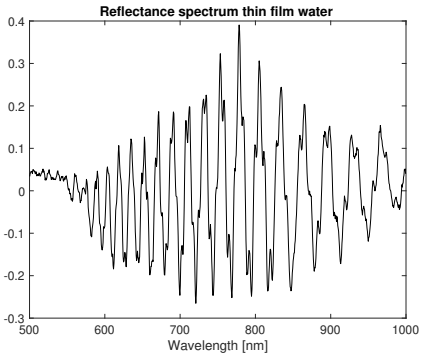

(a) Reflectance spectrum

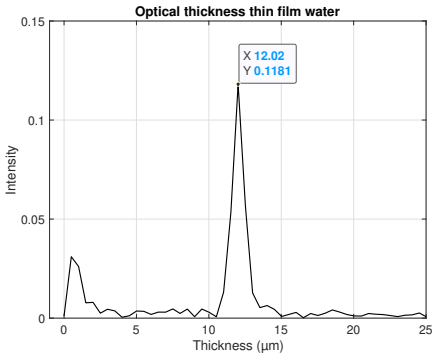

(b) Thickness determination (FFT).

Figure D.21: The measurement results from thin film of water between two incoherently thick glass substrates showing both Reflectance spectrum and FFT, first measurement.

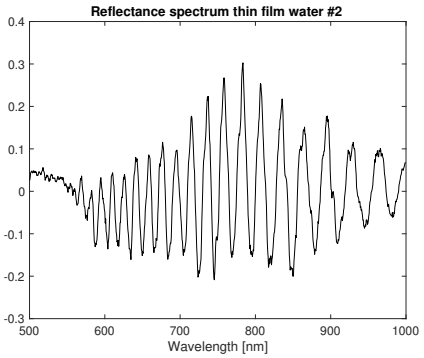

(a) Reflectance spectrum

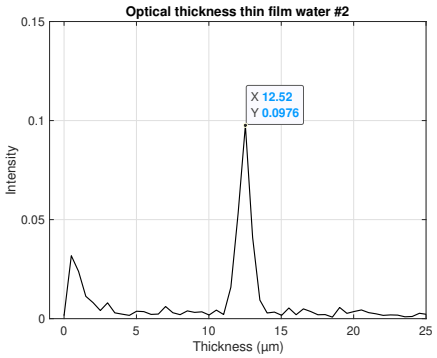

(b) Thickness determination (FFT).

Figure D.22: The measurement results from thin film of water between two incoherently thick glass substrates showing both Reflectance spectrum and FFT, second measurement.

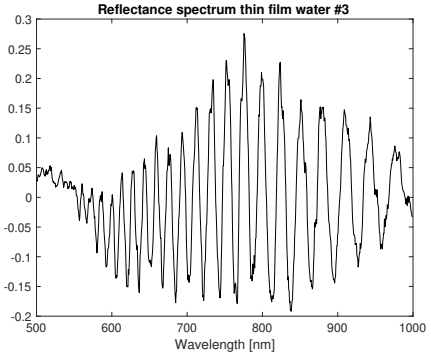

(a) Reflectance spectrum

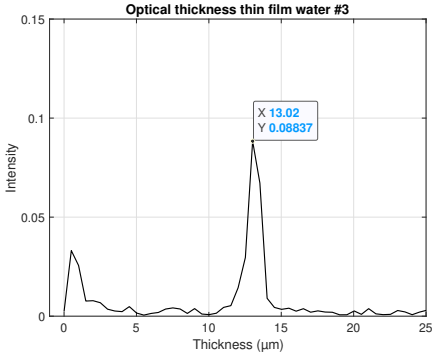

(b) Thickness determination (FFT).

Figure D.23: The measurement results from thin film of water between two incoherently thick glass substrates showing both Reflectance spectrum and FFT, third measurement.

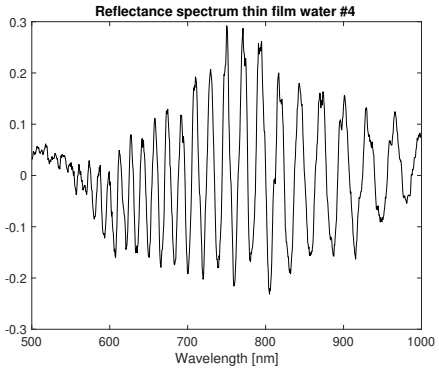

(a) Reflectance spectrum

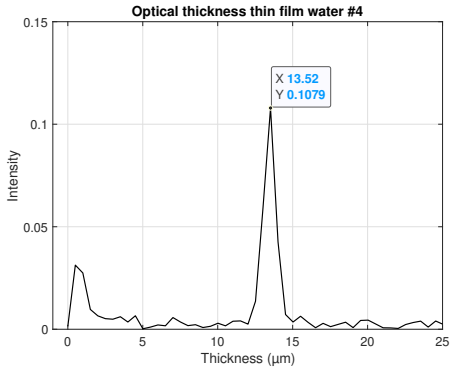

(b) Thickness determination (FFT).

Figure D.24: The measurement results from thin film of water between two incoherently thick glass substrates showing both Reflectance spectrum and FFT, fourth measurement.

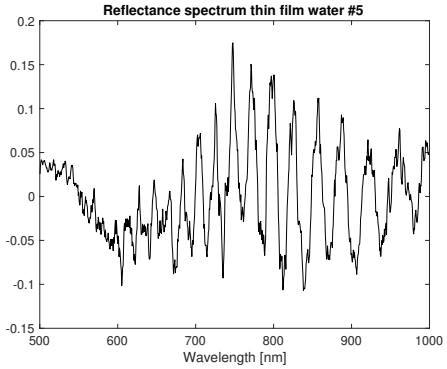

(a) Reflectance spectrum

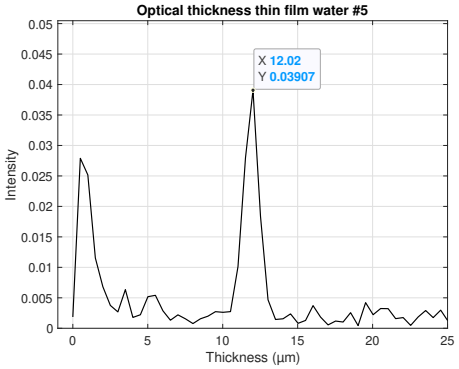

(b) Thickness determination (FFT).

Figure D.25: The measurement results from thin film of water between two incoherently thick glass substrates showing both Reflectance spectrum and FFT, fifth measurement.

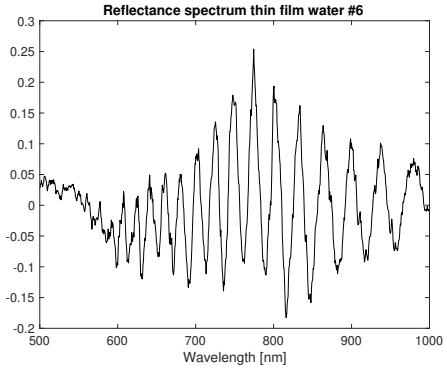

(a) Reflectance spectrum

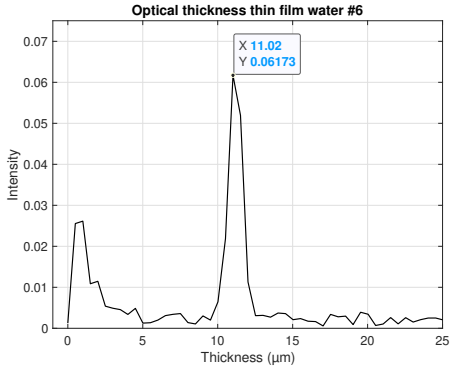

(b) Thickness determination (FFT).

Figure D.26: The measurement results from thin film of water between two incoherently thick glass substrates showing both Reflectance spectrum and FFT, sixth measurement.

E

Appendix reference thickness steps

The first thin film that was measured was cling foil which was stretched and fixed onto the setup with tape. But quickly problems occurred with stretching the foil so a new way to stretch the foil was thought of.

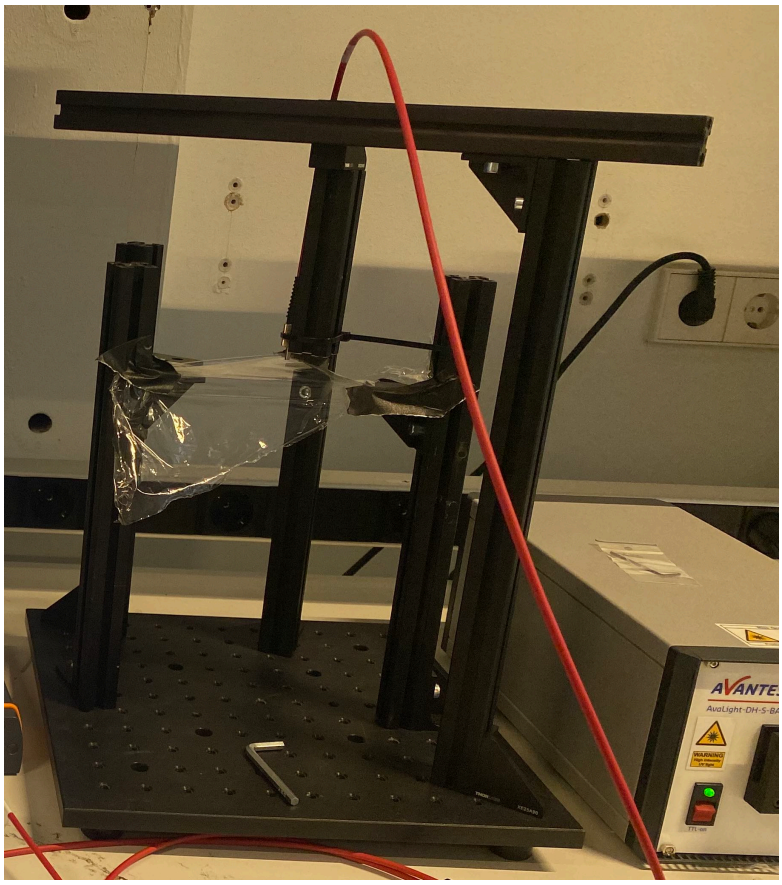

Figure E.1: Step 1: Foil stretched by fixing with tape.

.

The follow up step was stretching the foil between two glass substrates. This gave better results but it turned out to be rather difficult and time consuming to reproduce and stretch the foil.

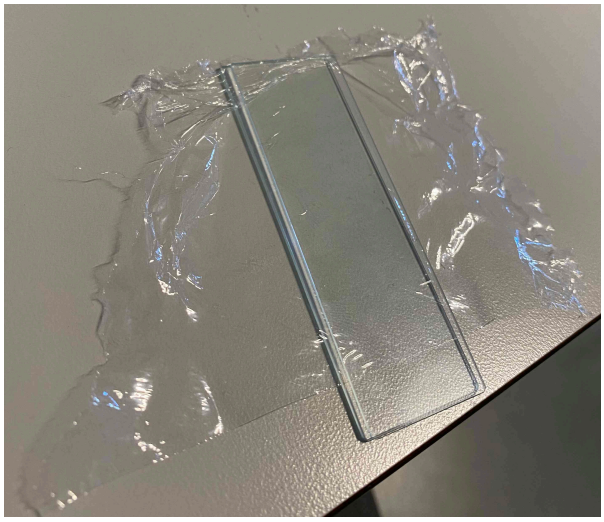

Figure E.2: Step 2: Foil stretched between glass substrates.

The next step was using a PVC sleeve and pipe that fit into it and with these two objects foil was stretched in between giving really clean thin film of foil. The foil gave great results in terms of reflectance spectra with a clear oscillation with a large amplitude. However, the thickness of the cling foil is not very accurate. The producer of the foil only gives an estimate. Even if that thickness estimate is assumed to be accurate enough, once the foil is stretched in the PVC pipes, the thickness changes considerably and becomes unknown. Hence a new method was looked into to use as a reference thickness.

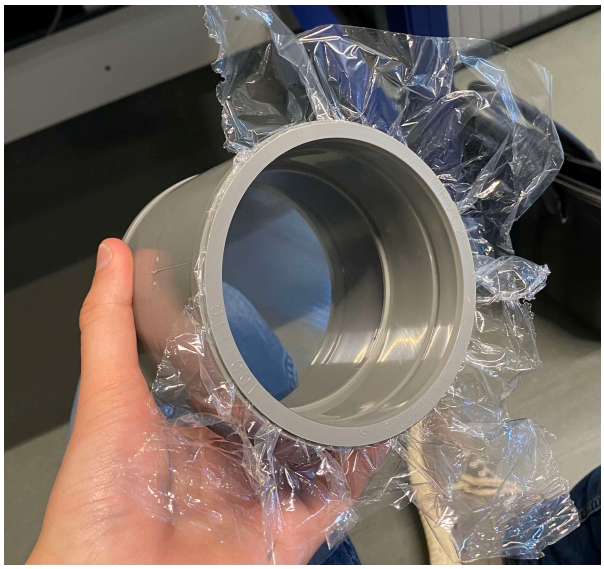

Figure E.3: Step 3: Foil stretched between PVC sleeve and pipe.

.

The next step was by using optical flats which have a properly calibrated surface roughness in combination with a gauge block resulting in a linearly increasing thin film of air between the optical flats. Since gauge blocks typically are 1 mm and then increased by several µm these gauge blocks turned out to be not very useful either since the spectral reflectance setup is not able to measure such thick layers. The follow up step was to look for an object that could figure as a gauge block which was found to be spring steel which has a really accurate thickness and also of the desired thicknesses.

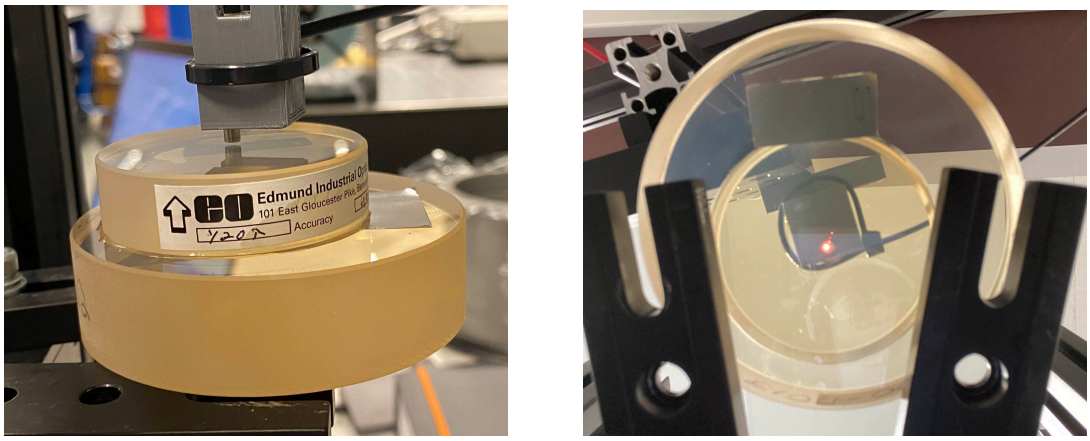

(a) Optical flats

(b) Measurement with spring steel

Figure E.4: Step 4: Optical flats with piece of spring steel.

Since the thickness measurements gave results that were not very logical since a problem was thought to be with cutting the spring steel. The cutted part of the spring steel may have caused significant errors in the expected thickness. This was solved by using longer pieces of spring steel. Still after making this adjustment, no logical results were found.

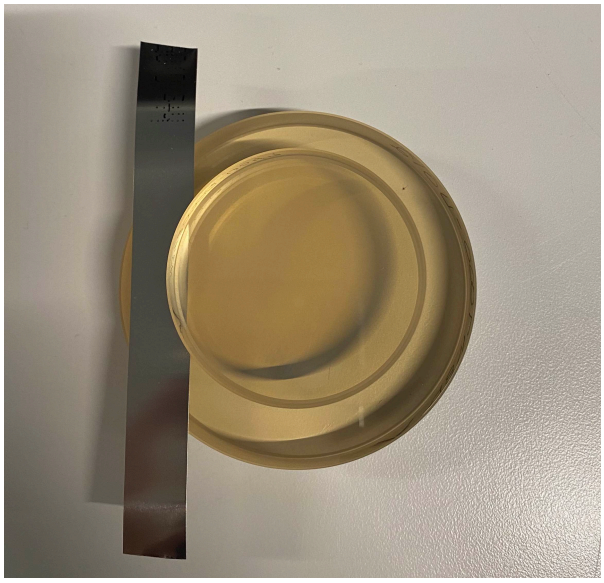

Figure E.5: Step 5: Optical flats with longer piece of spring steel.

.

Since the optical flats were now used, a new measurement was created again with the foil. This still turned out to be rather time consuming to stretch. The problem with unknown thickness of the foil was also still there.

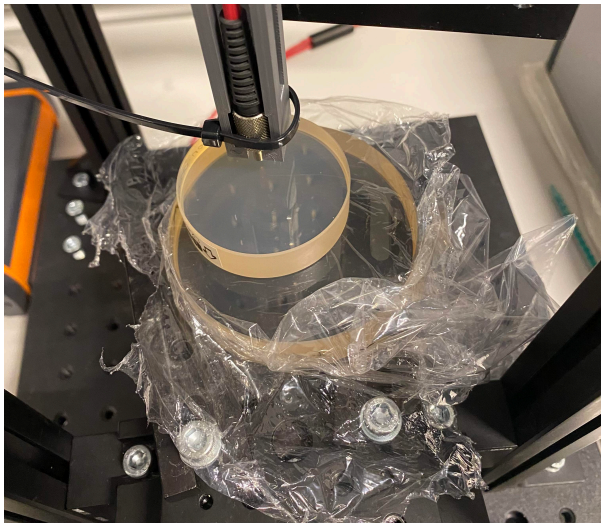

Figure E.6: Step 6: Optical flats with foil.

Going back to the spring steel gauge block idea but now instead of optical flats, regular microscope glasses were used to trap a thin film of air in between since the optical flats might be damaged due to the usage of the spring steel on their calibrated surfaces. By using the longer piece of spring steel, the cutted parts were not influence the thickness. A force was now applied to make sure there was contact between the spring steel and the glass. However, the results did not turn out to be as expected. Most likely due to trapped air between the steel and glass.

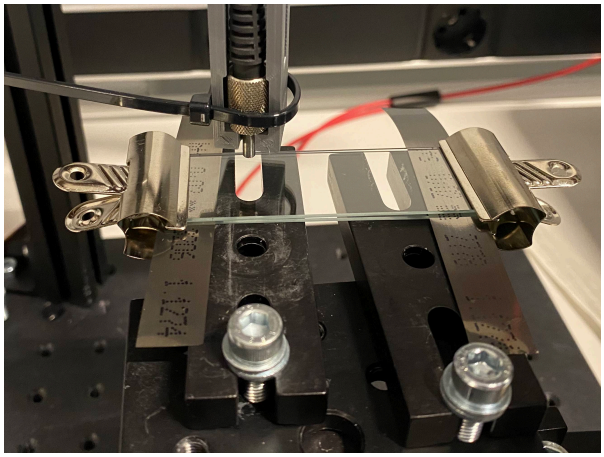

Figure E.7: Glass substrates with spring steel while applying a force.

.

A different method was tried, this time with the use of an accurate pipette. With the pipette, a droplet of water with known volume due to the pipette was deposited onto a microscope glass. By depositing another microscrop glass on top of it the water was smeared out into a certain shape between the microscope glasses. Since the area of this shape could be determined and the volume of the droplet was known, thickness could be determined.

(a) Pipette

(b) Example of a covered area between two glass substrates.

Figure E.8: Pipette method with volume droplet and area of thin film.

Since water was smeared out into a certain shape, the area had to be determined of that shape. After looking into a imaging technique, the technique could be used to determine area of complicated shapes from photos. However, since the water has roughly the same colour as the glass this became rather difficult. Colouring could be added to the water but but instead a different route was chosen.

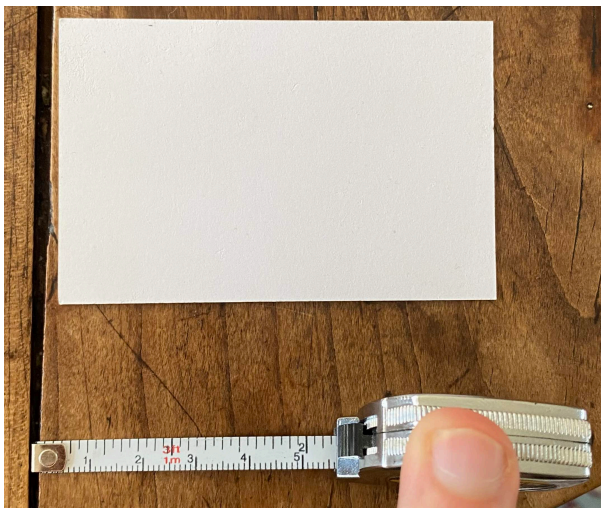

Figure E.9: Imaging technique to find area from photo.

.

Instead of using very little volume, bigger droplets were used causing the entire surface to be covered. Now the area could be determined more easily.

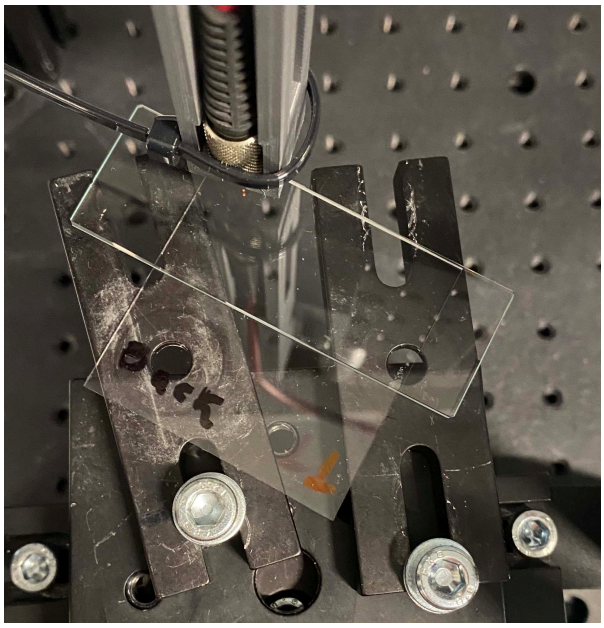

Figure E.10: Instead of partly covering, now covering entire area.

The determination of the area shown with the use of a simple ruler. In combination with the known volume of the water droplet due to the use of the pipette thicknesses of thin films of water could now be measured.

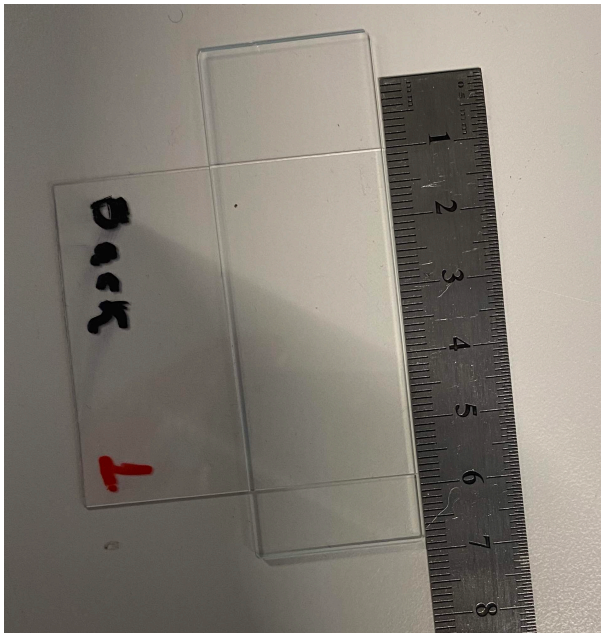

Figure E.11: Measuring the used area.

.

A first proper measurement result followed by using the square sample which was a glass substrate with a cured thin film of acrylic on top of it while using a droplet of water from the pipette, two layers could be measured at the same time. However, the water thin film thickness was not measured as expected. The thickness error was most likely due to the fact that the glass substrate was cut and therefore had edges that influenced the thin water film thickness.

Location	Volume [µl]	Area [mm2]	de_s [µm]	de_w [µm]	dm_s1 [µm]	dm_w1 [µm]
opposite of #	30	2400,75	25.7-26.4	12,49609497	25,86092715	16,81203008

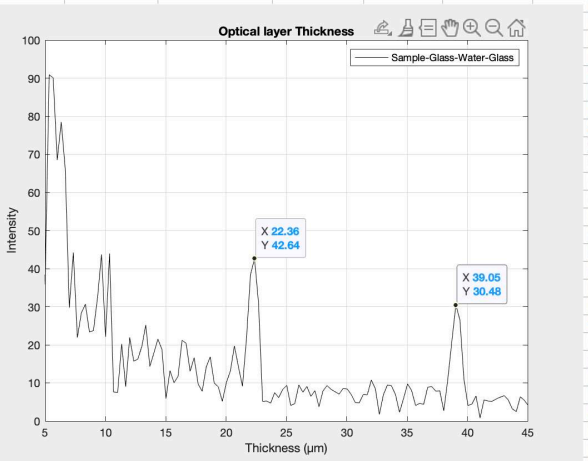

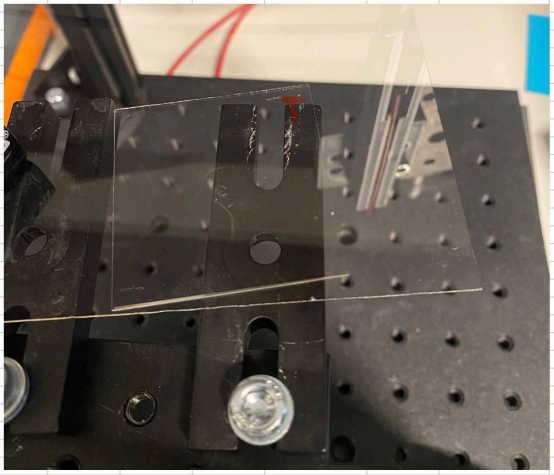

Figure E.12: Sample on top of a bigger piece of glass covering the square area with water.

By using a small optical flat on top of the sample, a thin film of water with a lot smaller volume could be created. However, now that the problem with the cutted edges of the glass was eliminated, another problem arised. The optical flat have rounded edge and due to the weight of the optical flat, water was pressured to go part into these edge and due to that the thickness was influenced making the measurement less accurate. The pro of using an optical flat is that water needs to spread out over a round surface which means that water will not have to be pushed into corners. In the case of using the square area of the sample, an additional force was needed to make sure the water spread out over the entire surface.

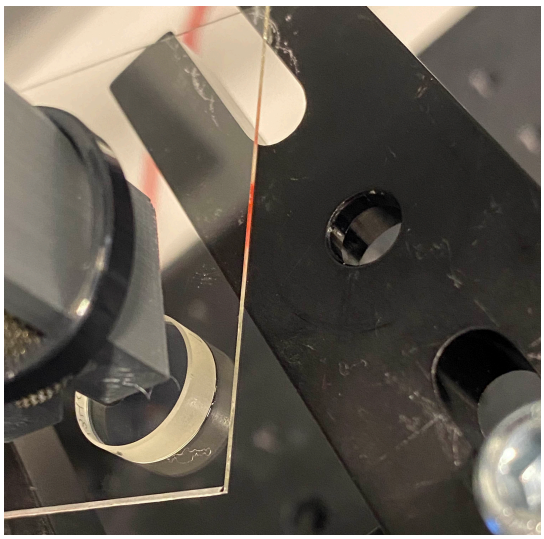

Figure E.13: Using small optical flat to cover with water on top of the sample.

By using a bigger optical flat and turning the situation up side down, meaning that the weight of the glass substrate made sure that the water spread out over the surface of the optical flat instead of the weight of the optical flat. Since the glass substrate was a lot thinner than the optical flat, no water is pushed into the rounded edge of the optical flat. This significantly improved the measurement results. Another issue that arised but was relatively small was that the center of mass of the glass substrate had to be in the middle of the optical flat since otherwise the glass substrate would be positioned slightly inclined and therefore slightly impacting the thickness of the water thin film.

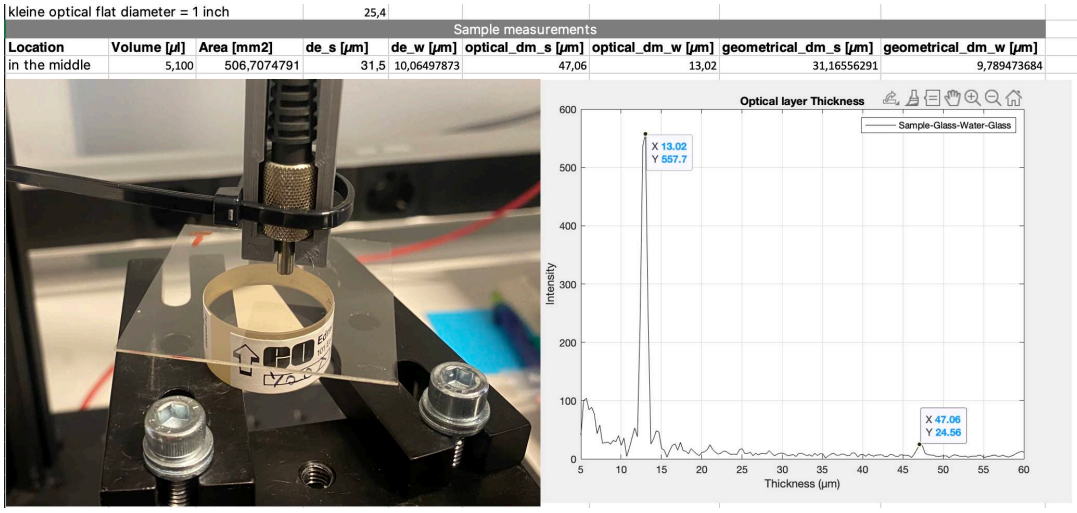

Figure E.14: Turning situation around while using a bigger optical flat.

F

Appendix mathematical derivations

F.1. Rewriting Fresnel equations

By using the Fresnel equations $r_{ij} = \frac{n_j - n_i}{n_j + n_i}$ and $t_{ij} = \frac{2 \cdot n_i}{n_j + n_i}$

Proof that: $r_{01} = -r_{10}$

$$r_{10} = \frac{n_0 - n_1}{n_0 + n_1}$$

$$r_{01} = \frac{n_1 - n_0}{n_0 + n_1}$$

Directly follows that: $r_{01} = -r_{10}$ (F.1)

F.2. Rewriting Fresnel equations

Proof that: $t_{10} \cdot t_{01} = 1 - r_{01}^2$

$$t_{10} = \frac{2n_1}{n_1 + n_0}$$

$$t_{01} = \frac{2n_0}{n_1 + n_0}$$

$$t_{10} \cdot t_{01} = \frac{4n_1 n_0}{(n_1 + n_0)^2}$$

$$1 - r_{01}^2 = 1 - (\frac{n_1 - n_0}{n_0 + n_1})^2$$

$$= 1 - \frac{-2n_1 n_0 + n_1^2 + n_0^2}{(n_1 + n_0)^2}$$

$$= \frac{2n_1 n_0 + n_1^2 + n_0^2}{(n_1 + n_0)^2} - \frac{-2n_1 n_0 + n_1^2 + n_0^2}{(n_1 + n_0)^2}$$

$$= \frac{4n_1 n_0}{(n_1 + n_0)^2}$$

From this follows that: $t_{10} \cdot t_{01} = 1 - r_{01}^2$ (F.2)

F.3. Infinite geometric series

$$B = A_0\left(r_{01} + t_{10}r_{12}t_{01}\exp\left(i\cdot n_1(\lambda)\cdot d\frac{4\pi}{\lambda}\right)\cdot\sum_{m=0}^{\infty}\left(r_{10}r_{12}\exp\left(i\cdot n_1(\lambda)\cdot d\frac{4\pi}{\lambda}\right)\right)^m\right)$$

Which can be rewritten to:

$$B = A_0\left(r_{01} + a_1\cdot\sum_{m=0}^{\infty}(R)^m\right)$$

According to the infinite geometric series: if |R| < 1, then:

$$a_1\sum_{m=0}^{\infty}(R)^m = \frac{a_1}{1-R}$$

This means that:

$$B = A_0\cdot r_{01} + A_0\cdot\frac{t_{10}r_{12}t_{01}\exp\left(i\cdot n_1(\lambda)\cdot d\frac{4\pi}{\lambda}\right)}{1-r_{10}r_{12}\exp\left(i\cdot n_1(\lambda)\cdot d\frac{4\pi}{\lambda}\right)}$$

Now by using results from the previous two derivations F.1 and F.2 this can be rewritten to:

$$B = A_0\cdot r_{01} + A_0\cdot\frac{\left(r_{12}-r_{12}r_{01}^2\right)\exp\left(i\cdot n_1(\lambda)\cdot d\frac{4\pi}{\lambda}\right)}{1+r_{01}r_{12}\exp\left(i\cdot n_1(\lambda)\cdot d\frac{4\pi}{\lambda}\right)}$$

$$= A_0\cdot r_{01}\cdot\frac{1+r_{01}r_{12}\exp\left(i\cdot n_1(\lambda)\cdot d\frac{4\pi}{\lambda}\right)}{1+r_{01}r_{12}\exp\left(i\cdot n_1(\lambda)\cdot d\frac{4\pi}{\lambda}\right)} + A_0\cdot\frac{\left(r_{12}-r_{12}r_{01}^2\right)\exp\left(i\cdot n_1(\lambda)\cdot d\frac{4\pi}{\lambda}\right)}{1+r_{01}r_{12}\exp\left(i\cdot n_1(\lambda)\cdot d\frac{4\pi}{\lambda}\right)}$$

$$= A_0\cdot\frac{r_{01}+r_{01}^2r_{12}\exp\left(i\cdot n_1(\lambda)\cdot d\frac{4\pi}{\lambda}\right)}{1+r_{01}r_{12}\exp\left(i\cdot n_1(\lambda)\cdot d\frac{4\pi}{\lambda}\right)} + A_0\cdot\frac{\left(r_{12}-r_{12}r_{01}^2\right)\exp\left(i\cdot n_1(\lambda)\cdot d\frac{4\pi}{\lambda}\right)}{1+r_{01}r_{12}\exp\left(i\cdot n_1(\lambda)\cdot d\frac{4\pi}{\lambda}\right)}$$

$$= A_0\cdot\frac{r_{01}+r_{12}\exp\left(i\cdot n_1(\lambda)\cdot d\frac{4\pi}{\lambda}\right)}{1+r_{01}r_{12}\exp\left(i\cdot n_1(\lambda)\cdot d\frac{4\pi}{\lambda}\right)}$$

From this follows that: $$B = A_0\cdot\frac{r_{01}+r_{12}\exp\left(i\cdot n_1(\lambda)\cdot d\frac{4\pi}{\lambda}\right)}{1+r_{01}r_{12}\exp\left(i\cdot n_1(\lambda)\cdot d\frac{4\pi}{\lambda}\right)} \quad \text{(F.3)}$$

G

Appendix MATLAB codes

G.1. Simulation single thin film

```
%% Layer information
clearvars
close all
clc

% Wavelength range and step
% Assumption that both incident and substrate material are of infinite
    thickness.
lambdaStart = 400e-9;    % [m] wavelength start
lambdaEnd   = 1000e-9;    % [m] wavelength end
dlambda     = 1.4e-9; % [m] wavelength step
lambda      = lambdaStart:dlambda:lambdaEnd-dlambda;    % [m] Wavelength
    range

% Layer thickness
d = 0.4e-6;

% Refractive index data
load SiO2
SiO2 = table2array(SiO2);
nsio2 = SiO2(:,2);
ds_lambda = SiO2(:,1)*10^-9;

n_SiO2 = interp1(ds_lambda,nsio2,lambda);

% Refractive indices
for j = 1:length(lambda)
n0 = 1;                     % Air
n1(j) = n_SiO2(j);
n2 = 1;                     % Air
end

figure
plot(lambda,n1)
xlabel('Wavelength')
ylabel('Refractive index')
title('Refractive index of SiO2 as a function of the wavelength')

```

```
%  Reflection and Transmission coefficients
for j=1:length(lambda)

r01(j) = (n1(j)-n0)/(n1(j)+n0);      % Reflection at first interface (
    Incident light)
r12(j) = (n2-n1(j))/(n2+n1(j));      % Reflection at second interface (
    After transmition of light through first interface)
r10(j) = (n0-n1(j))/(n0+n1(j));      % Reflection at first interface (
    After transmition of light through first interface and reflected at
    second interface)

t01(j) = 2*n0/(n1(j)+n0);          % Transmission through first interface (
    Indicent light)
t10(j) = 2*n1(j)/(n0+n1(j));         % Transmission through first
    interface (After reflection at second interface)

% Phase change
delta(j) = (2*n1(j)*pi*d) ./ lambda(j);

% Equations phase & reflection for a single thickness
 r012x = r01 + ( ( t01.*r12.*t10 .* exp(2*1i*delta) ) ./ ( 1 - r10.*r12.*
     exp(2*1i*delta) ) );
R(j) = abs(r012x(j)).^2;
end

% Reflectance spectrum for a single layer
figure
plot(lambda*1e9,R,'k')
xlabel('Wavelength (nm)')
ylabel('Reflected power')
title('Thin film SiO2 with d = 0.4 µm')

%% Fast Fourier Transform
v = 1./lambda;

figure
plot(v,R)
xlabel('Wavenumber (1/nm)')
ylabel('Reflected power')
title('Single layer of SiO2 of thickness 1000 nm')

% Step 2
v_max = max(v);
v_min = min(v);
L = length(v);
N = 2^nextpow2(L);
dv = (v_max - v_min) / N;
vi = v_min:dv:v_max;
Ri = interp1(v,R,vi);

% Step 3 - https://nl.mathworks.com/help/matlab/ref/fft.html
Y = fft(Ri);
P2 = abs(Y/N);
P1 = P2(1:N/2+1);
P1(2:end-1) = 2*P1(2:end-1);

```

```
86 for j=1:length(lambda)
87 d = (0:N/2)./(2*n1(j)*(v_max-v_min));              % Optical thickness
88 end
89
90 % Thickness plot
91 figure
92 plot(d*1e6,P1,k)
93 xlabel('Thickness (µm)')
94 ylabel('Intensity')
95 title('Optical layer Thickness')
96 grid on
97 legend('Sample-Glass-Water-Glass')
```

G.2. Simulation multilayer

```
%% Layer information
clearvars
close all
clc

% Parameters
% Assumption that both incident and substrate material are of infinite
    thickness.
lambdaStart = 550e-9;    % [m] wavelength start
lambdaEnd   = 700e-9;    % [m] wavelength end
dlambda     = 0.01e-9; % [m] wavelength step
lambda      = lambdaStart:dlambda:lambdaEnd-dlambda;     % [m] Wavelength
    range

d1 = 20e-6; % Layer 1
d2 = 10e-6; % Layer 2

% Refractive indices
load SiO2
SiO2 = table2array(SiO2);
nsio2 = SiO2(:,2);
ds_lambda = SiO2(:,1)*10^-9;

n_SiO2 = interp1(ds_lambda,nsio2,lambda);

Acr = readtable('Acrylic.txt');
Acr = table2array(Acr);
nacr = Acr(:,2);
ds_lambda_acr = Acr(:,1)*10^-9;

n_acr = interp1(ds_lambda_acr,nacr,lambda);

load Al2O3
Al2O3 = table2array(Al2O3);
nal2o3 = Al2O3(:,2);
ds_lambda = Al2O3(:,1)*10^-9;

n_Al2O3 = interp1(ds_lambda,nal2o3,lambda);

load PET
PET = table2array(PET);
npet = PET(:,2);
ds_lambda = PET(:,1)*10^-9;

n_PET = interp1(ds_lambda,npet,lambda);

load PE
PE = table2array(PE);
npe = PE(:,2);
ds_lambda_PE = PE(:,1)*10^-9;

n_PE = interp1(ds_lambda_PE,npe,lambda);

H2O = readtable('n_h20.csv');
```

```
H2O = table2array(H2O);
nh2o = H2O(:,2);
ds_lambda_h2o = H2O(:,1)*10^-6;

n_H2O = interp1(ds_lambda_h2o,nh2o,lambda);

n_mat1 = n_acr;
n_mat2 = n_PET;

figure(1);
subplot(211), plot(lambda*10^9,n_mat1);
xlabel('Wavelength [nm]')
ylabel('n')
title('Refractive index Acrylic')
subplot(212), plot(lambda*10^9,n_mat2);
xlabel('Wavelength [nm]')
ylabel('n')
title('Refractive index PET')

for j = 1:length(lambda)
n0 = 1;
n1(j) = n_mat1(j);
n2(j) = n_mat2(j);
n3 = n0;
end

% Transfer Matrix method
for j=1:length(lambda)
M_1 = [ cos( (2*pi*n1(j)*d1)./lambda(j) )      , -(1i/n1(j))*sin( (2*pi*n1(
    j)*d1)./lambda(j) )
          -(1i*n1(j))*sin((2*pi*n1(j)*d1)./lambda(j)) ,    cos( (2*pi*n1(j)
             *d1)./lambda(j) )];

M_2 = [ cos((2*pi*n2(j)*d2)./lambda(j))      , -(1i/n2(j))*sin((2*pi*n2(j)*
    d2)./lambda(j))
          -(1i*n2(j))*sin((2*pi*n2(j)*d2)./lambda(j)) ,    cos((2*pi*n2(j)*
             d2)./lambda(j))];

M = M_1*M_2;
A = M(1,1);
B = M(1,2);
C = M(2,1);
D = M(2,2);

nt(j) = n3;

r2(j) = ( ( A+B*nt(j) ) - (1/n0)*( C+D*nt(j) ) ) / ( ( A+B*nt(j) ) + (1/n0
    )*( C+D*nt(j) ) );
R2(j) = abs(r2(j)).^2;
end

figure
plot(lambda*1e9,R2)
xlabel('Wavelength (nm)')
ylabel('Reflected power')
title('Reflectance spectrum for two thin films of acrylic and PET')
```

```
104
105 %% see Page 123 in the book by Michael Quinten
106 % https://nl.mathworks.com/help/matlab/ref/fft.html
107 v = 1./lambda;
108
109 v_max = max(v);
110 v_min = min(v);
111
112 L = length(v);
113 N = 2^nextpow2(L);
114 dv = (v_max - v_min) / N;
115 vi = v_min:dv:v_max;
116 Ri = interp1(v,R2,vi);
117
118 Y = fft(Ri);
119 P2 = abs(Y/N);
120 P1 = P2(1:N/2+1);
121 P1(2:end-1) = 2*P1(2:end-1);
122
123 for j=1:length(lambda)
124 d = (0:N/2)./(2*(v_max-v_min));              % Optical thickness
125 end
126
127 % Thickness plot
128 figure
129 plot(d*1e6,P1)
130 xlabel('Thickness (µm)')
131 ylabel('Intensity')
132 xlim([2,75])
133 ylim(['auto'])
134 title('Optical layer Thickness')
135 grid on
136 legend('Arylic and PET thin films')
```

G.3. From measurement data to thickness determination

```
%% Reflectance spectrum - Measurement data
clear all
clc

% setting the Wavelength range
lambda_start   = 500*10^-9;
lambda_end     = 1000*10^-9;

% loading measurement dataset
meting = readtable('waterfilm_5.1microliter.txt');
meting = table2array(meting);

light_source = readtable('Reference (light source).txt');
light_source = table2array(light_source);


% Parameters
lambda = (meting(:,1)).'*10^-9;

A = find( lambda>lambda_start & lambda<lambda_end );

lambda = lambda(A);
c = meting(A,5);                          % Corrected for Dark
R2 = c

c_light = light_source(A,2);                            % Sample
R2_light = c_light;

R2 =  normalize(c)-normalize(c_light);

% loading refractive index datasets
load SiO2
SiO2 = table2array(SiO2);
nsio2 = SiO2(:,2);
ds_lambda = SiO2(:,1)*10^-9;

n_SiO2 = interp1(ds_lambda,nsio2,lambda);

load Al2O3
Al2O3 = table2array(Al2O3);
nal2o3 = Al2O3(:,2);
ds_lambda = Al2O3(:,1)*10^-9;

n_Al2O3 = interp1(ds_lambda,nal2o3,lambda);

load PET
PET = table2array(PET);
npet = PET(:,2);
ds_lambda = PET(:,1)*10^-9;

n_PET = interp1(ds_lambda,npet,lambda);

load PE
PE = table2array(PE);
```

```
npe = PE(:,2);
ds_lambda = PE(:,1)*10^-9;

n_PE = interp1(ds_lambda,npe,lambda);

acr = readtable('Acrylic.txt');
acr = table2array(acr);
nacr = acr(:,2);
ds_lambda = acr(:,1)*10^-9;

n_acr = interp1(ds_lambda,nacr,lambda);

% Choose material, refractive index n
n_mat = n_PE;

figure
plot(lambda*10^9,c,k)
title('Reflectance spectrum rawdata')
xlabel('Wavelength [nm]')
legend('Sample-Glass-Water-Glass')

figure
plot(lambda*10^9,R2,k)
title('Reflectance spectrum')
xlabel('Wavelength [nm]')
legend('Sample-Glass-Water-Glass')

%% Fast Fourier Transform - Thickness determination - Measurement data
% https://nl.mathworks.com/help/matlab/ref/fft.html
v = 1./lambda;
v_max = max(v);
v_min = min(v);
L = length(v);
N = 2^nextpow2(L);
dv = (v_max - v_min) / N;
vi = v_min:dv:v_max;
Ri = interp1(v,R2,vi);

Y = fft(Ri);
P2 = abs(Y/N);
P1 = P2(1:N/2+1);
P1(2:end-1) = 2*P1(2:end-1);

for j=1:length(lambda)
d = (0:N/2)./(2*(v_max-v_min));              % Optical thickness
end

% Thickness plot
figure
plot(d*1e6,P1)
xlabel('Thickness (µm)')
ylabel('Intensity')
xlim([-2,75])
ylim(['auto'])
title('Optical layer Thickness')
legend('Sample-Glass-Water-Glass')
```

Bibliography

[1] Avantes spectrometer, avaspec, 2022. URL https://www.avantes.com/products/spectrometers/starline/avaspec-uls2048cl-evo/.

[2] Enlightening spectroscopy, 2022. URL https://in-science.ru/f/avantes_catalog_xi_1-183.pdf.

[3] Avantes light source, avalight, 2023. URL https://www.avantes.com/products/light-sources/halogen-and-deuterium-halogen/avalight-dh-s-bal/.

[4] Fiber optic cables, 2023. URL https://www.avantes.com/products/fiber-optics/fiber-optic-cables/.

[5] Avantes, 2023. URL https://www.avantes.com/.

[6] M Bender, A Fuchs, U Plachetka, and H Kurz. Status and prospects of uv-nanoimprint technology. *Microelectronic Engineering*, 83(4-9):827–830, 2006.

[7] Steven J Byrnes. Multilayer optical calculations. *arXiv preprint arXiv:1603.02720*, 2016.

[8] Capp. Pipetting errors, 2023. URL https://capp.dk/blog/common-pipetting-errors/.

[9] Stephen Y Chou, Peter R Krauss, and Preston J Renstrom. Imprint of sub-25 nm vias and trenches in polymers. *Applied physics letters*, 67(21):3114–3116, 1995.

[10] Stephen Y Chou, Peter R Krauss, and Preston J Renstrom. Nanoimprint lithography. *Journal of Vacuum Science & Technology B: Microelectronics and Nanometer Structures Processing, Measurement, and Phenomena*, 14(6):4129–4133, 1996.

[11] EdmundOptics. Optical flat, zerodur, 2023. URL https://www.edmundoptics.eu/p/254mm-dia-lambda10-zerodurreg-optical-flat/2210/#.

[12] Filmetrics. Filmetrics refractive index database, 2023. URL https://www.filmetrics.com/refractive-index-database.

[13] A Hunter, R Dwyer-Joyce, and P Harper. Calibration and validation of ultrasonic reflection methods for thin-film measurement in tribology. *Measurement Science and Technology*, 23(10):105605, 2012.

[14] Anita C Jones, M Millington, J Muhl, JM De Freitas, James S Barton, and G Gregory. Calibration of an optical fluorescence method for film thickness measurement. *Measurement Science and Technology*, 12(5):N23, 2001.

[15] Keyence. 3d laser scanning confocal microscope, 2023. URL https://www.keyence.eu/products/microscope/laser-microscope/vk-x100_x200/models/vk-x1100/.

[16] Jin Young Kim, In Gyu Hwang, and Byung Mook Weon. Evaporation of inclined water droplets. *Scientific reports*, 7(1):1–7, 2017.

[17] Nazrin Kooy, Khairudin Mohamed, Lee Tze Pin, and Ooi Su Guan. A review of roll-to-roll nanoimprint lithography. *Nanoscale research letters*, 9(1):1–13, 2014.

[18] Hongbo Lan. Large-area nanoimprint lithography and applications. *Micro/Nanolithography-A heuristic aspect on the enduring technology*, pages 43–68, 2018.

[19] Hongbo Lan and Hongzhong Liu. Uv-nanoimprint lithography: structure, materials and fabrication of flexible molds. *Journal of nanoscience and nanotechnology*, 13(5):3145–3172, 2013.

[20] Xingxin Liang, Xinping Yan, Wu Ouyang, Robert JK Wood, Fuming Kuang, Zhenglin Liu, and Xincong Zhou. Comparison of measured and calculated water film thickness of a water-lubricated elastically supported tilting pad thrust bearing. *Surface Topography: Metrology and Properties*, 7 (4):045010, 2019.

[21] BR Marshall. Glue film thickness measurements by spectral reflectance. Technical report, National Security Technologies, LLC (United States), 2010.

[22] Mathworks. Spectral leakage fft, 2023. URL `https://blogs.mathworks.com/steve/2021/02/26/fft-spectral-leakage/`.

[23] Morphotonics. Morphotonics, 2023. URL `https://morphotonics.com/`.

[24] Ashish Pandey, Sivan Tzadka, Dor Yehuda, and Mark Schvartzman. Soft thermal nanoimprint with a 10 nm feature size. *Soft Matter*, 15(13):2897–2904, 2019.

[25] Michael Quinten. *A practical guide to optical metrology for thin films*. John Wiley & Sons, 2012.

[26] Michael Quinten. On the use of fast fourier transform for optical layer thickness determination. *SN Applied Sciences*, 1(8):823, 2019.

[27] refractivexindex.info. Refractive index database, 2023. URL `https://refractiveindex.info/`.

[28] Alaa Abdulwahid Sharhan. Transfer matrix mathematical method for evaluation the dbr mirror for light emitting diode and laser. In *Journal of Physics: Conference Series*, volume 1535, page 012018. IOP Publishing, 2020.

[29] Olaf Stenzel et al. *The physics of thin film optical spectra*. Springer, 2015.

[30] Thorlabs. Numerical aperture, 2023. URL `https://www.thorlabs.com/newgrouppage9.cfm?objectgroup_id=6689`.

[31] Vera Trabadelo, Helmut Schift, Santos Merino, Sandro Bellini, and Jens Gobrecht. Measurement of demolding forces in full wafer thermal nanoimprint. *Microelectronic Engineering*, 85(5-6):907–909, 2008.